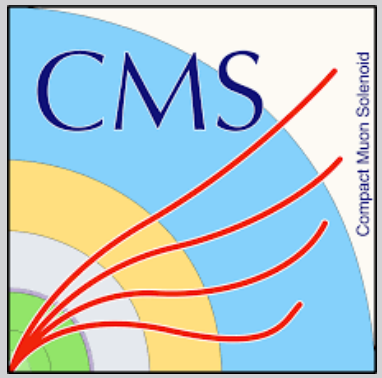

Diffractive results from CMS

István Szanyi
on behalf of the CMS and TOTEM Collaborations

University of Kansas, Lawrence, USA
MATE Institute of Technology, KRC, Gyöngyös, Hungary
HUN-REN Wigner RCP, Budapest, Hungary

Diffraction and Low-x 2024

8 – 14 September 2024, Palermo, Italy

Outline

- basic diffractive scattering events in pp collisions
- the CMS and TOTEM detectors at LHC
- nonresonant central exclusive production of charged-hadron pairs in pp collisions at $\sqrt{s}$ = 13 TeV Phys. Rev. D **109** (2024) 112013
- dijet events with hard color-singlet exchange (jet-gap-jet events) in pp collisions at $\sqrt{s}$ = 13 TeV Phys. Rev. D **104** (2021) 032009
- single-diffractive dijet production in pp collisions at $\sqrt{s}$ = 8 TeV Eur. Phys. J. C 80 (2020) 1164
- summary

Basic diffractive scattering events in pp collisions

Basic diffractive scattering events in pp collisions

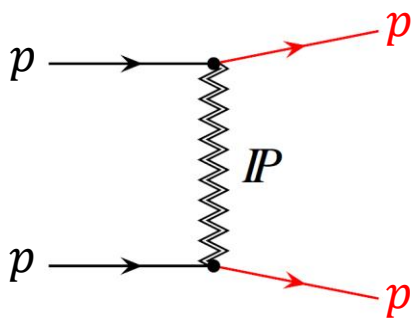

elastic

Basic diffractive scattering events in pp collisions

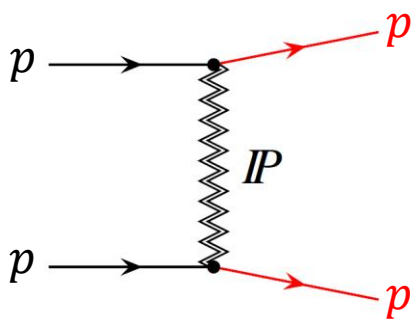

elastic

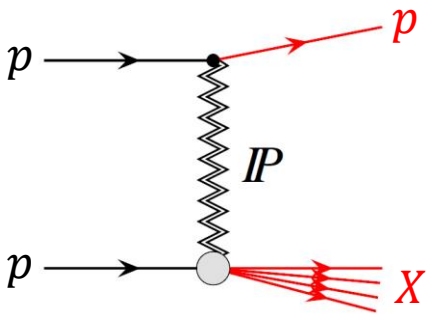

single-diffractive

Basic diffractive scattering events in pp collisions

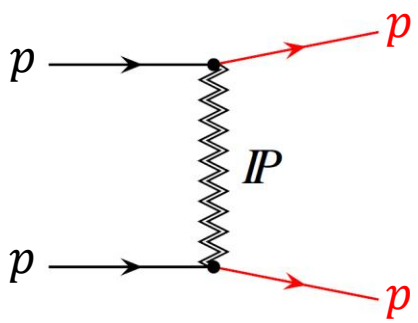

elastic

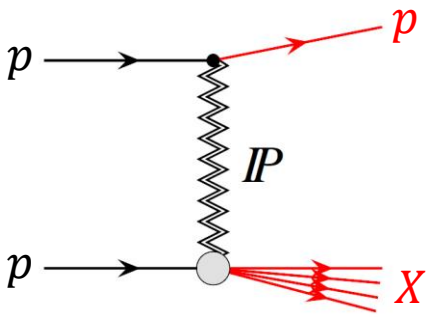

single-diffractive

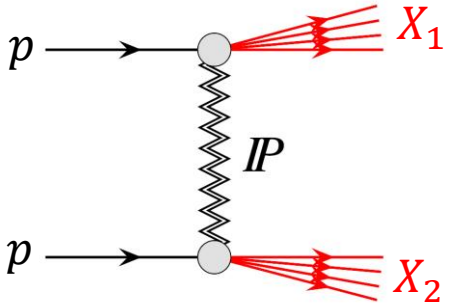

double-diffractive

Basic diffractive scattering events in pp collisions

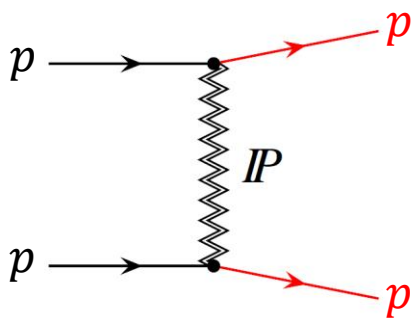

elastic

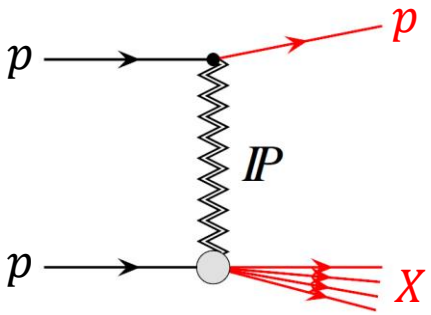

single-diffractive

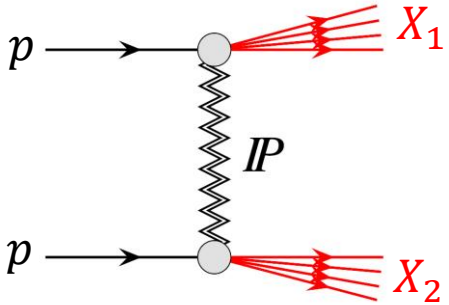

double-diffractive

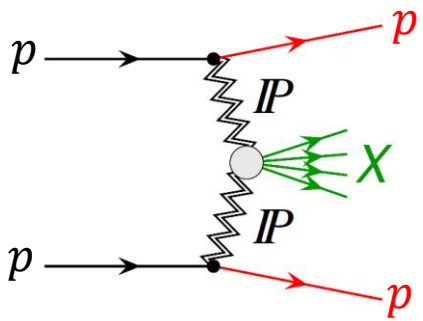

double pomeron exchange
(central exclusive production)

Basic diffractive scattering events in pp collisions

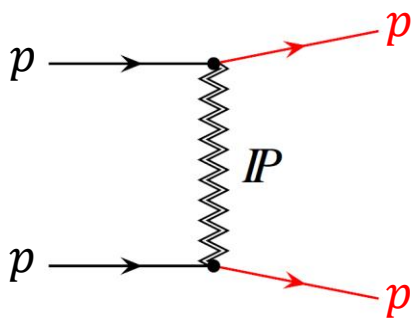

elastic

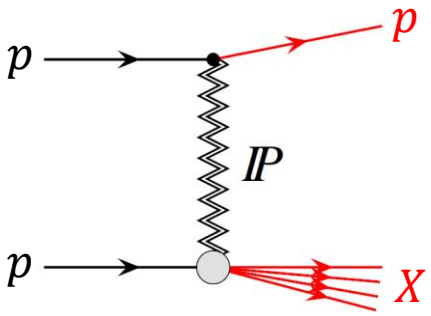

single-diffractive

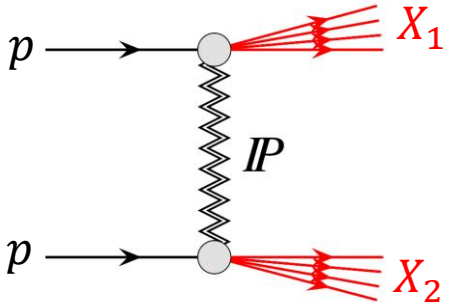

double-diffractive

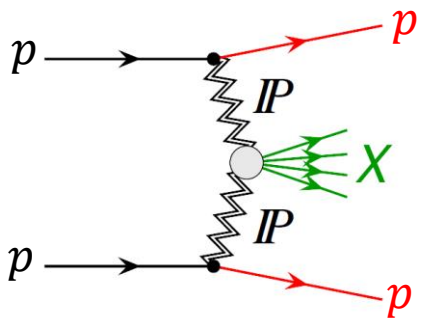

double pomeron exchange
(central exclusive production)

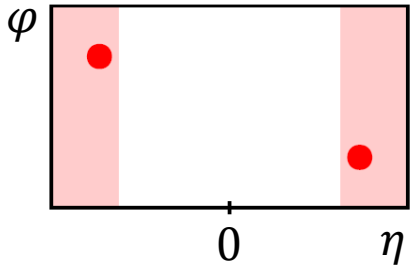

Basic diffractive scattering events in pp collisions

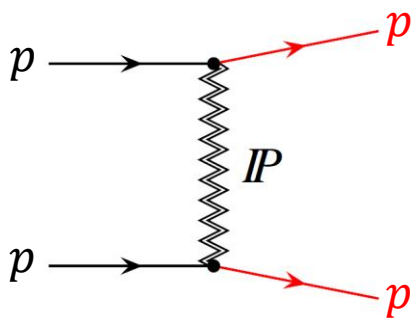

elastic

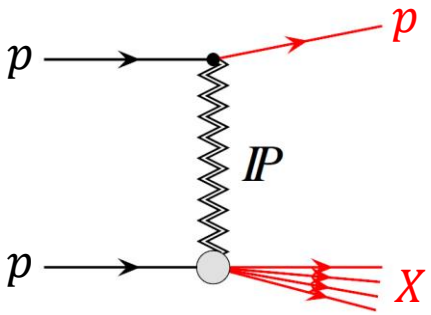

single-diffractive

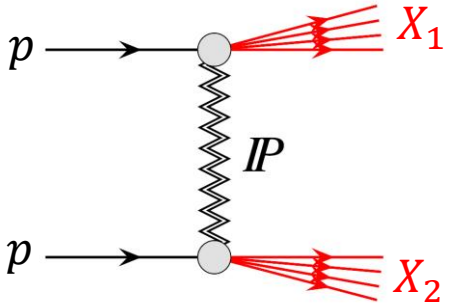

double-diffractive

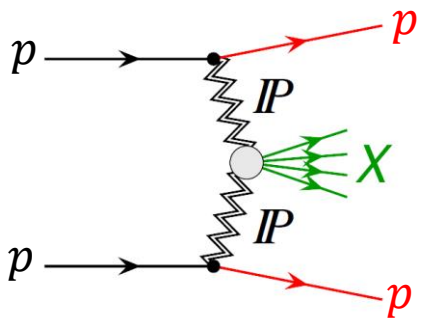

double pomeron exchange
(central exclusive production)

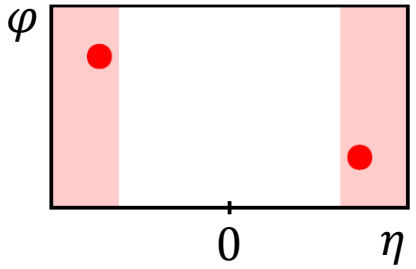

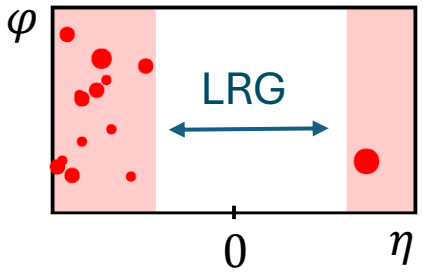

Basic diffractive scattering events in pp collisions

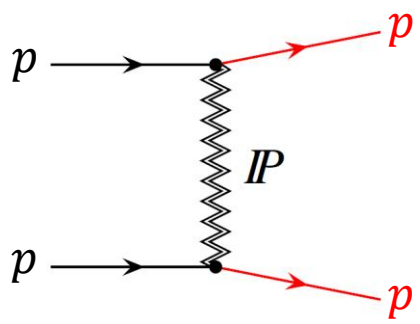

elastic

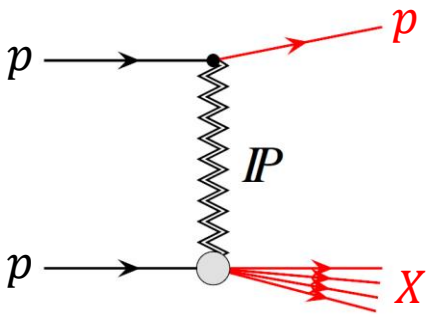

single-diffractive

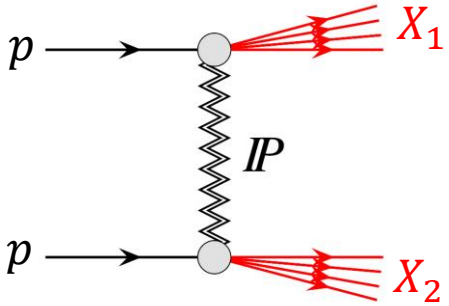

double-diffractive

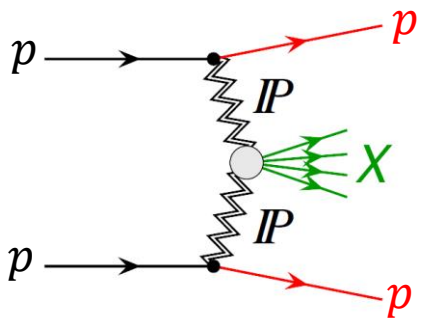

double pomeron exchange
(central exclusive production)

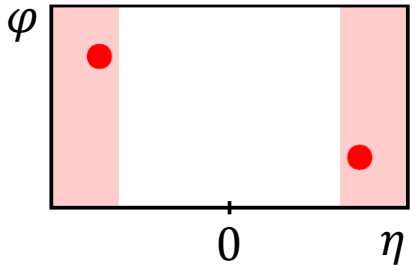

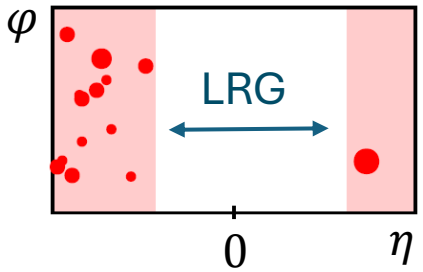

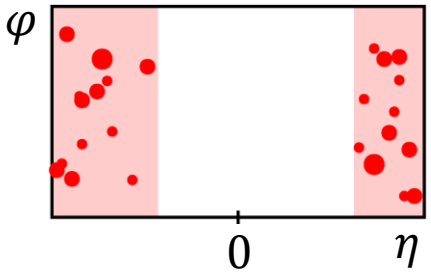

Basic diffractive scattering events in pp collisions

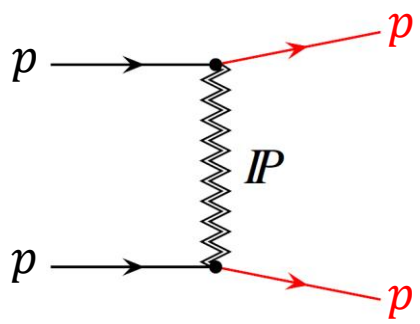

elastic

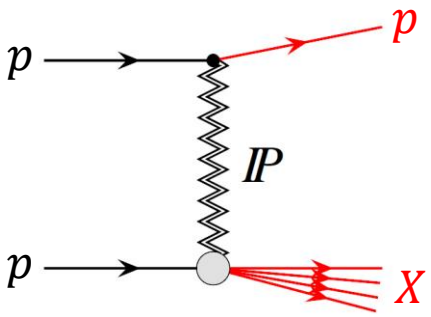

single-diffractive

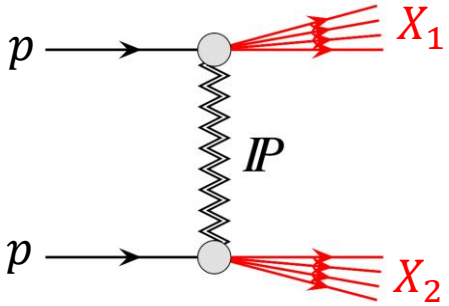

double-diffractive

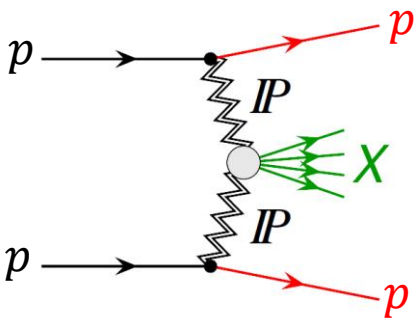

double pomeron exchange
(central exclusive production)

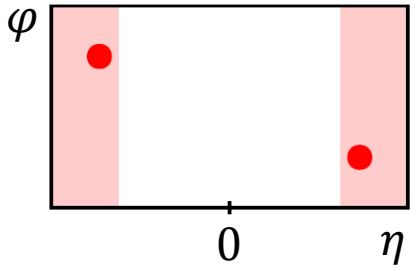

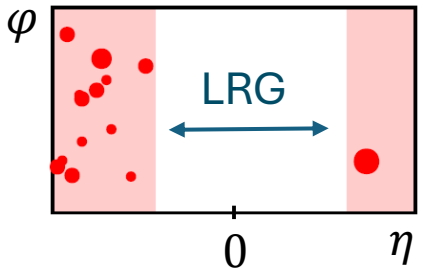

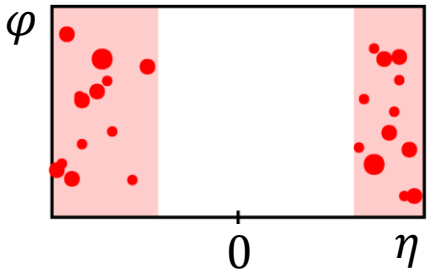

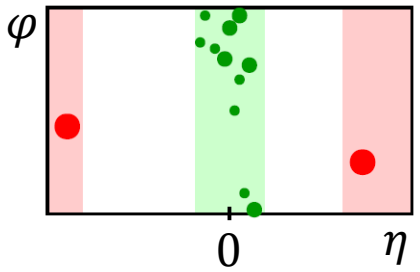

Basic diffractive scattering events in pp collisions

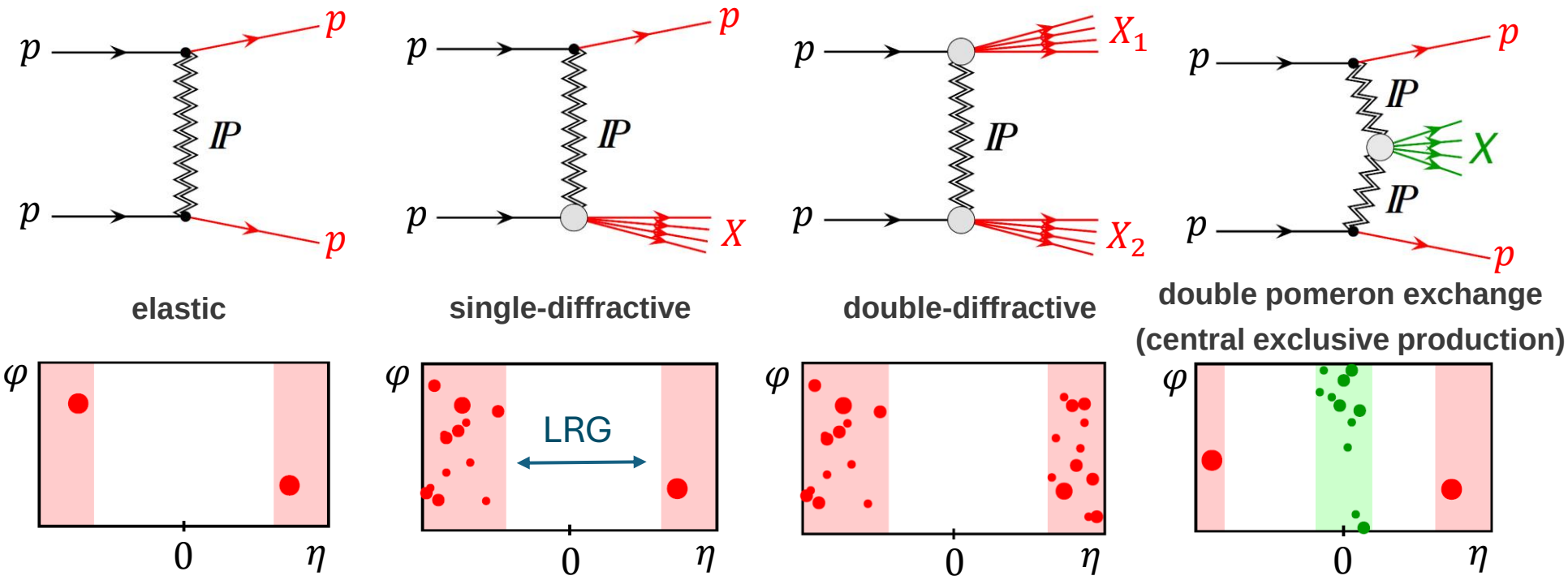

dominant **pomeron exchange** leading to a **large rapidity gap** (LRG),
a wide region devoid of particle activity

Basic diffractive scattering events in pp collisions

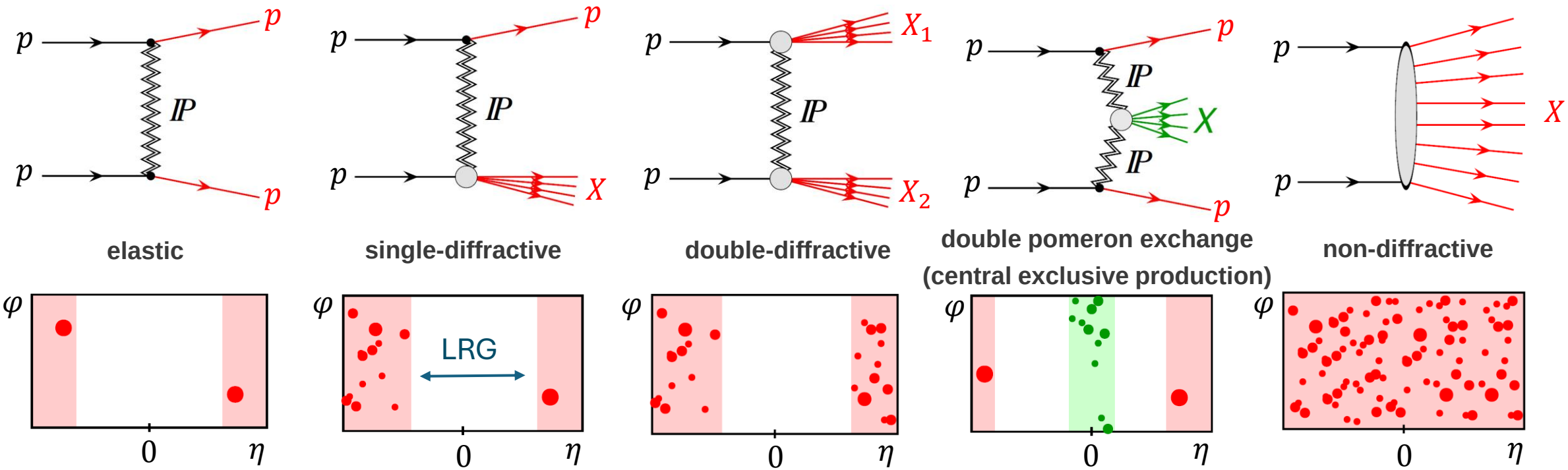

dominant **pomeron exchange** leading to a **large rapidity gap** (LRG),
a wide region devoid of particle activity

Basic diffractive scattering events in pp collisions

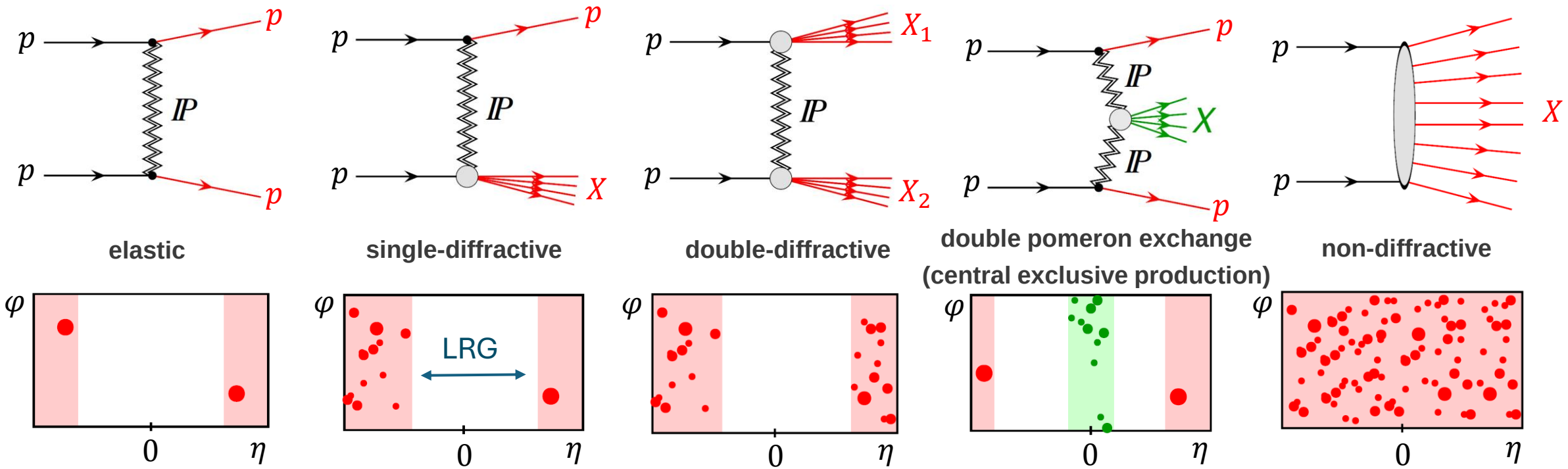

dominant **pomeron exchange** leading to a **large rapidity gap** (LRG), a wide region devoid of particle activity

"soft" pomeron in Regge theory: whole family of particles with vacuum quantum numbers; it accounts for the rising hadronic cross sections with $\sqrt{s}$

Basic diffractive scattering events in pp collisions

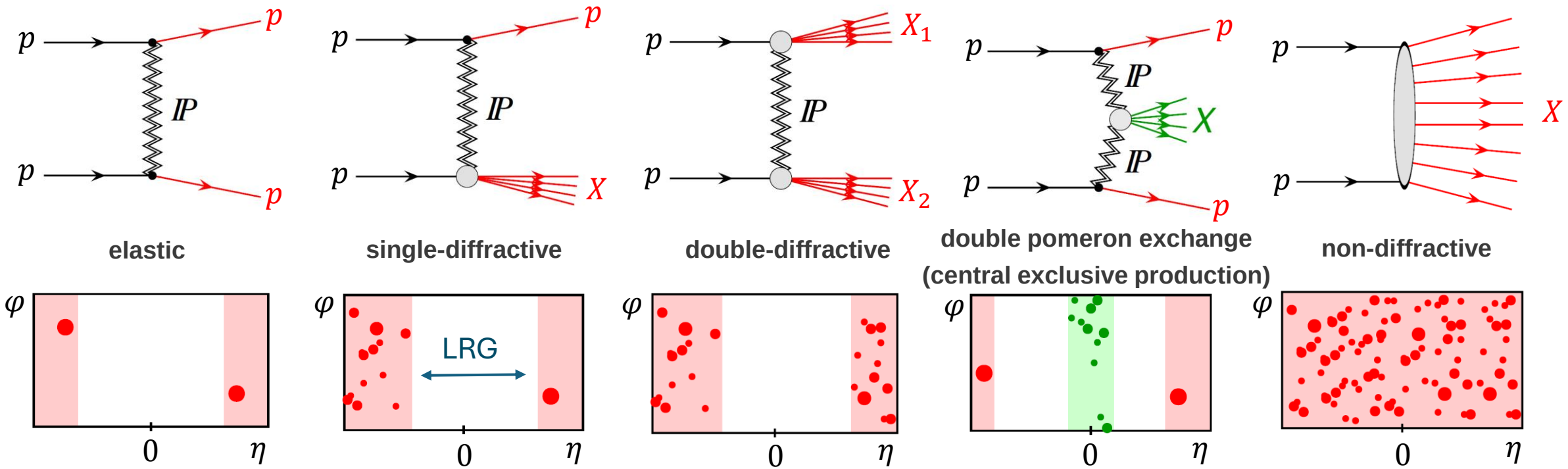

dominant **pomeron exchange** leading to a **large rapidity gap** (LRG), a wide region devoid of particle activity

"soft" pomeron in Regge theory: whole family of particles with vacuum quantum numbers; it accounts for the rising hadronic cross sections with $\sqrt{s}$

"hard" (BFKL) pomeron in pQCD: colorless compound of two interacting gluons

Basic diffractive scattering events in pp collisions

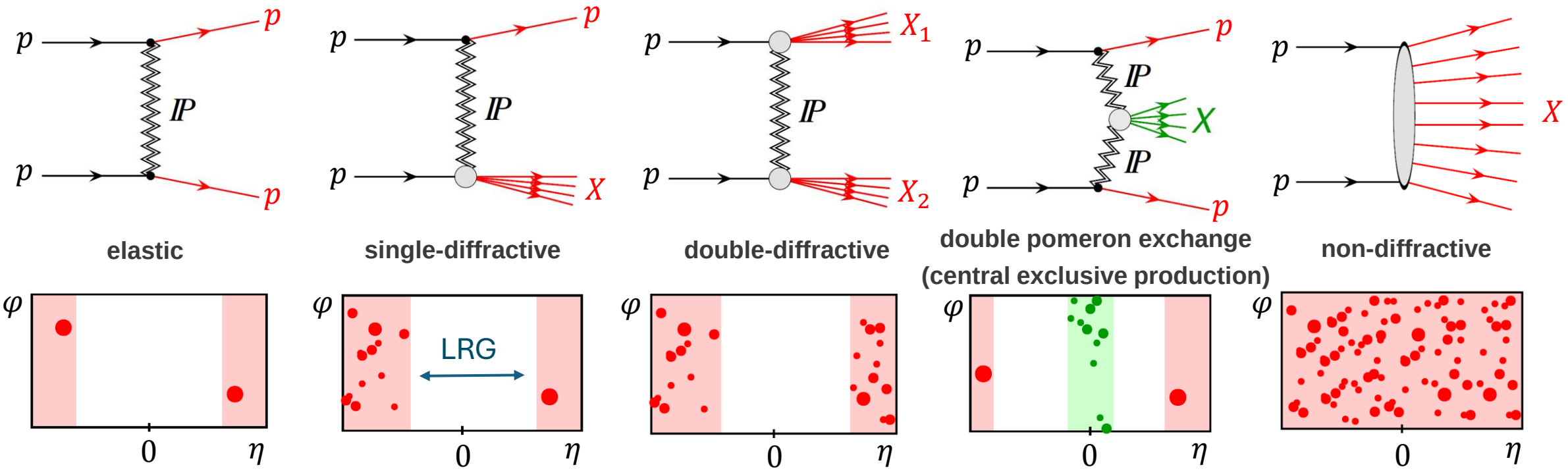

dominant **pomeron exchange** leading to a **large rapidity gap** (LRG), a wide region devoid of particle activity

"soft" pomeron in Regge theory: whole family of particles with vacuum quantum numbers; it accounts for the rising hadronic cross sections with $\sqrt{s}$

"hard" (BFKL) pomeron in pQCD: colorless compound of two interacting gluons

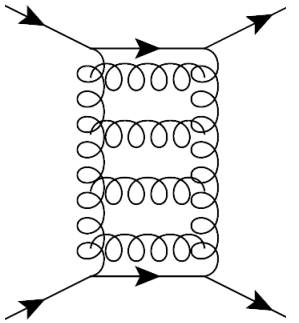

BFKL pomeron

Basic diffractive scattering events in pp collisions

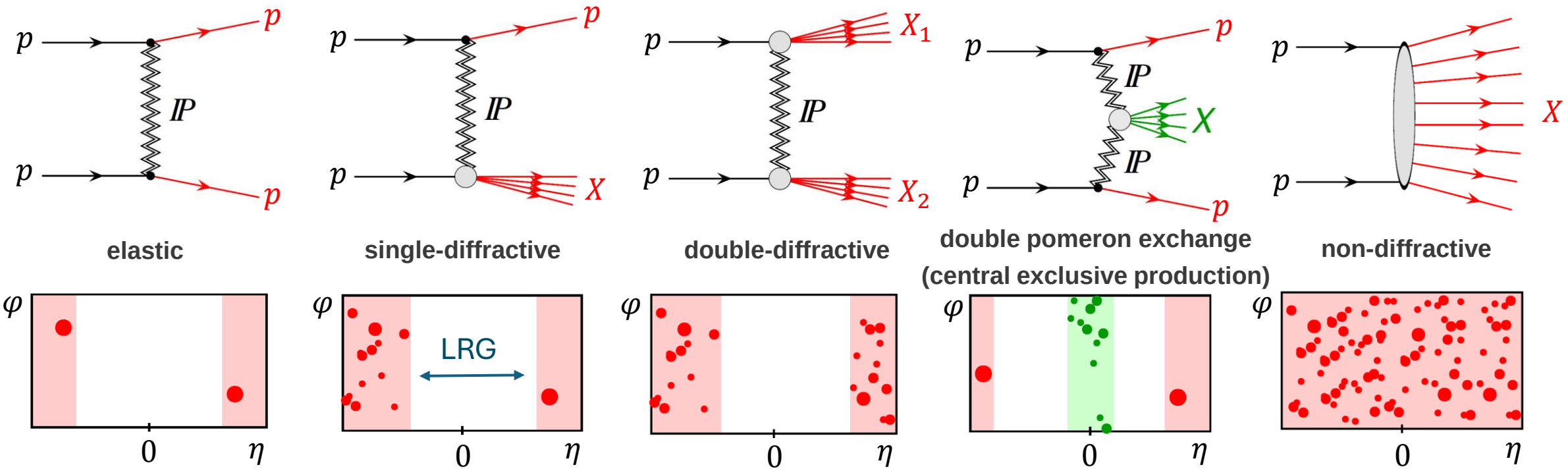

dominant **pomeron exchange** leading to a **large rapidity gap** (LRG), a wide region devoid of particle activity

"soft" pomeron in Regge theory: whole family of particles with vacuum quantum numbers; it accounts for the rising hadronic cross sections with $\sqrt{s}$

"hard" (BFKL) pomeron in pQCD: colorless compound of two interacting gluons

pomeron physics is an ongoing research topic both experimentally and theoretically

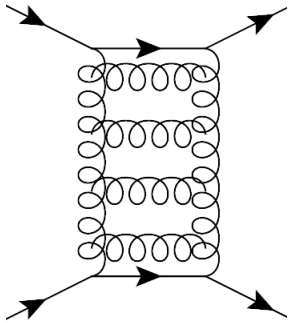

BFKL pomeron

CMS and TOTEM detectors at the LHC

CMS and TOTEM detectors at the LHC

CMS
central detector

IP5

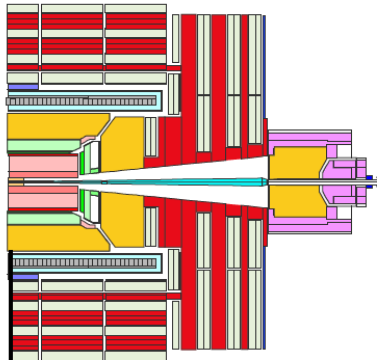

CMS and TOTEM detectors at the LHC

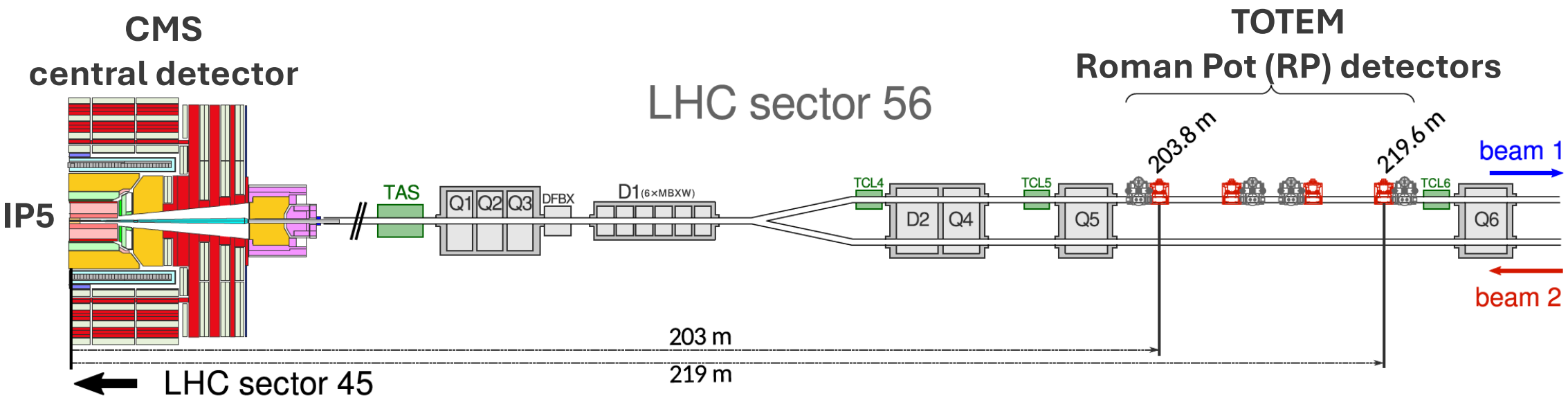

CMS and TOTEM detectors at the LHC

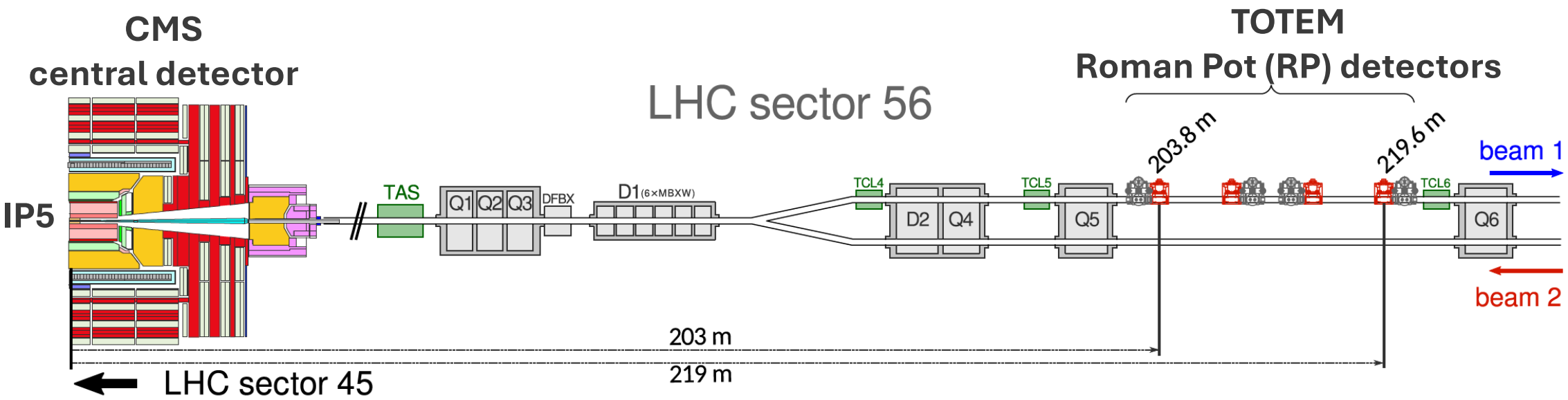

TOTEM RP detectors are located about 200-220 m away from IP5 on **both sides** of CMS

CMS and TOTEM detectors at the LHC

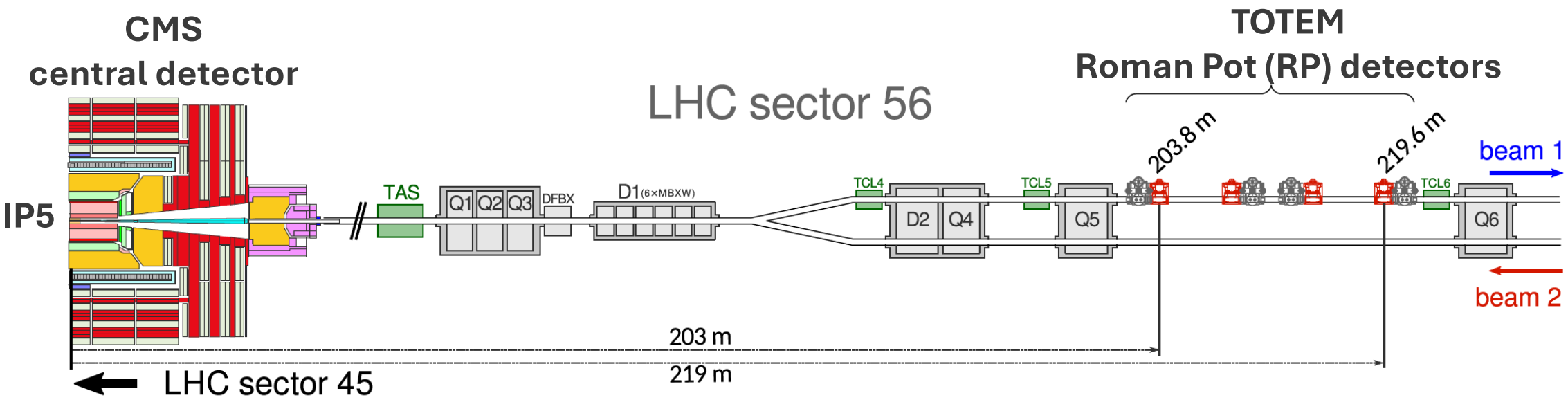

TOTEM RP detectors are located about 200-220 m away from IP5 on **both sides** of CMS

diffractively produced particles are measured by CMS detector; intact protons are measured by TOTEM RP detectors

CMS and TOTEM detectors at the LHC

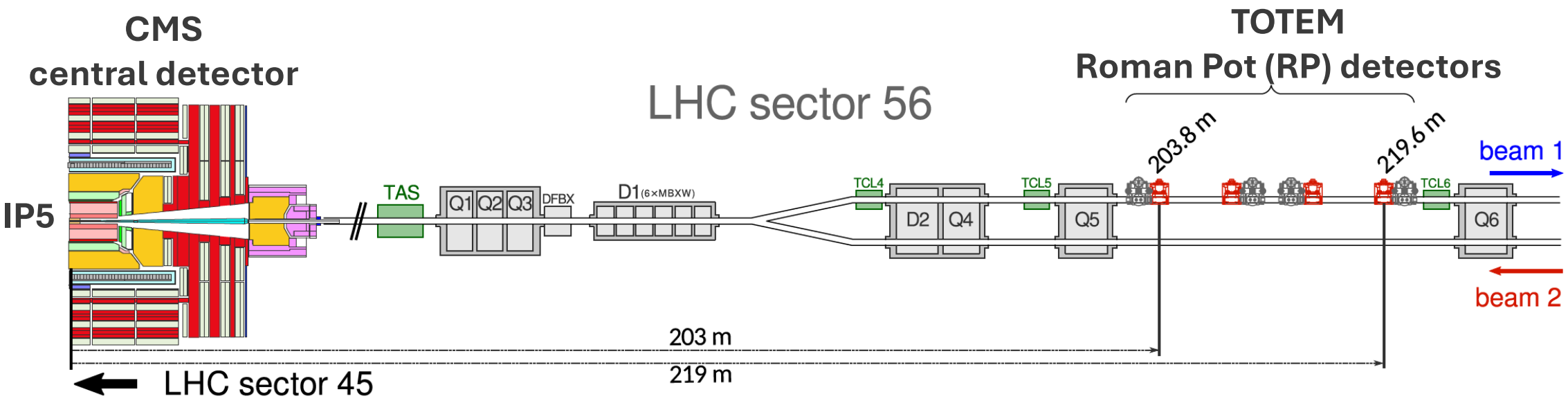

TOTEM RP detectors are located about 200-220 m away from IP5 on **both sides** of CMS

diffractively produced particles are measured by CMS detector; intact protons are measured by TOTEM RP detectors

RPs (equipped with 10 planes of Si strip sensors) approach the beam horizontally or vertically

CMS and TOTEM detectors at the LHC

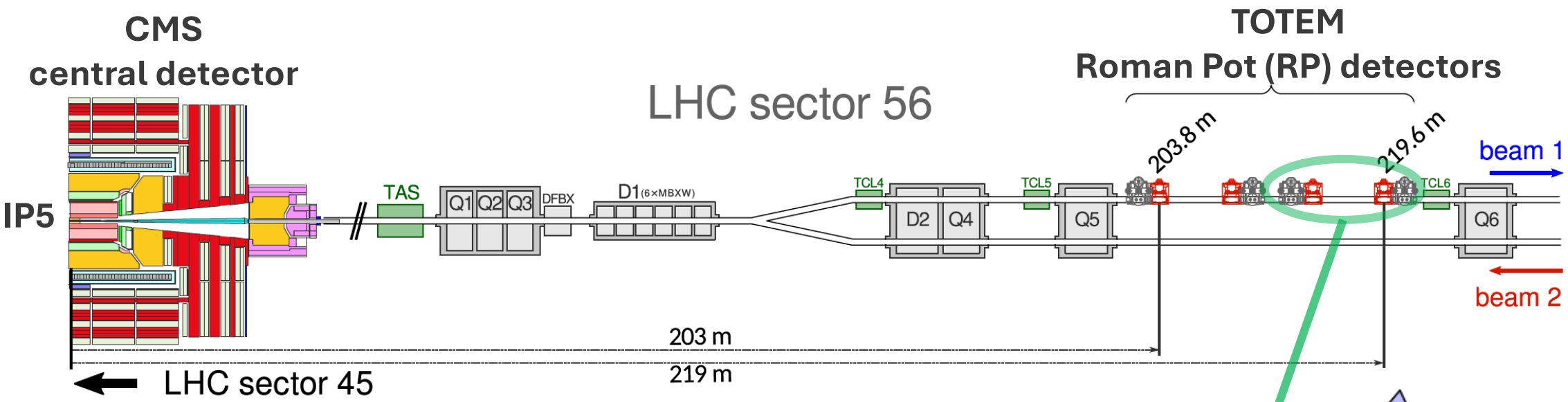

TOTEM RP detectors are located about 200-220 m away from IP5 on **both sides** of CMS

diffractively produced particles are measured by CMS detector; intact protons are measured by TOTEM RP detectors

RPs (equipped with 10 planes of Si strip sensors) approach the beam horizontally or vertically

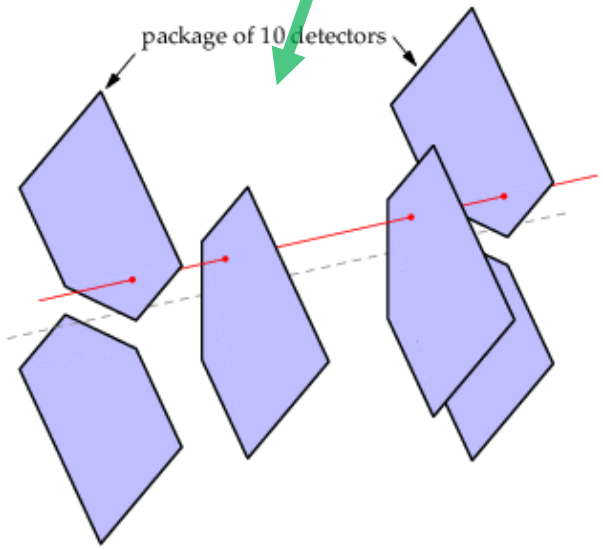

CMS and TOTEM detectors at the LHC

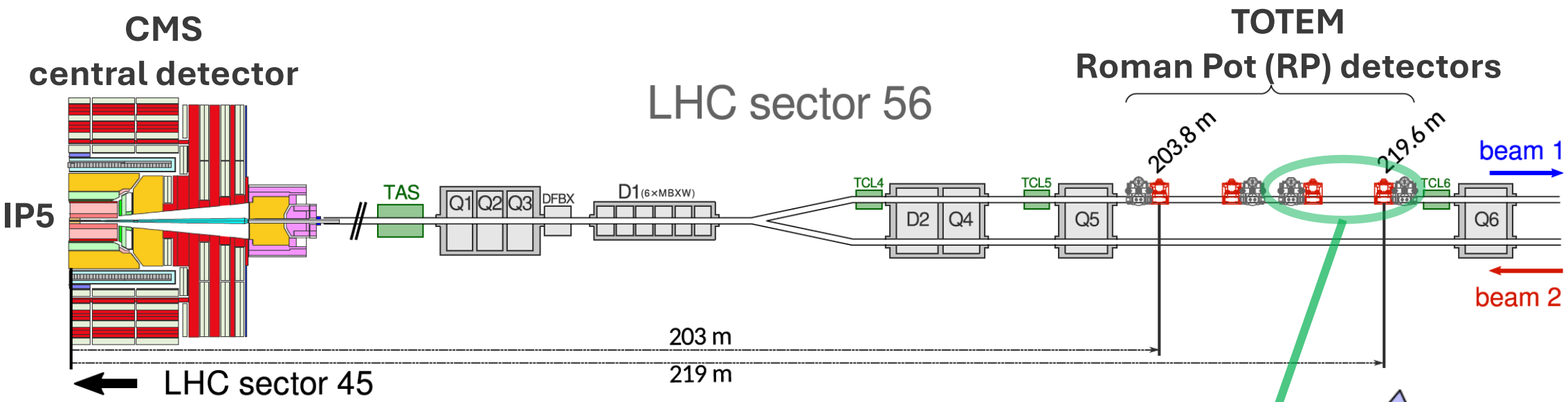

TOTEM RP detectors are located about 200-220 m away from IP5 on **both sides** of CMS

diffractively produced particles are measured by CMS detector; intact protons are measured by TOTEM RP detectors

RPs (equipped with 10 planes of Si strip sensors) approach the beam horizontally or vertically

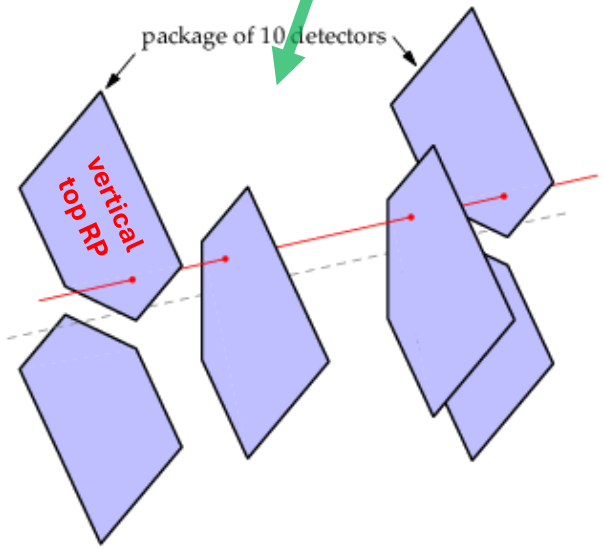

CMS and TOTEM detectors at the LHC

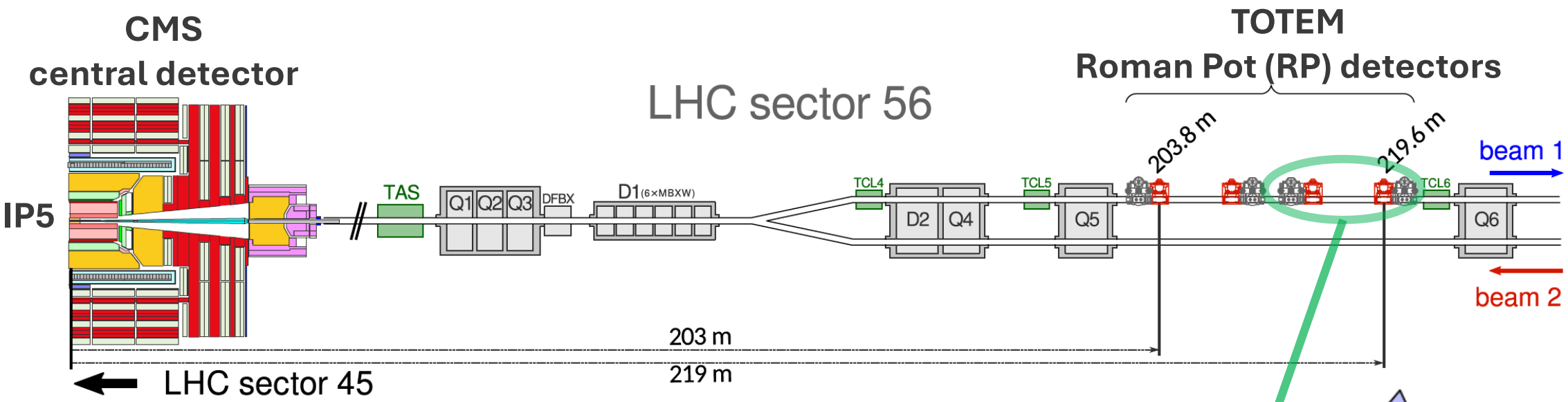

TOTEM RP detectors are located about 200-220 m away from IP5 on **both sides** of CMS

diffractively produced particles are measured by CMS detector; intact protons are measured by TOTEM RP detectors

RPs (equipped with 10 planes of Si strip sensors) approach the beam horizontally or vertically

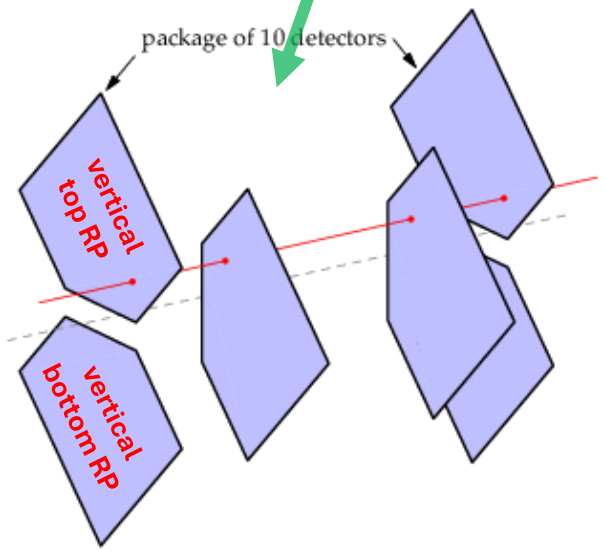

CMS and TOTEM detectors at the LHC

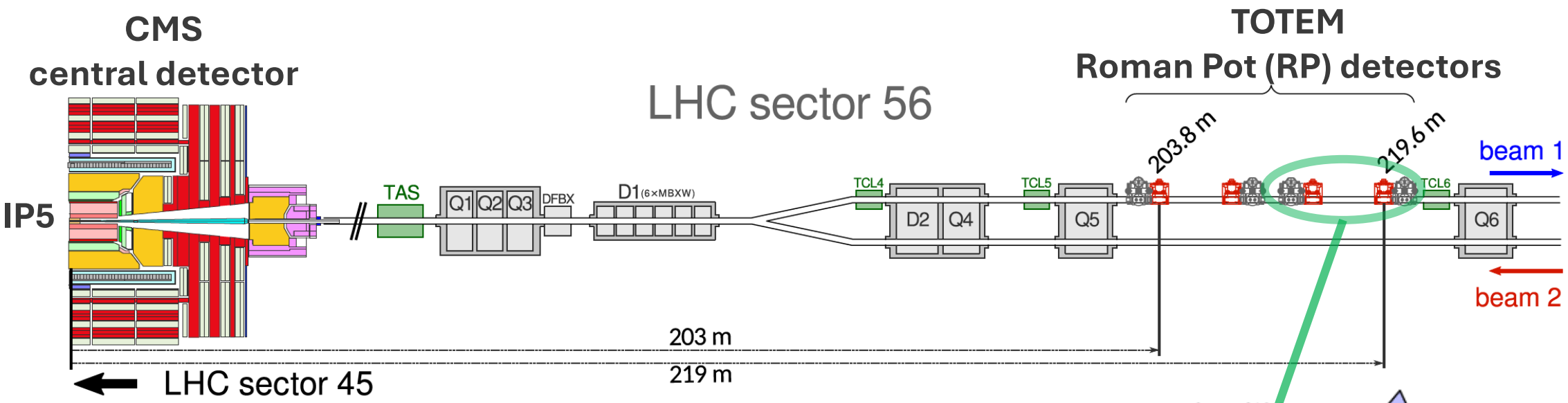

TOTEM RP detectors are located about 200-220 m away from IP5 on **both sides** of CMS

diffractively produced particles are measured by CMS detector; intact protons are measured by TOTEM RP detectors

RPs (equipped with 10 planes of Si strip sensors) approach the beam horizontally or vertically

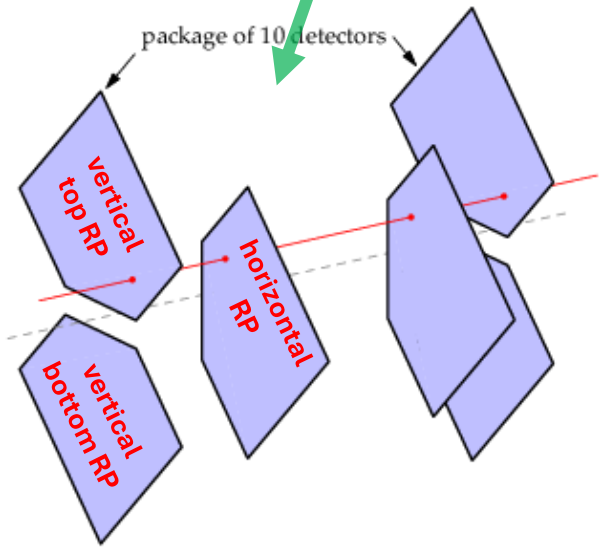

CMS and TOTEM detectors at the LHC

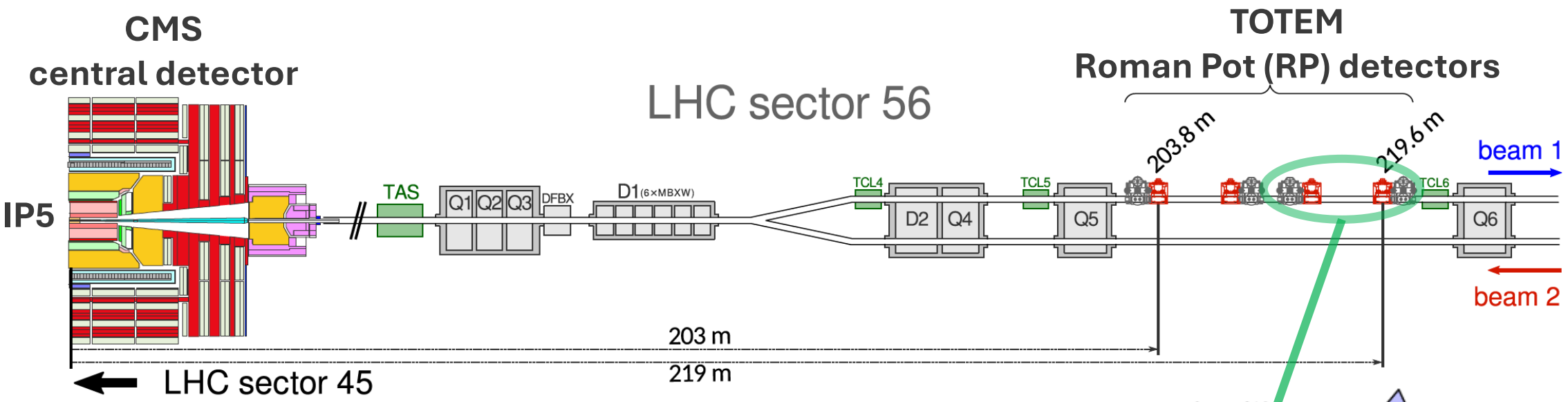

TOTEM RP detectors are located about 200-220 m away from IP5 on **both sides** of CMS

diffractively produced particles are measured by CMS detector; intact protons are measured by TOTEM RP detectors

RPs (equipped with 10 planes of Si strip sensors) approach the beam horizontally or vertically

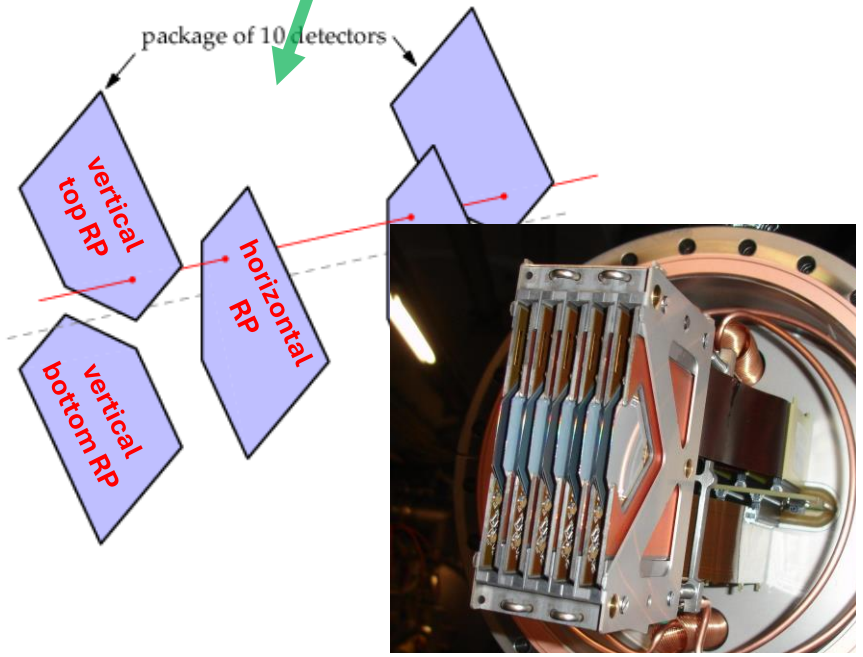

CMS and TOTEM detectors at the LHC

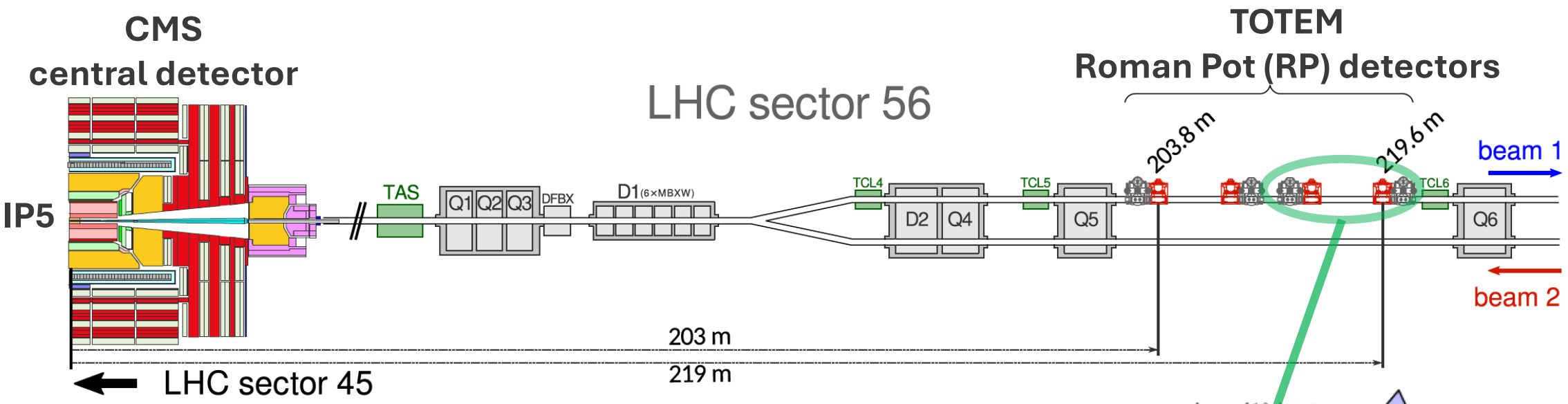

TOTEM RP detectors are located about 200-220 m away from IP5 on **both sides** of CMS

diffractively produced particles are measured by CMS detector; intact protons are measured by TOTEM RP detectors

RPs (equipped with 10 planes of Si strip sensors) approach the beam horizontally or vertically

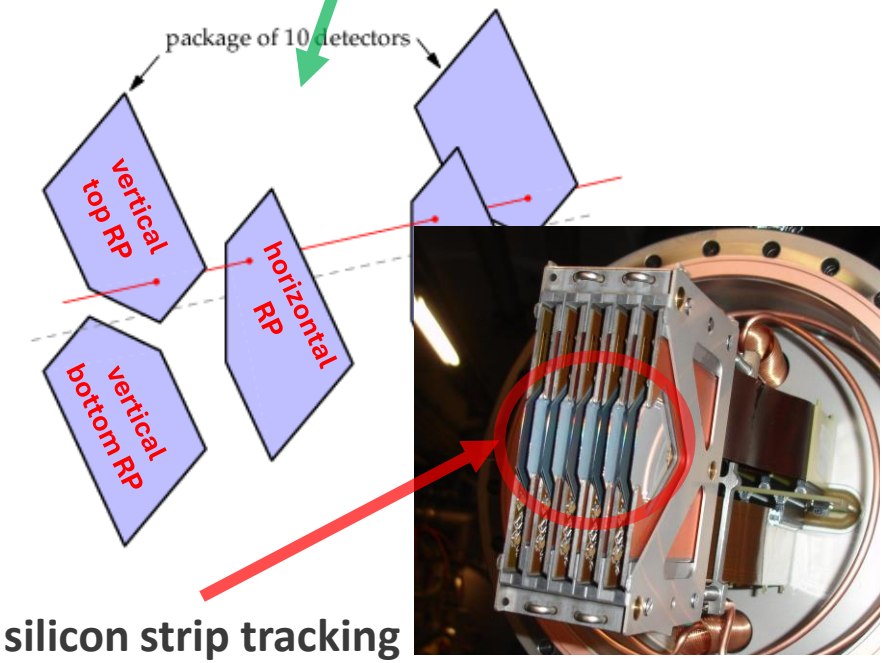

CMS and TOTEM detectors at the LHC

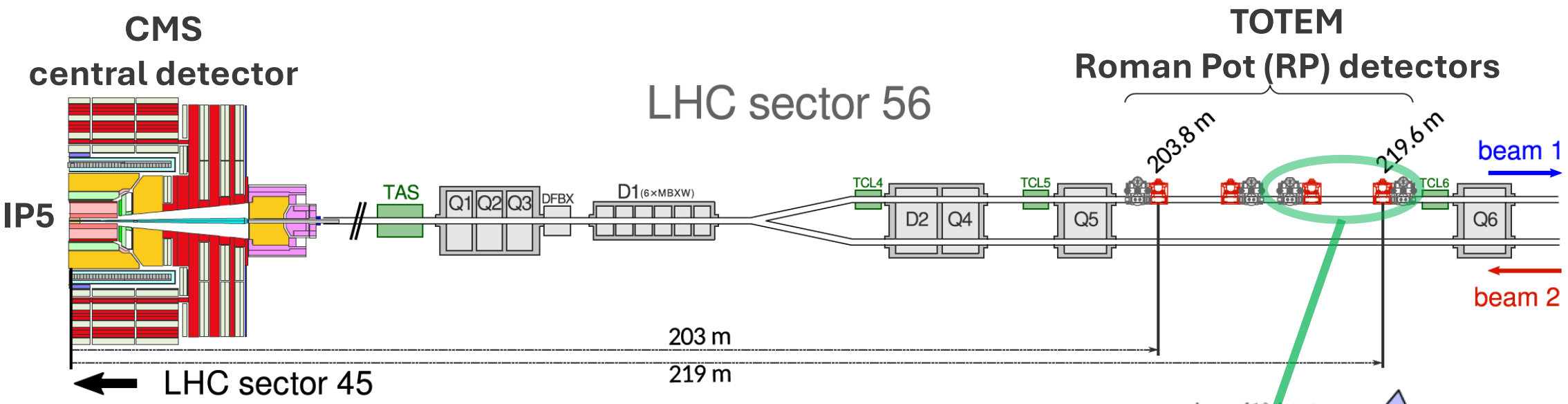

TOTEM RP detectors are located about 200-220 m away from IP5 on **both sides** of CMS

diffractively produced particles are measured by CMS detector; intact protons are measured by TOTEM RP detectors

RPs (equipped with 10 planes of Si strip sensors) approach the beam horizontally or vertically

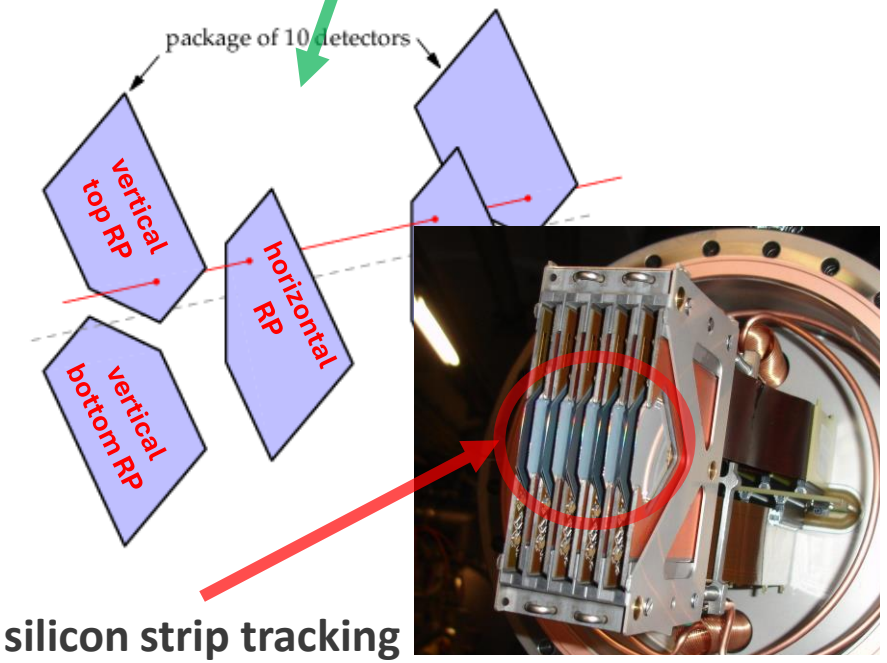

CMS and TOTEM detectors at the LHC

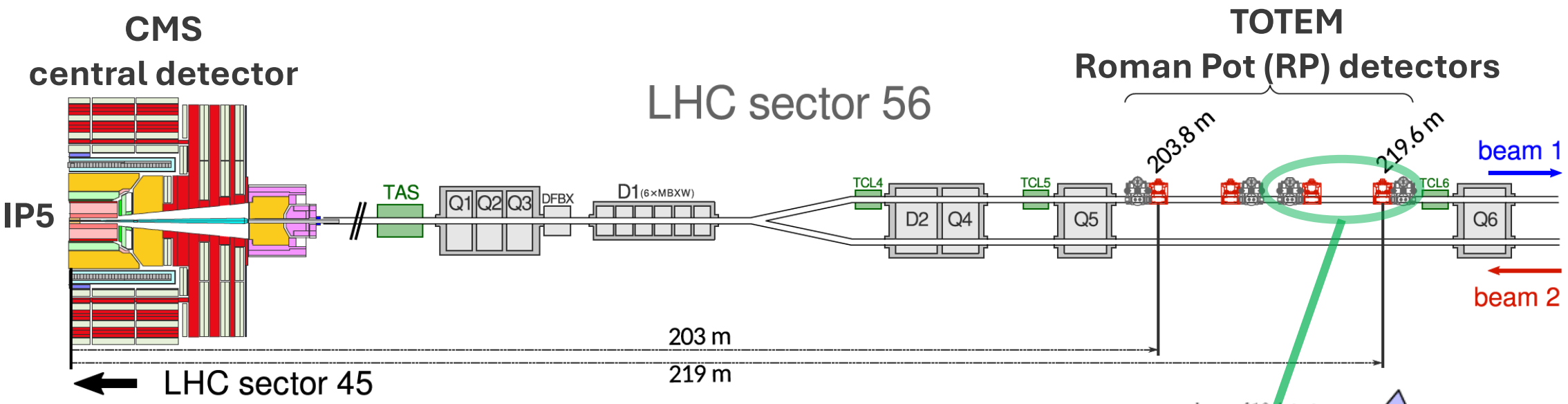

TOTEM RP detectors are located about 200-220 m away from IP5 on **both sides** of CMS

diffractively produced particles are measured by CMS detector; intact protons are measured by TOTEM RP detectors

RPs (equipped with 10 planes of Si strip sensors) approach the beam horizontally or vertically

acceptance down to near zero in fractional momentum loss (ξ) and squared transferred 4-momentum (t)

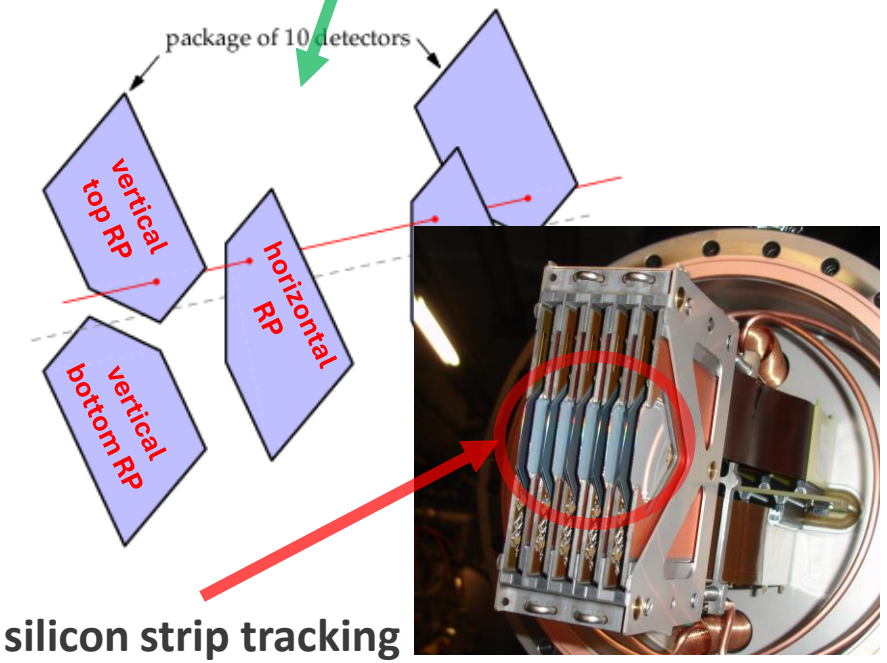

Central exclusive production (CEP) of charged pion pairs

Central exclusive production (CEP) of charged pion pairs

resonant component (Born-level)

Central exclusive production (CEP) of charged pion pairs

resonant component (Born-level)

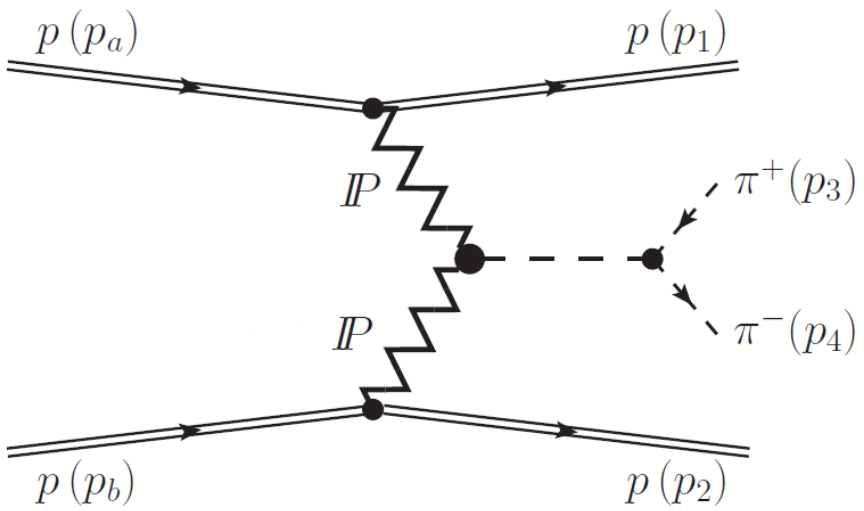

Central exclusive production (CEP) of charged pion pairs

resonant component (Born-level)

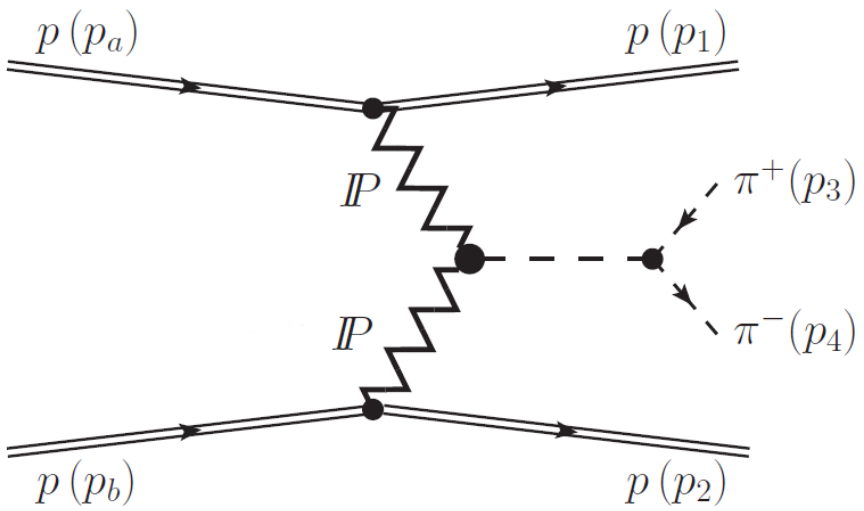

nonresonant continuum component (Born-level)

Central exclusive production (CEP) of charged pion pairs

resonant component (Born-level)

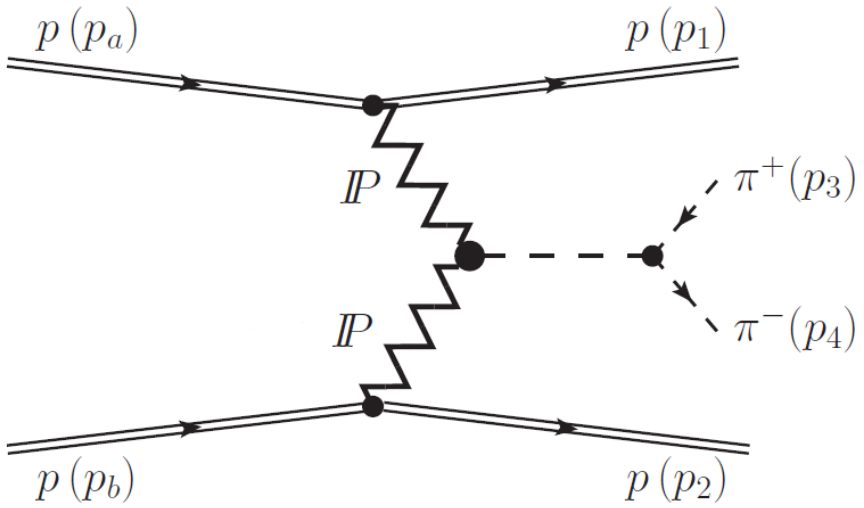

nonresonant continuum component (Born-level)

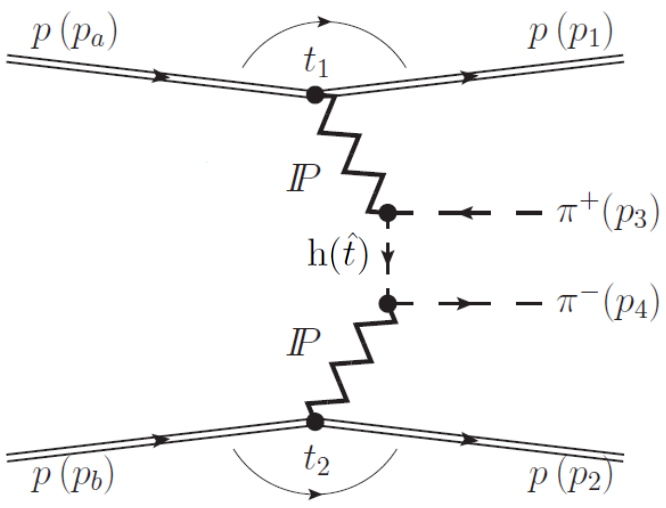

Central exclusive production (CEP) of charged pion pairs

resonant component (Born-level)

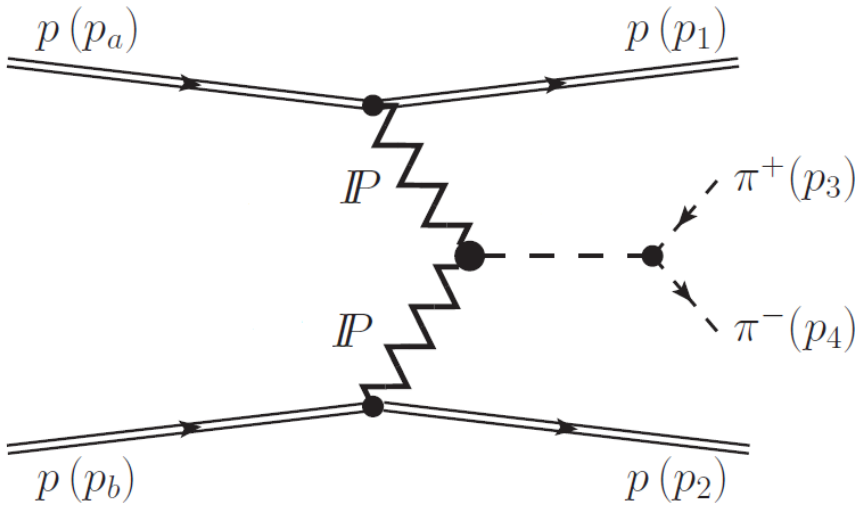

nonresonant continuum component (Born-level)

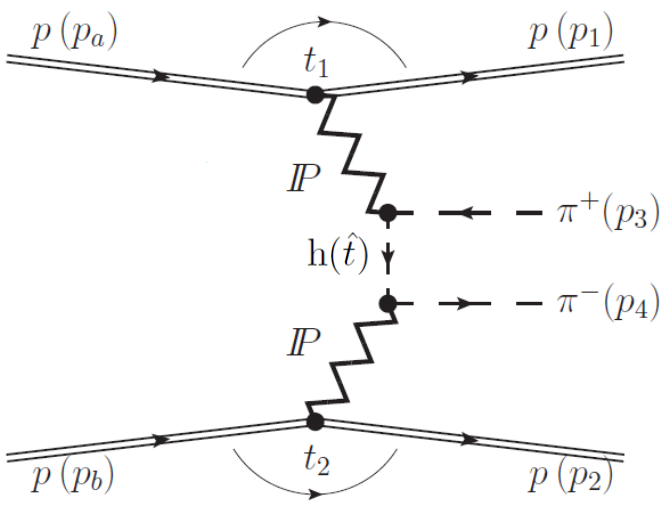

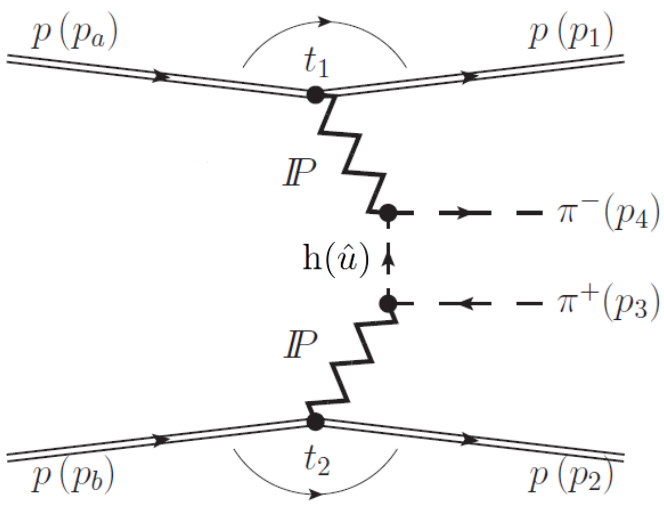

Central exclusive production (CEP) of charged pion pairs

resonant component (Born-level)

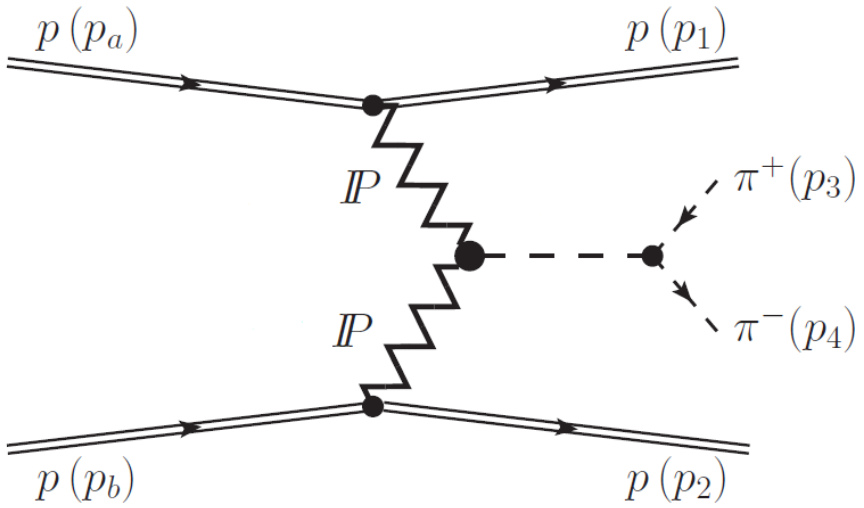

nonresonant continuum component (Born-level)

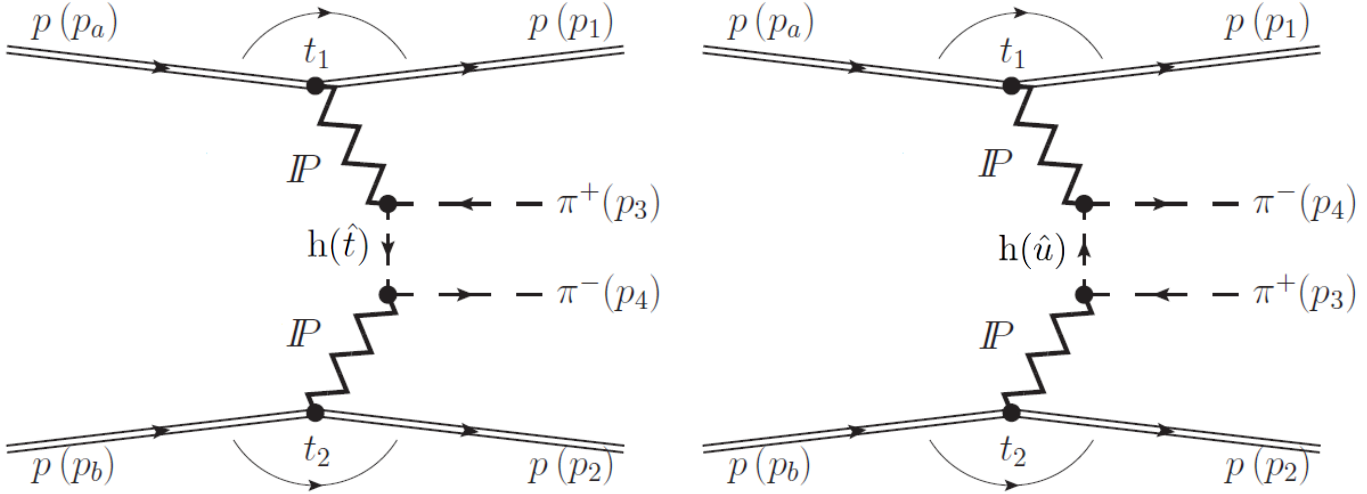

nonresonant continuum production of charged pion pairs
is studied by CMS and TOTEM experiments

in pp collisions at $\sqrt{s}$ = 13 TeV in a special run (β^* = 90m, L_{int} = 4.7 pb^{-1}),
in the resonance-free region: $m_{\pi^+\pi^-} < 0.7$ GeV, $m_{\pi^+\pi^-} > 1.8$ GeV
(scattered proton p_T: 0.2 GeV $< (p_{1,T}, p_{2,T}) <$ 0.8 GeV; pion rapidities: $|y| < 2$)

Central exclusive production (CEP) of charged pion pairs

resonant component (Born-level)

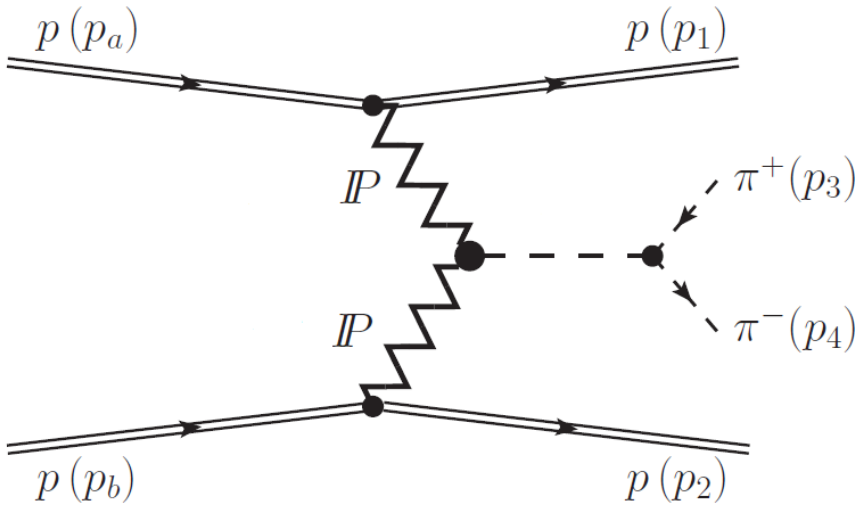

nonresonant continuum component (Born-level)

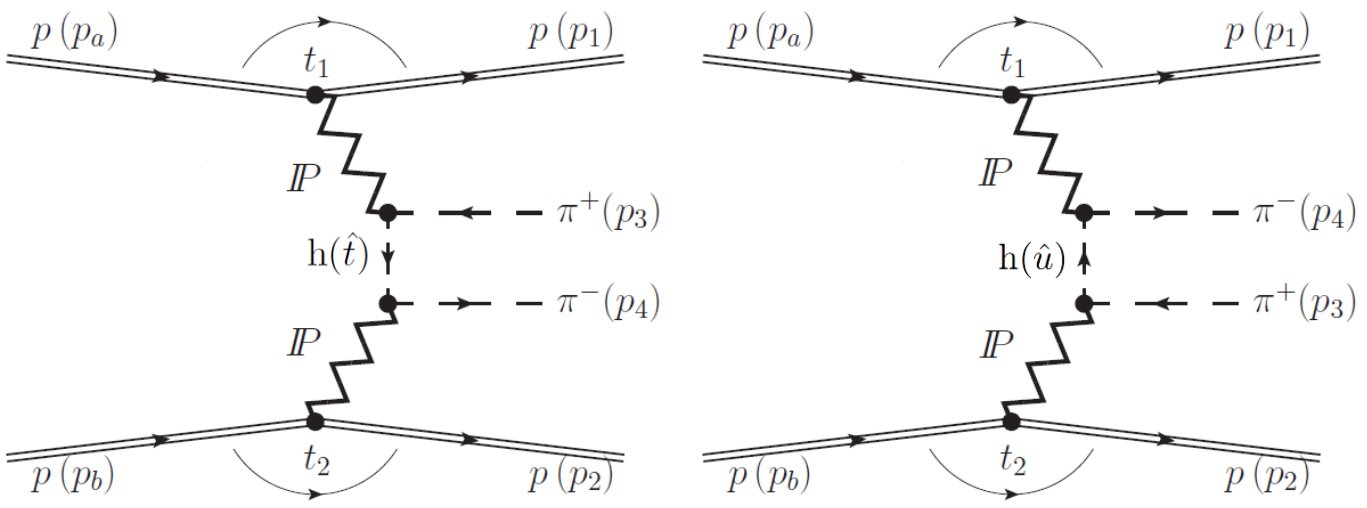

nonresonant continuum production of charged pion pairs
is studied by CMS and TOTEM experiments
in pp collisions at $\sqrt{s}$ = 13 TeV in a special run (β^* = 90m, L_{int} = 4.7 pb^{-1}),
in the resonance-free region: $m_{\pi^+\pi^-} < 0.7$ GeV, $m_{\pi^+\pi^-} > 1.8$ GeV
(scattered proton p_T: 0.2 GeV $< (p_{1,T}, p_{2,T}) <$ 0.8 GeV; pion rapidities: $|y| < 2$)

Phys. Rev. D **109** (2024) 112013

Central exclusive $\pi^+\pi^-$ production event classification

Central exclusive $\pi^+\pi^-$ production event classification

very clean pp → pππp **events:**
2 pions measured in CMS
and 2 protons measured in TOTEM

Central exclusive $\pi^+\pi^-$ production event classification

very clean pp → pππp **events:**
2 pions measured in CMS
and 2 protons measured in TOTEM

main background:
elastic and inelastic pileup

Central exclusive $\pi^+\pi^-$ production event classification

very clean pp → pππp **events:**
2 pions measured in CMS
and 2 protons measured in TOTEM

main background:
elastic and inelastic pileup

background removal is based on momentum conservation in the transverse plane

Central exclusive $\pi^+\pi^-$ production event classification

very clean pp → pππp **events:**
2 pions measured in CMS
and 2 protons measured in TOTEM

main background:
elastic and inelastic pileup

background removal is based on momentum conservation in the transverse plane

the sum of $\mathbf{p_{Tx,y}}$ of the two protons

$$\sum_{2} p_{x,y}$$

Central exclusive $\pi^+\pi^-$ production event classification

very clean pp → pππp **events:**
2 pions measured in CMS
and 2 protons measured in TOTEM

main background:
elastic and inelastic pileup

background removal is based on momentum conservation in the transverse plane

the sum of $\mathbf{p_{Tx,y}}$ of the two protons

$$\sum_{2} p_{x,y}$$

vs.

Central exclusive $\pi^+\pi^-$ production event classification

very clean pp → pππp **events:**
2 pions measured in CMS
and 2 protons measured in TOTEM

main background:
elastic and inelastic pileup

background removal is based on momentum conservation in the transverse plane

the sum of $\mathbf{p_{Tx,y}}$ of the two protons

$$\sum_{2} p_{x,y}$$

vs.

the sum of $\mathbf{p_{Tx,y}}$ of the two protons and the two pions

$$\sum_{4} p_{x,y}$$

Central exclusive $\pi^+\pi^-$ production event classification

very clean pp → pππp **events:**
2 pions measured in CMS
and 2 protons measured in TOTEM

main background:
elastic and inelastic pileup

background removal is based on momentum conservation in the transverse plane

the sum of $\mathbf{p_{Tx,y}}$ of the two protons

$$\sum_{2} p_{x,y}$$

vs.

the sum of $\mathbf{p_{Tx,y}}$ of the two protons and the two pions

$$\sum_{4} p_{x,y}$$

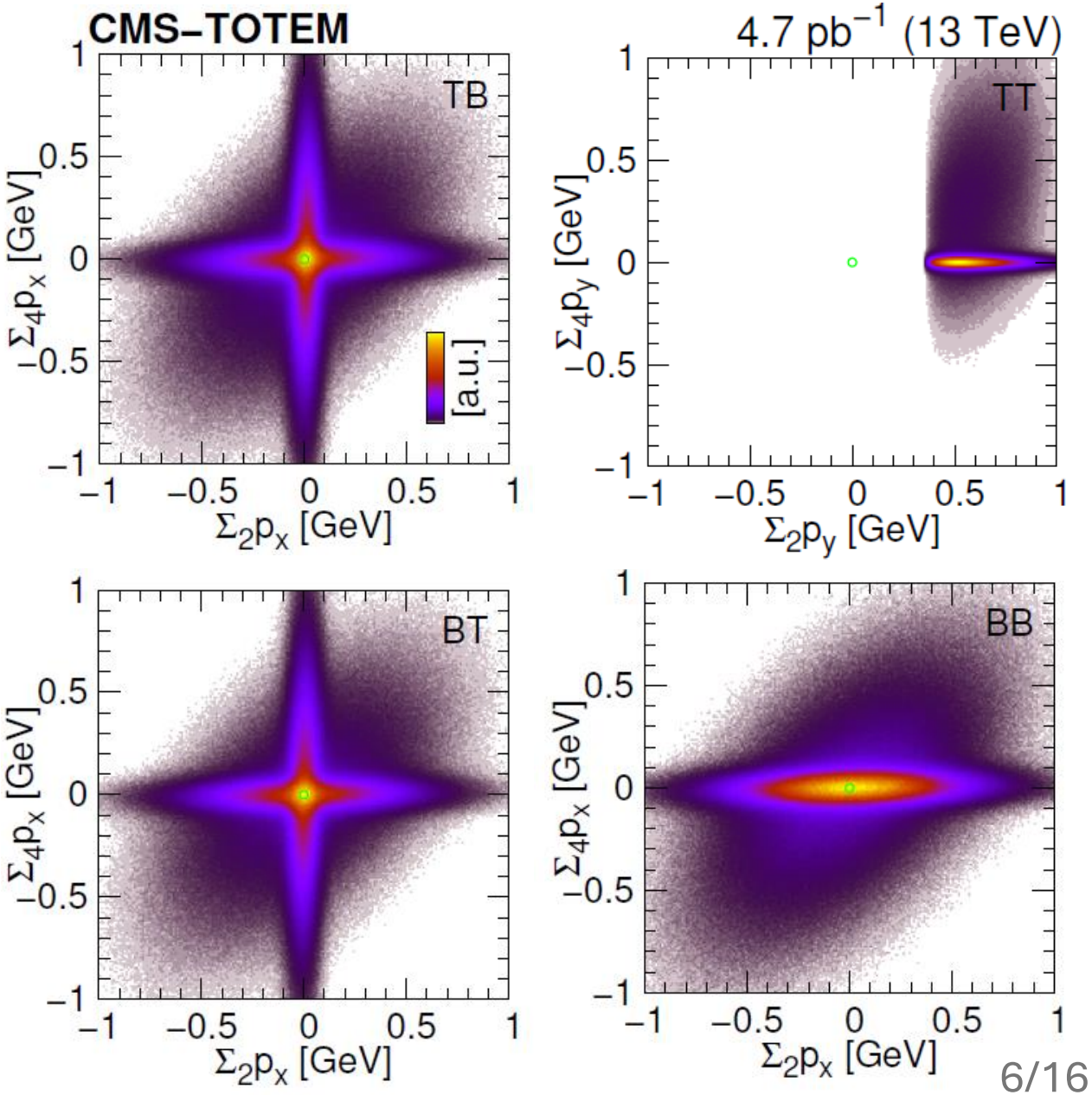

Central exclusive $\pi^+\pi^-$ production event classification

very clean pp → pππp **events:**
2 pions measured in CMS
and 2 protons measured in TOTEM

main background:
elastic and inelastic pileup

background removal is based on momentum conservation in the transverse plane

the sum of $p_{Tx,y}$ of the two protons

$$\sum_{2} p_{x,y}$$

vs.

the sum of $p_{Tx,y}$ of the two protons and the two pions

$$\sum_{4} p_{x,y}$$

for exclusive events: $\sum_4 p_{x,y} \sim 0$

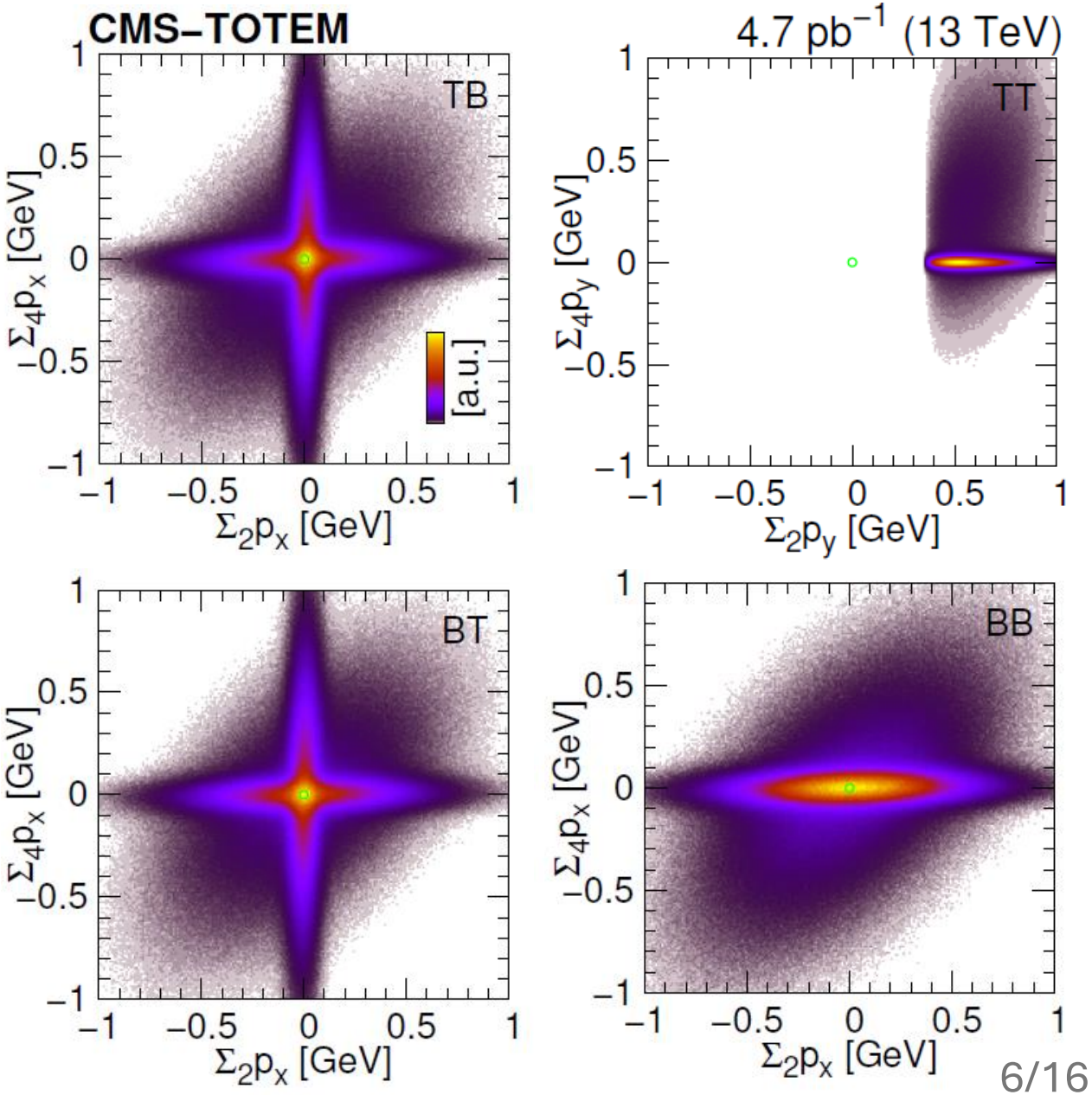

Central exclusive $\pi^+\pi^-$ production event classification

very clean pp → pππp **events:**
2 pions measured in CMS
and 2 protons measured in TOTEM

main background:
elastic and inelastic pileup

background removal is based on momentum conservation in the transverse plane

the sum of $p_{Tx,y}$ of the two protons

$$\sum_{2} p_{x,y}$$

vs.

the sum of $p_{Tx,y}$ of the two protons and the two pions

$$\sum_{4} p_{x,y}$$

for exclusive events: $\sum_4 p_{x,y} \sim 0$

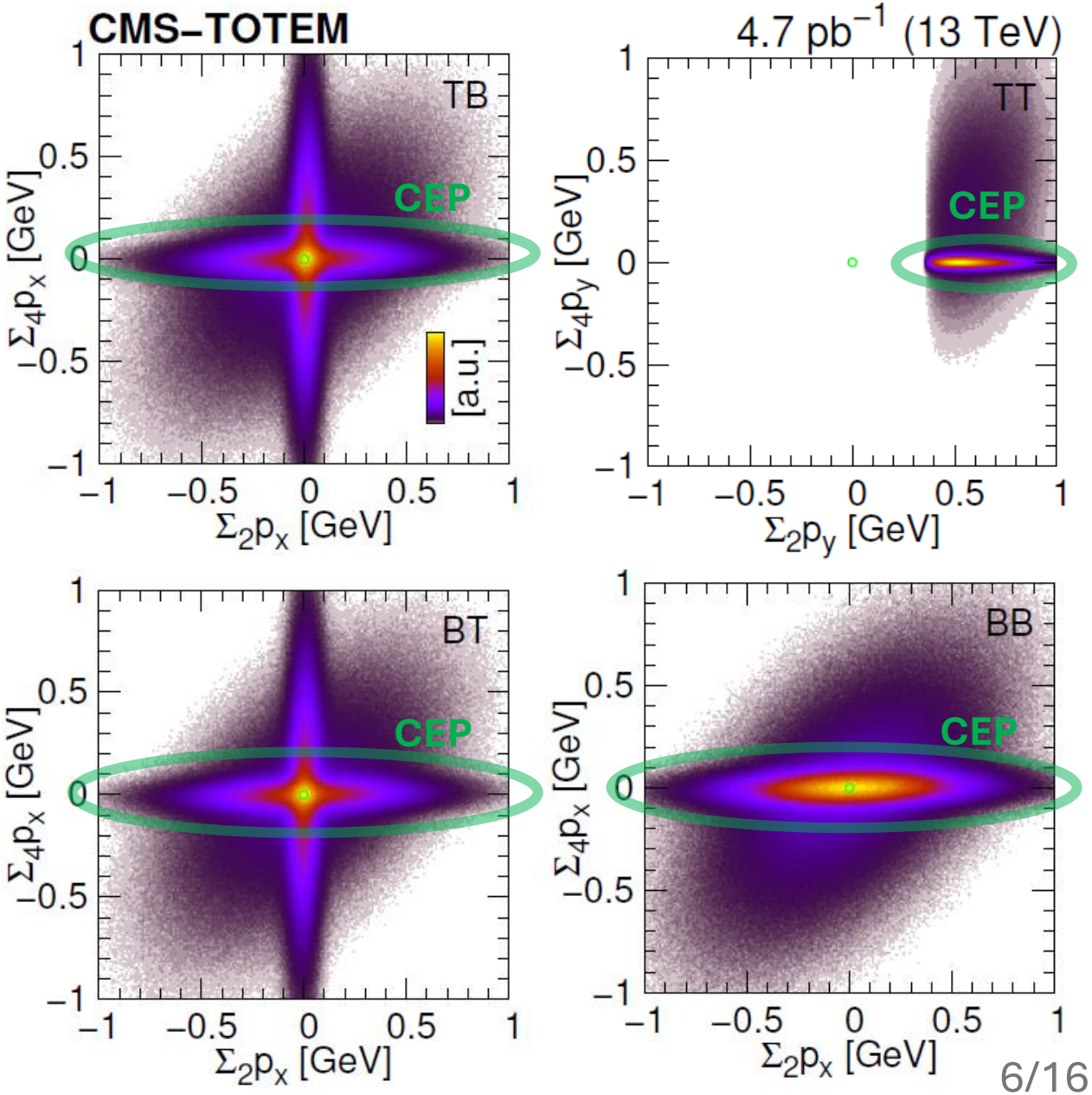

Central exclusive $\pi^+\pi^-$ production event classification

very clean pp → pππp **events:**
2 pions measured in CMS
and 2 protons measured in TOTEM

main background:
elastic and inelastic pileup

background removal is based on momentum conservation in the transverse plane

the sum of $p_{Tx,y}$ of the two protons

$$\sum_{2} p_{x,y}$$

vs.

the sum of $p_{Tx,y}$ of the two protons and the two pions

$$\sum_{4} p_{x,y}$$

for exclusive events: $\sum_4 p_{x,y} \sim 0$

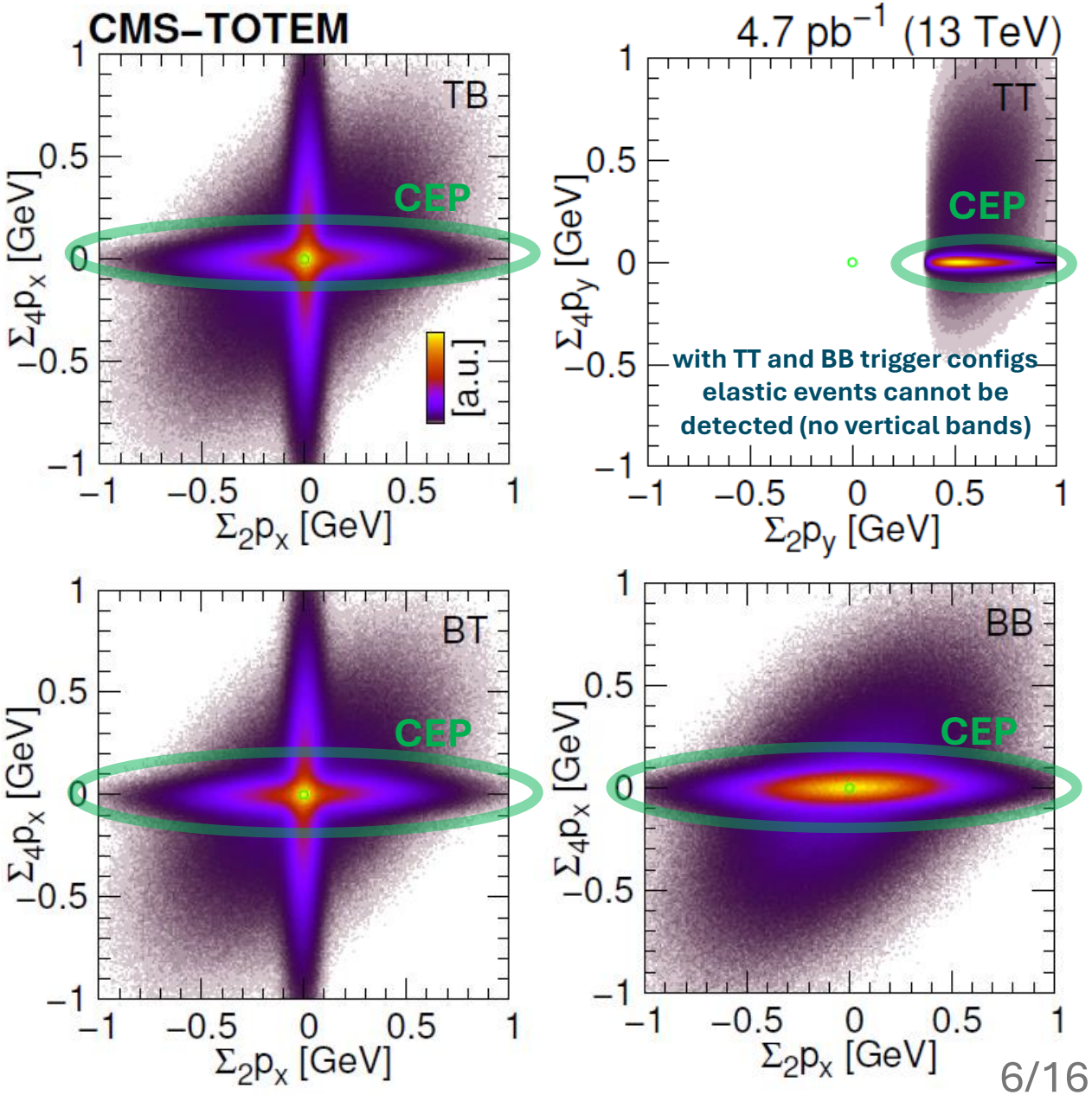

Results, $\mathrm{d}^3\sigma/\mathrm{d}p_{1,\mathrm{T}}\,\mathrm{d}p_{2,\mathrm{T}}\,\mathrm{d}\phi$

Results, $d^3\sigma/dp_{1,T}\,dp_{2,T}\,d\phi$

studied variables:

$p_{1,T}$ and $p_{2,T}$, the transverse momenta of final state protons;

ϕ, the azimuthal angle between the scattered protons;

m, the invariant mass of the pion pair;

$\max(t, u)$ squared four momentum of the virtual meson

Results, $d^3\sigma/dp_{1,T}\,dp_{2,T}\,d\phi$

studied variables:

$p_{1,T}$ and $p_{2,T}$, the transverse momenta of final state protons;

ϕ, the azimuthal angle between the scattered protons;

m, the invariant mass of the pion pair;

$\max(t, u)$ squared four momentum of the virtual meson

triple differential cross sections:

in ranges of $p_{1,T}$ and $p_{2,T}$, distributions of ϕ, m, and $\max(t, u)$

Results, $d^3\sigma/dp_{1,T}\,dp_{2,T}\,d\phi$

studied variables:

$p_{1,T}$ and $p_{2,T}$, the transverse momenta of final state protons;

ϕ, the azimuthal angle between the scattered protons;

m, the invariant mass of the pion pair;

$\max(t, u)$ squared four momentum of the virtual meson

triple differential cross sections:

in ranges of $p_{1,T}$ and $p_{2,T}$, distributions of ϕ, m, and $\max(t, u)$

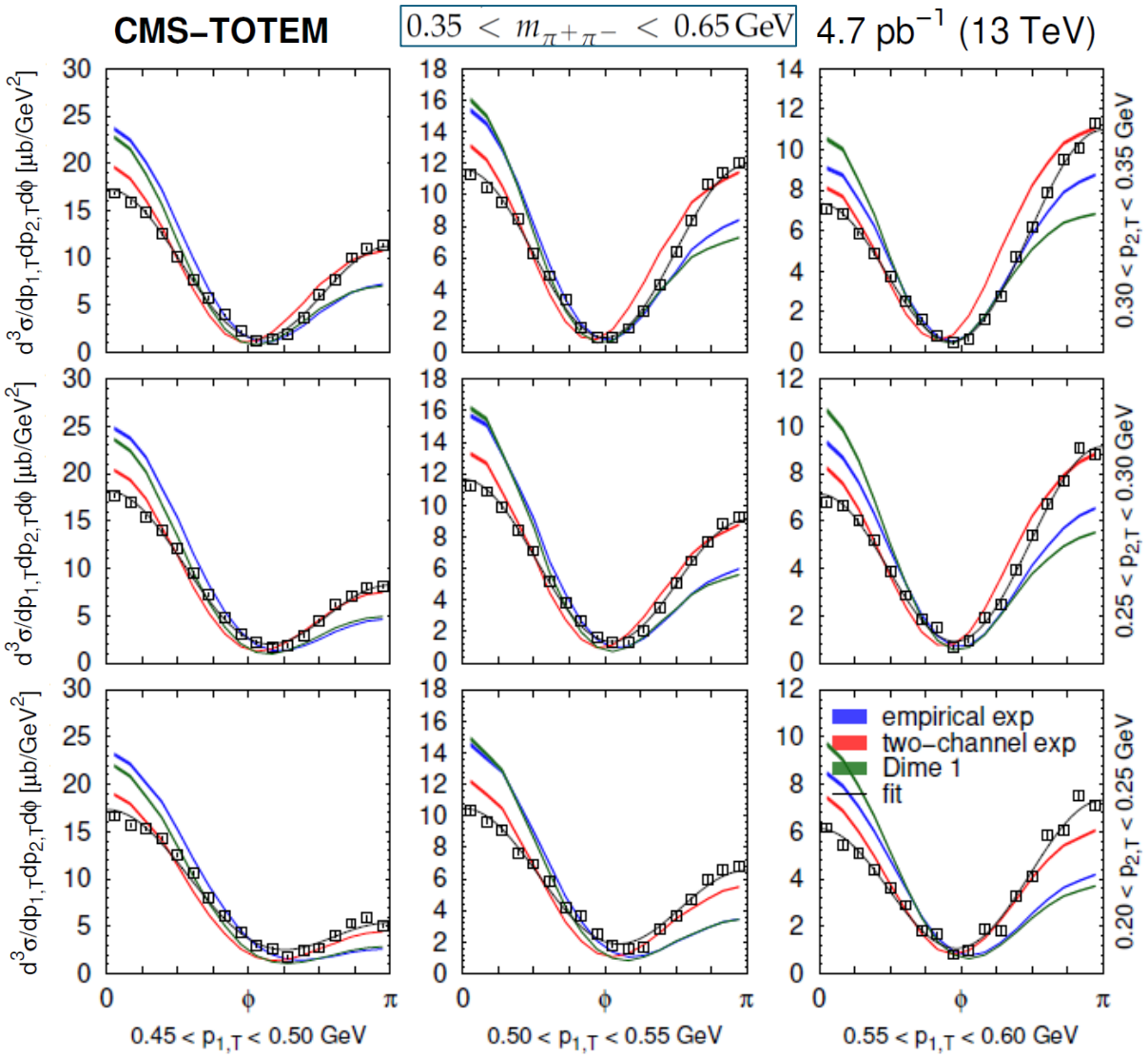

Results, $d^3\sigma/dp_{1,T}\,dp_{2,T}\,d\phi$

studied variables:

$p_{1,T}$ and $p_{2,T}$, the transverse momenta of final state protons;

ϕ, the azimuthal angle between the scattered protons;

m, the invariant mass of the pion pair;

$\max(t, u)$ squared four momentum of the virtual meson

triple differential cross sections:

in ranges of $p_{1,T}$ and $p_{2,T}$, distributions of ϕ, m, and $\max(t, u)$

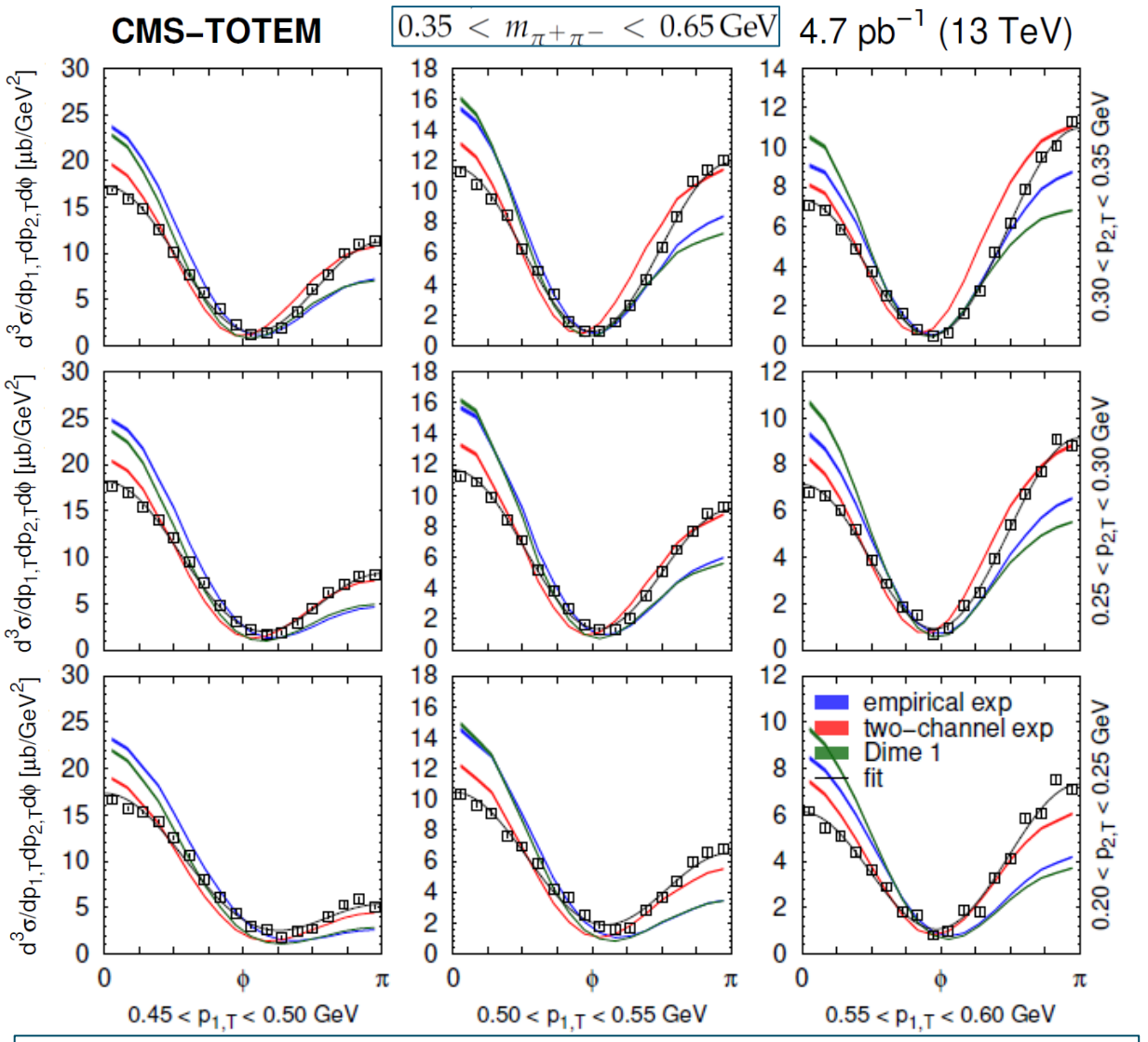

models after tuning give better descriptions but still need for further theoretical developments

Results, $d^3\sigma/dp_{1,T}\,dp_{2,T}\,d\phi$

studied variables:

$p_{1,T}$ and $p_{2,T}$, the transverse momenta of final state protons;

ϕ, the azimuthal angle between the scattered protons;

m, the invariant mass of the pion pair;

$\max(t, u)$ squared four momentum of the virtual meson

triple differential cross sections:

in ranges of $p_{1,T}$ and $p_{2,T}$, distributions of ϕ, m, and $\max(t, u)$

a parabolic minimum in the distribution of ϕ is observed for the first time

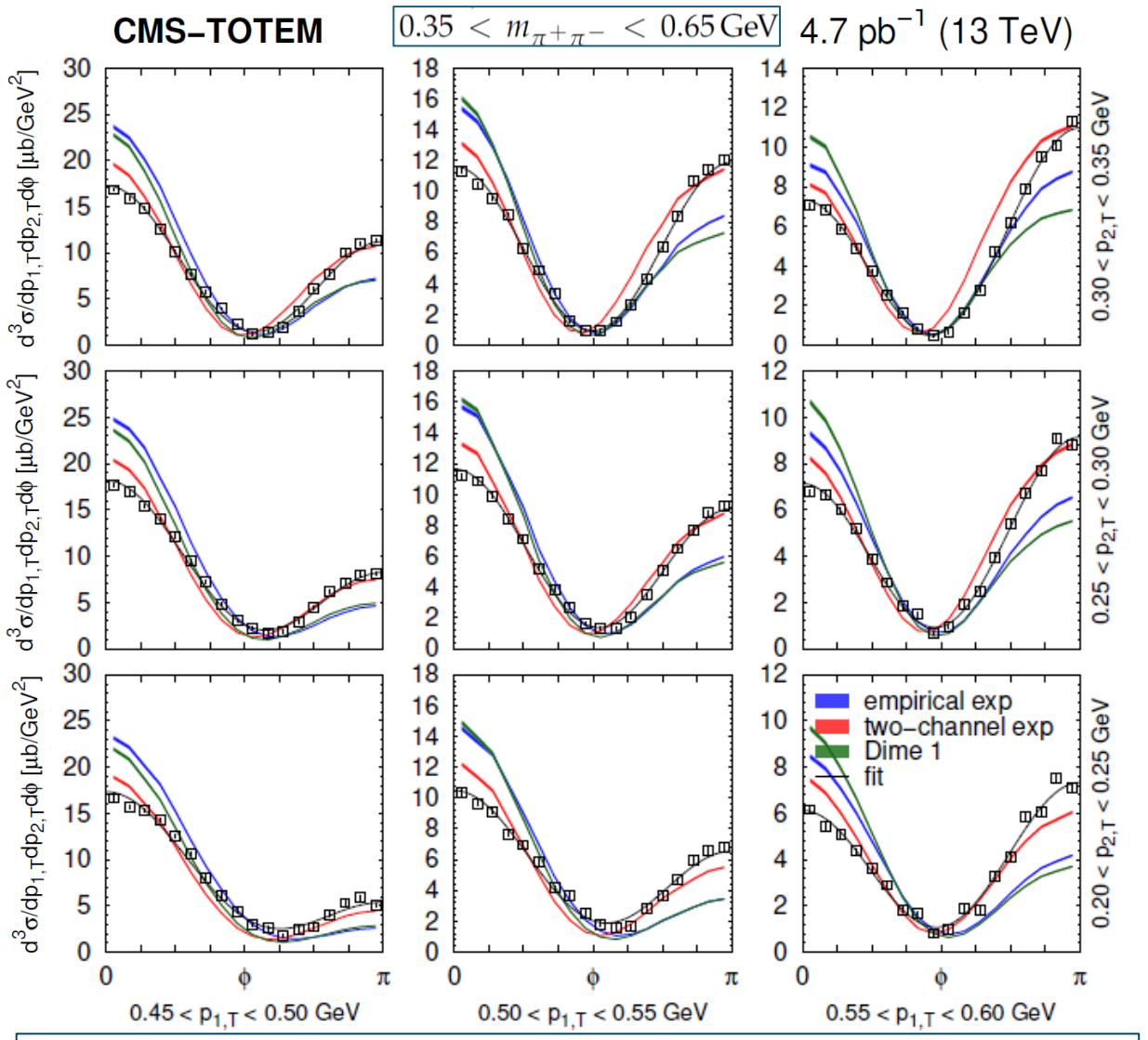

models after tuning give better descriptions but still need for further theoretical developments

Results, $d^3\sigma/dp_{1,T}\,dp_{2,T}\,d\phi$

studied variables:

$p_{1,T}$ and $p_{2,T}$, the transverse momenta of final state protons;

ϕ, the azimuthal angle between the scattered protons;

m, the invariant mass of the pion pair;

$\max(t, u)$ squared four momentum of the virtual meson

triple differential cross sections:

in ranges of $p_{1,T}$ and $p_{2,T}$, distributions of ϕ, m, and $\max(t, u)$

a parabolic minimum in the distribution of ϕ is observed for the first time

the minimum can be interpreted as an effect due to rescattering (absorption) corrections

Harland-Lang, Khoze, Ryskin, Eur. Phys. J. C 74 (2014) 2848

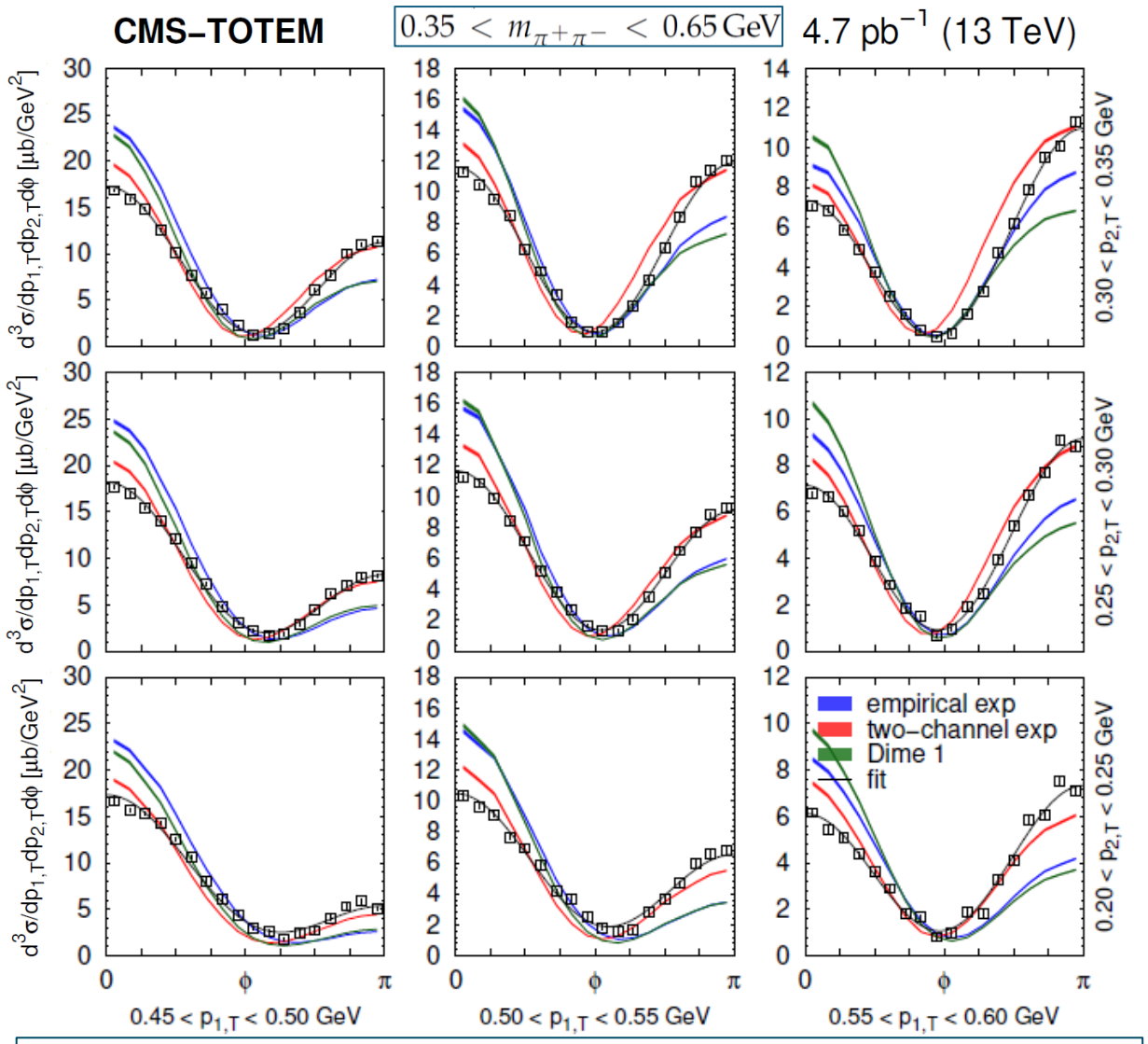

models after tuning give better descriptions but still need for further theoretical developments

$d^3\sigma/dp_{1,T}\,dp_{2,T}\,dm$ and $d^3\sigma/dp_{1,T}\,dp_{2,T}\,d\max(t,u)$

$d^3\sigma/dp_{1,T}\,dp_{2,T}\,dm$ and $d^3\sigma/dp_{1,T}\,dp_{2,T}\,dmax(t,u)$

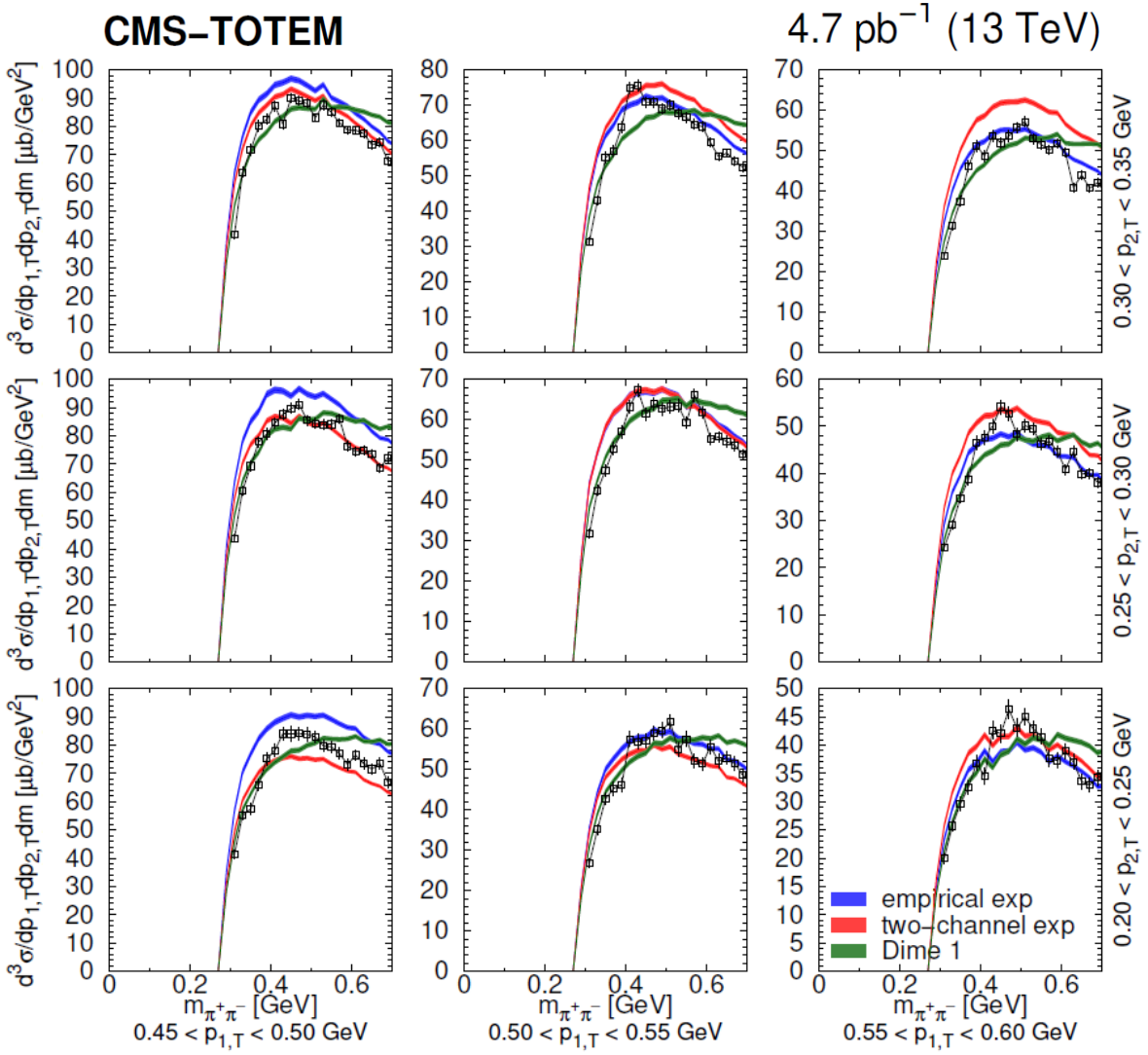

$d^3\sigma/dp_{1,T}\,dp_{2,T}\,dm$ and $d^3\sigma/dp_{1,T}\,dp_{2,T}\,dmax(t,u)$

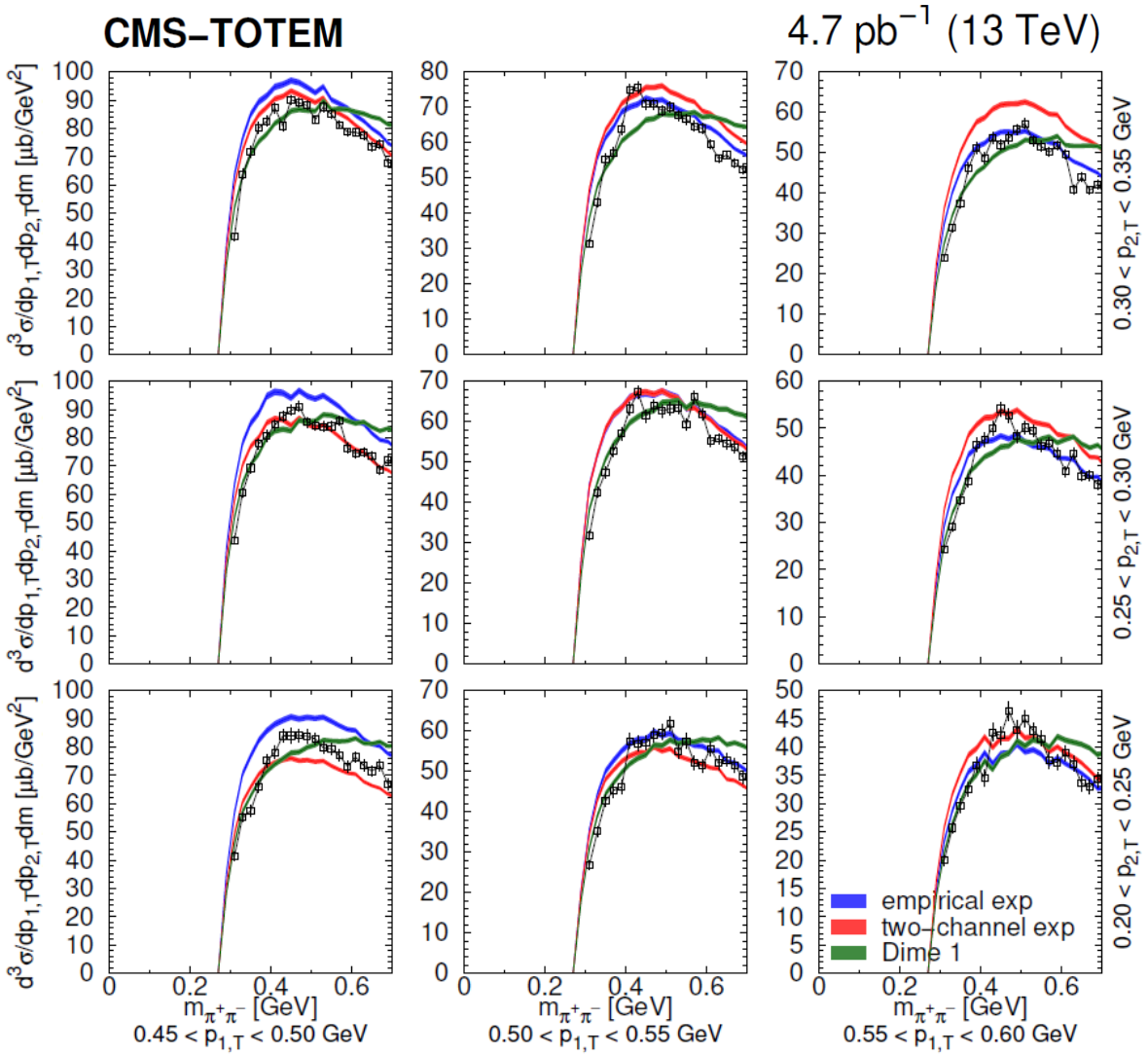

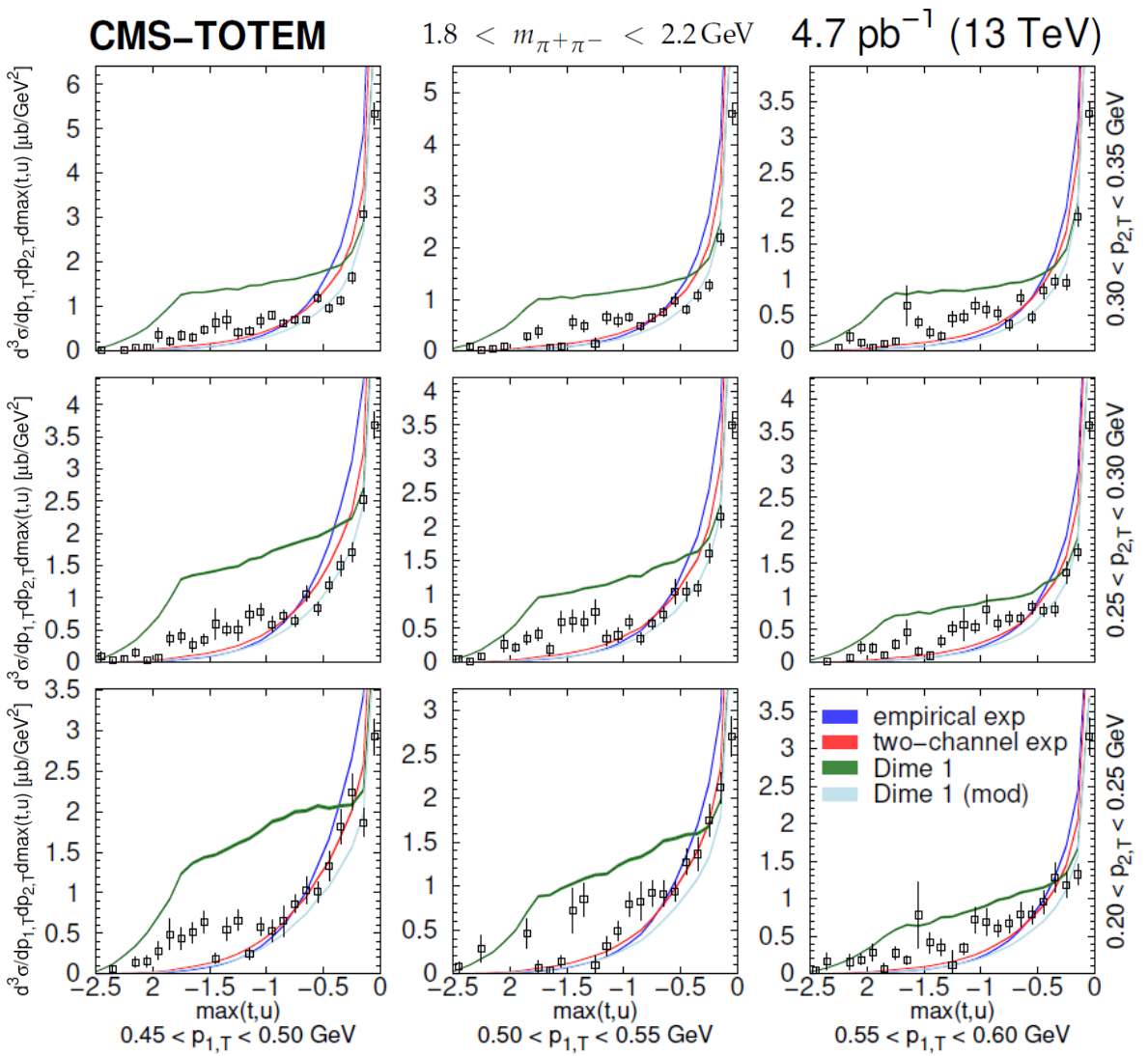

$d^3\sigma/dp_{1,T}\,dp_{2,T}\,dm$ and $d^3\sigma/dp_{1,T}\,dp_{2,T}\,dmax(t,u)$

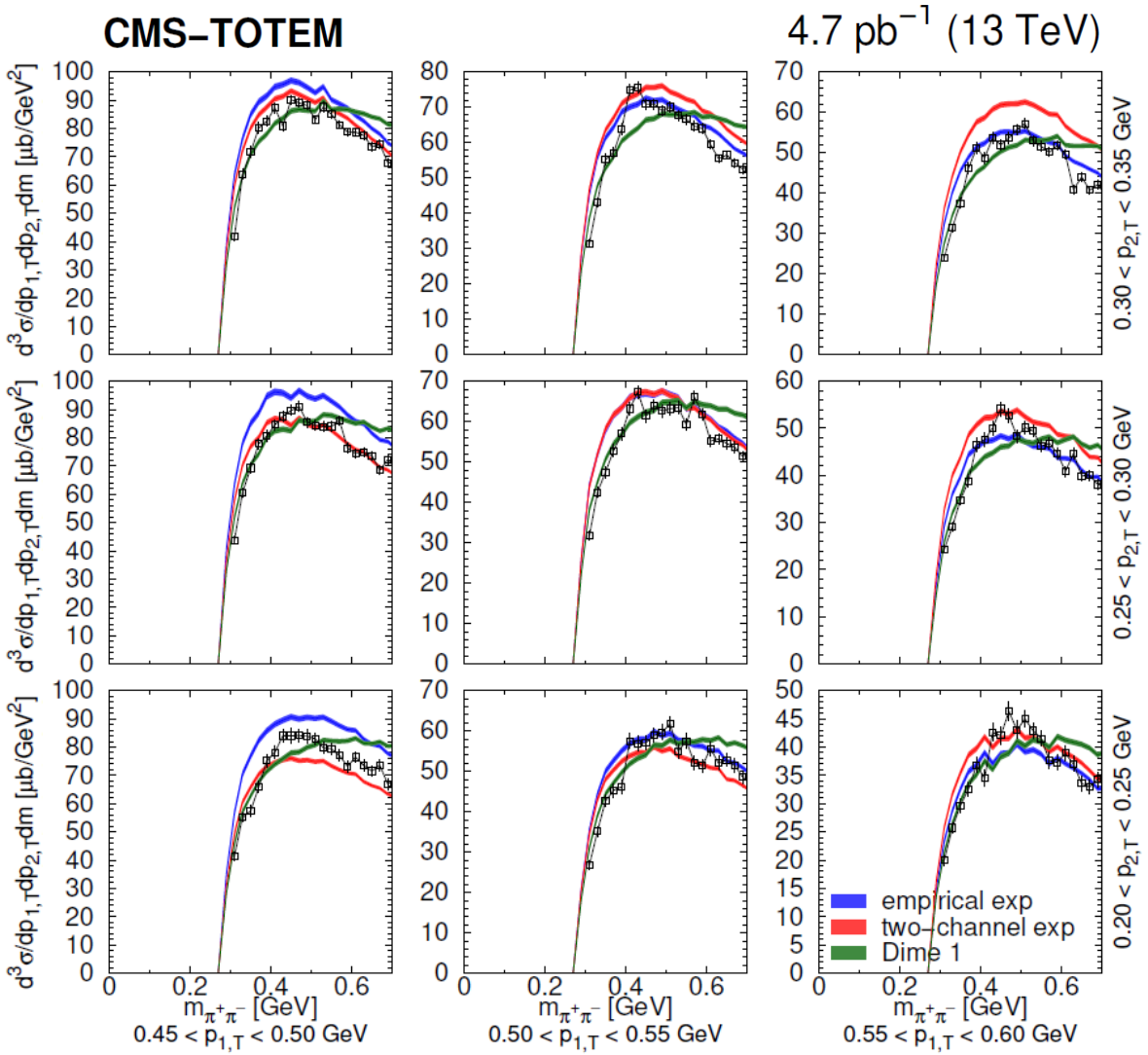

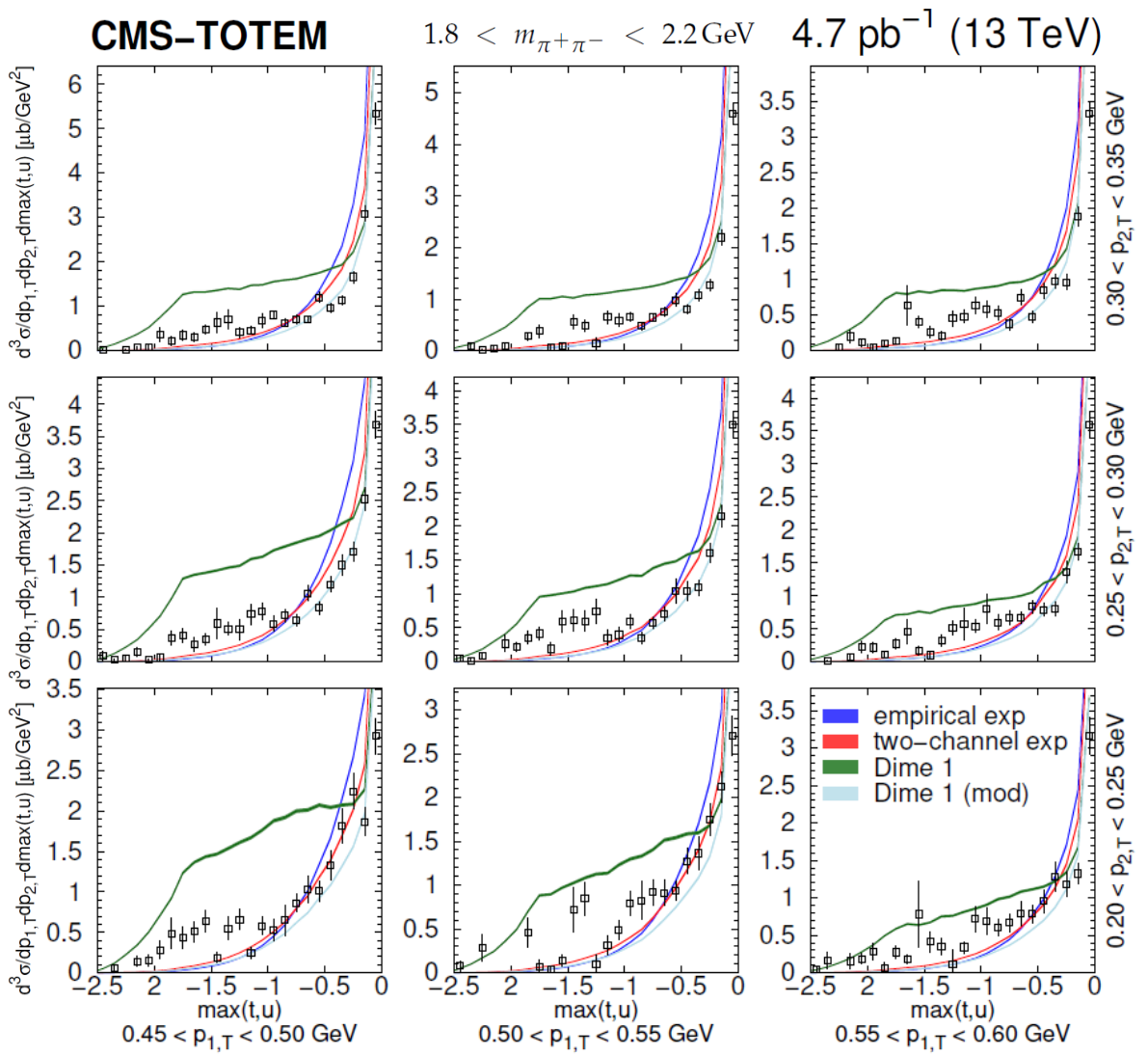

based on the measured distributions, models are tuned and various physical parameters related to pomeron physics are determined

Dijet events with hard color-singlet exchange

Dijet events with hard color-singlet exchange

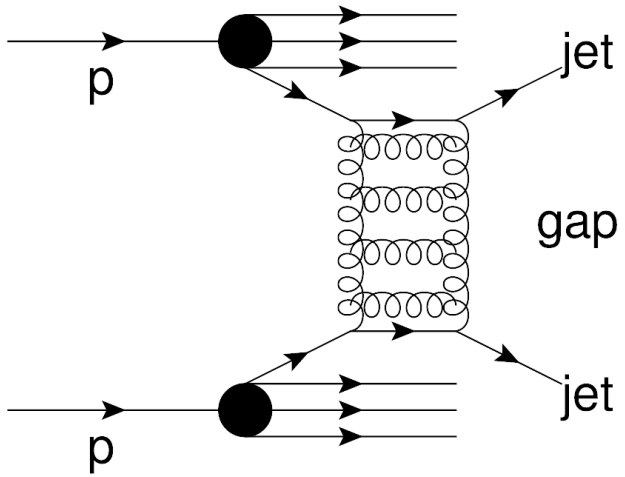

jet-gap-jet event
by hard color-singlet exchange

Dijet events with hard color-singlet exchange

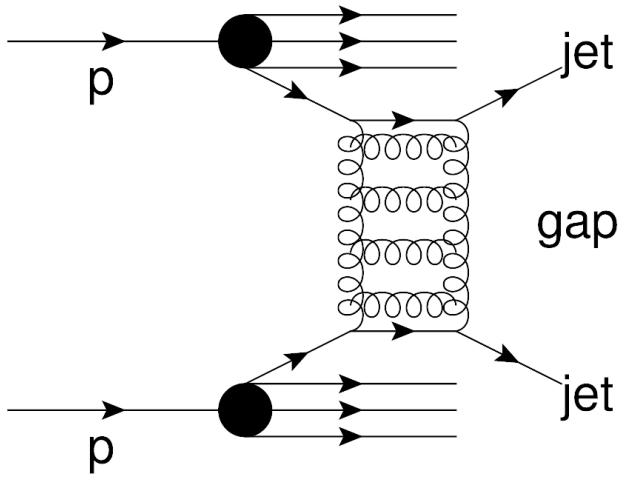

jet-gap-jet event
by hard color-singlet exchange

devoid of particle activity between the final-state jets due to **BFKL pomeron exchange**

Dijet events with hard color-singlet exchange

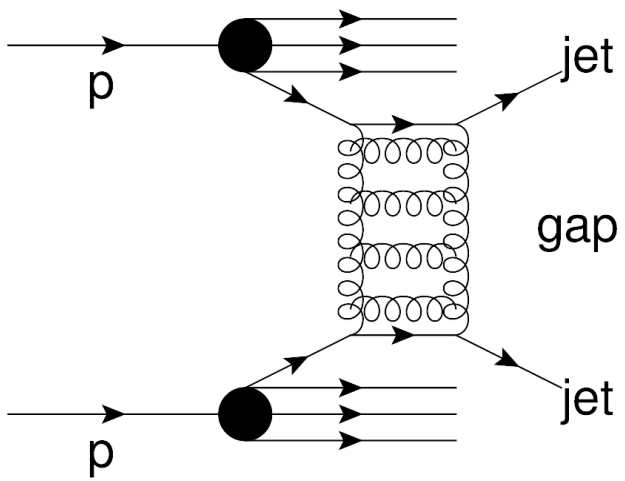

jet-gap-jet event
by hard color-singlet exchange

devoid of particle activity between the final-state jets due to **BFKL pomeron exchange**

tool to study BFKL dynamics

Dijet events with hard color-singlet exchange

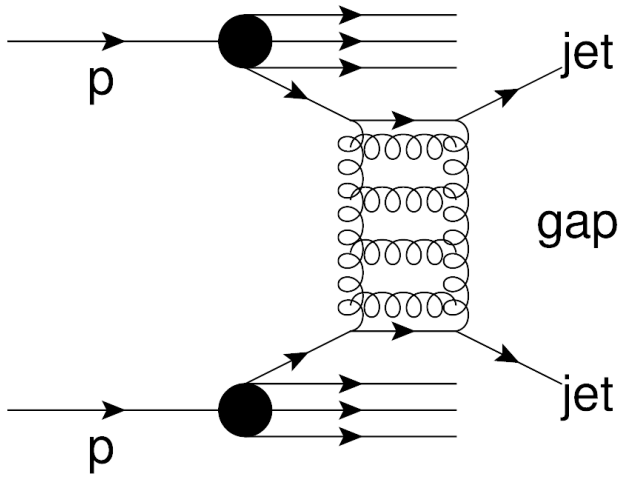

jet-gap-jet event
by hard color-singlet exchange

devoid of particle activity between the final-state jets due to **BFKL pomeron exchange**

tool to study BFKL dynamics

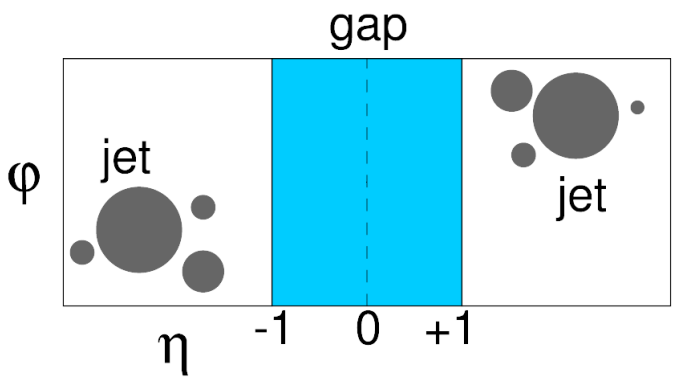

jet-gap-jet event signature in the φ-η plane

measured by CMS

Dijet events with hard color-singlet exchange

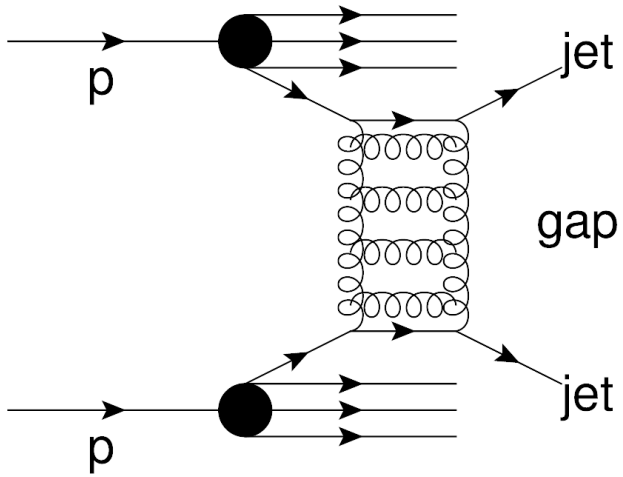

jet-gap-jet event
by hard color-singlet exchange

devoid of particle activity between the final-state jets due to **BFKL pomeron exchange**

tool to study BFKL dynamics

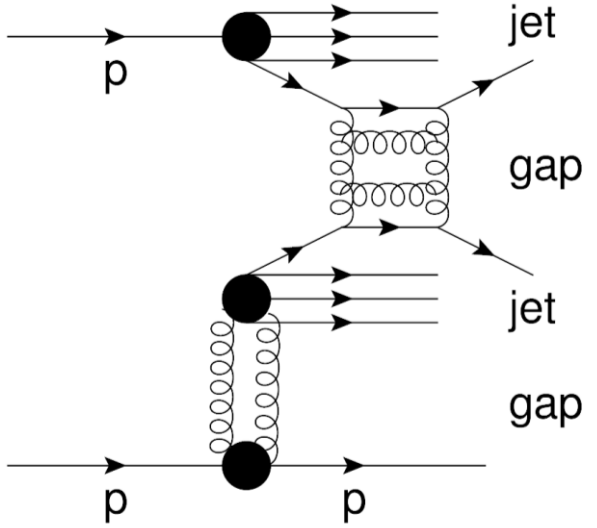

jet-gap-jet with intact proton event
by hard color-singlet exchange

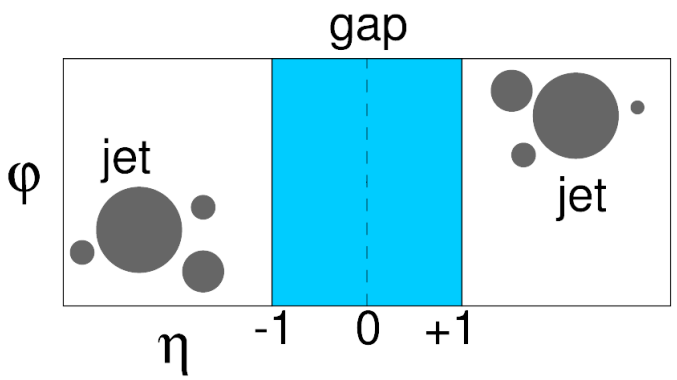

jet-gap-jet event signature in the
φ-η plane

measured by CMS

Dijet events with hard color-singlet exchange

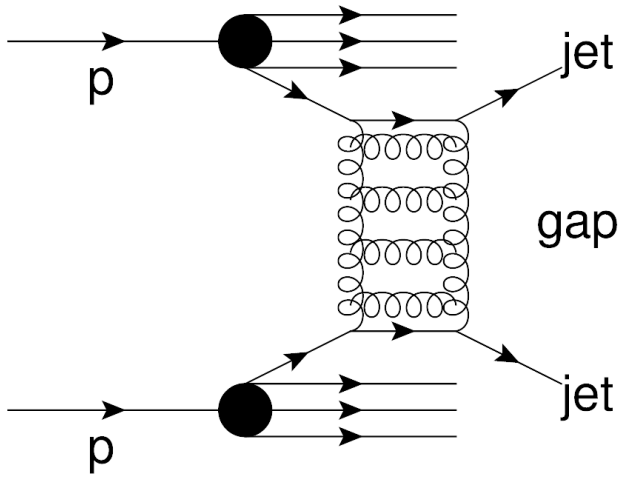

jet-gap-jet event
by hard color-singlet exchange

devoid of particle activity between the final-state jets due to **BFKL pomeron exchange**

tool to study BFKL dynamics

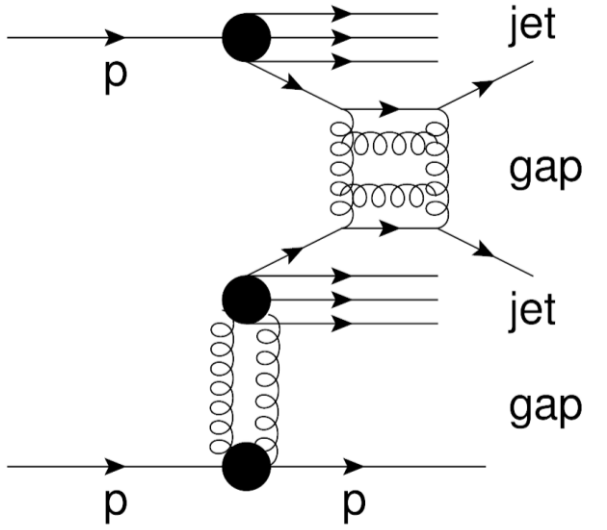

jet-gap-jet with intact proton event
by hard color-singlet exchange

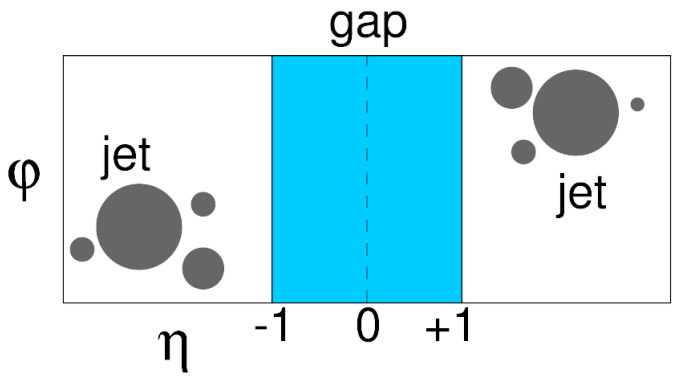

jet-gap-jet event signature in the
φ-η plane

measured by CMS

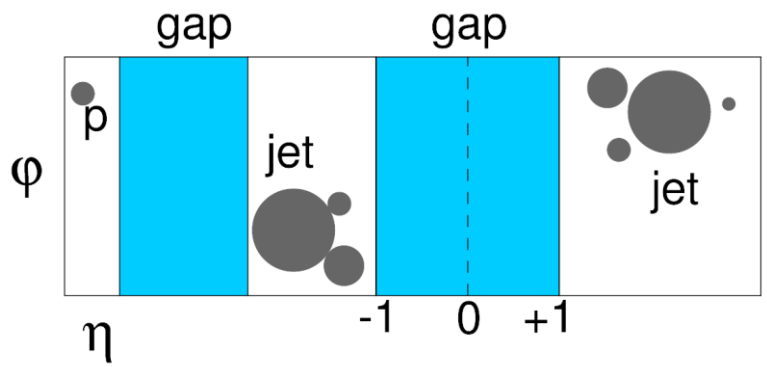

jet-gap-jet + intact proton event
signature in the φ-η plane

Dijet events with hard color-singlet exchange

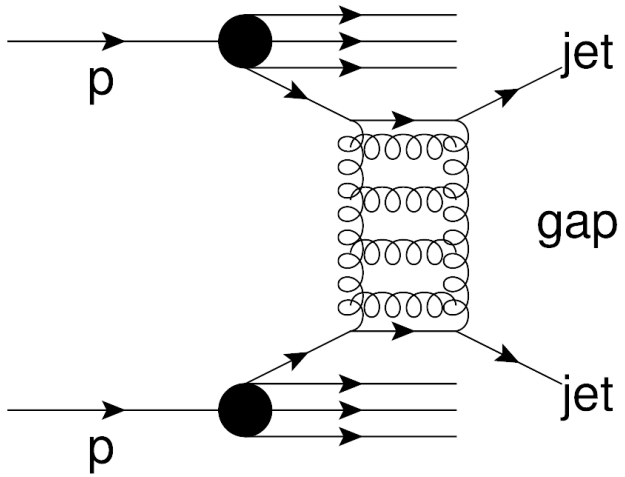

jet-gap-jet event
by hard color-singlet exchange

devoid of particle activity between the final-state jets due to **BFKL pomeron exchange**

tool to study BFKL dynamics

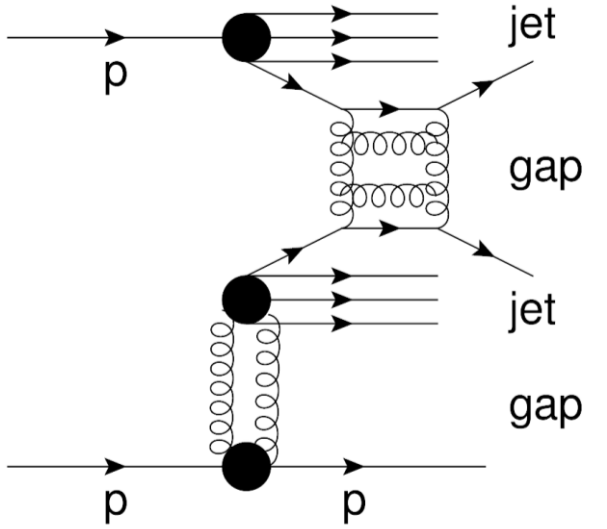

jet-gap-jet with intact proton event
by hard color-singlet exchange

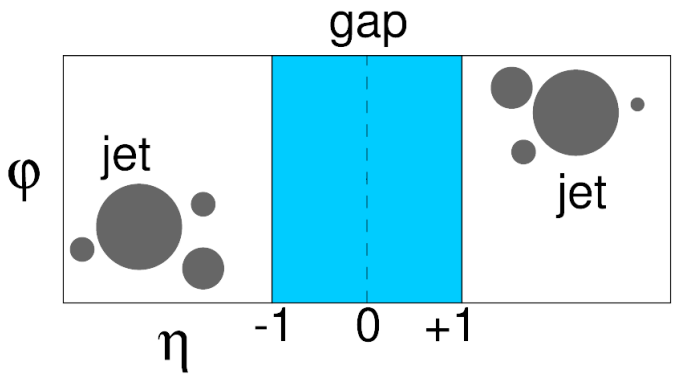

jet-gap-jet event signature in the
φ-η plane

measured by CMS

measured by CMS+TOTEM

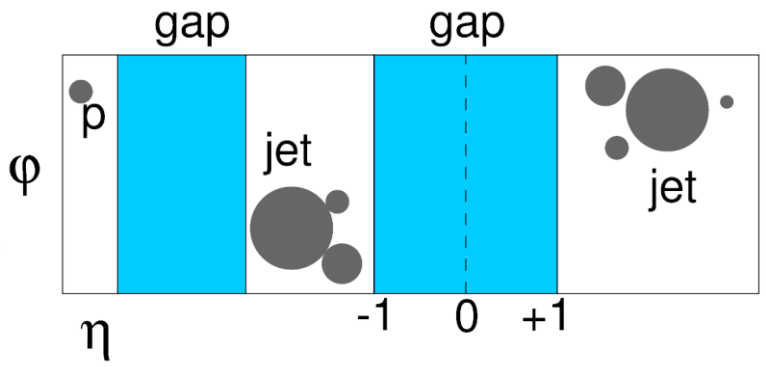

jet-gap-jet + intact proton event
signature in the φ-η plane

Dijet events with hard color-singlet exchange

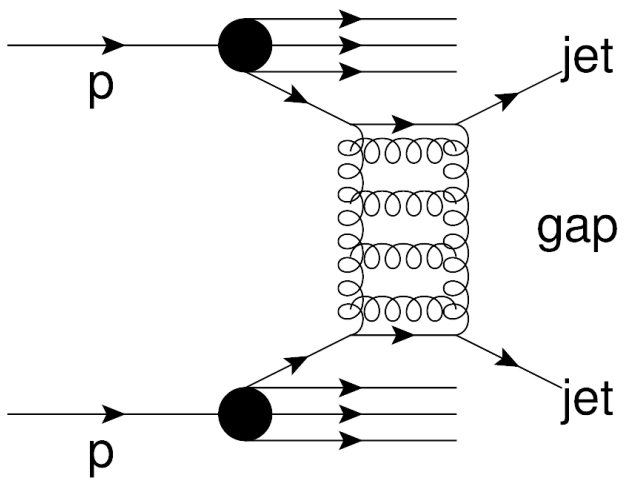

jet-gap-jet event
by hard color-singlet exchange

devoid of particle activity between the final-state jets due to **BFKL pomeron exchange**

tool to study BFKL dynamics

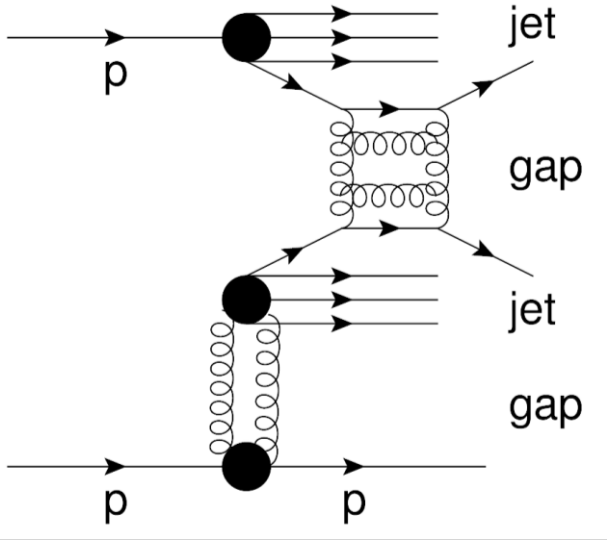

jet-gap-jet with intact proton event
by hard color-singlet exchange

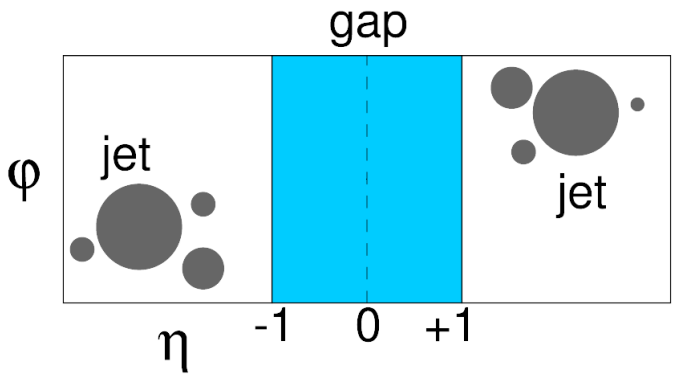

jet-gap-jet event signature in the
φ-η plane

measured by CMS

measured by CMS+TOTEM

$\sqrt{s}$ = 13 TeV, L_{int}^{CMS} = 0.66 pb^{-1}
$L_{int}^{CMS-TOTEM}$ = 0.4 pb^{-1}, β^* = 90m

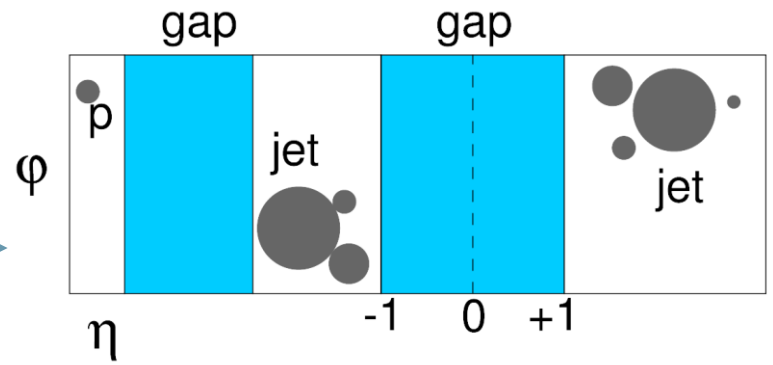

jet-gap-jet + intact proton event
signature in the φ-η plane

Dijet events with hard color-singlet exchange

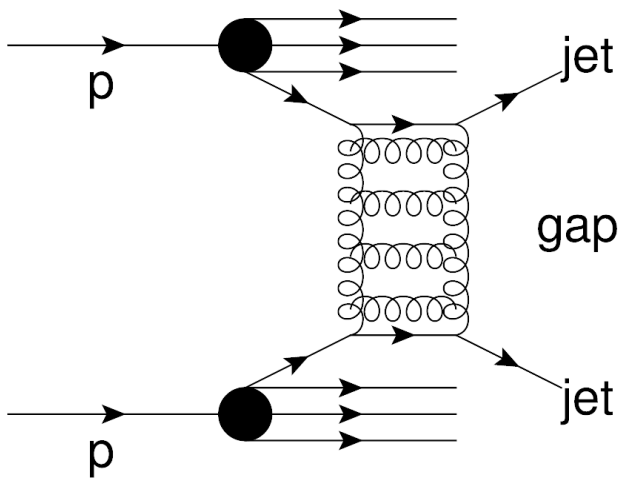

jet-gap-jet event
by hard color-singlet exchange

devoid of particle activity between the final-state jets due to **BFKL pomeron exchange**

tool to study BFKL dynamics

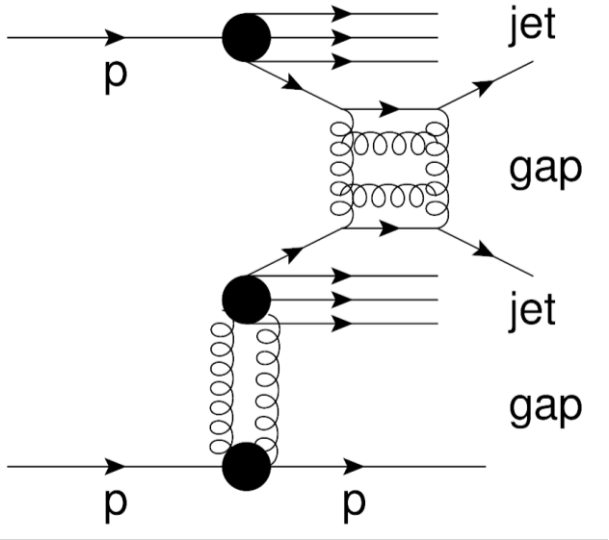

jet-gap-jet with intact proton event
by hard color-singlet exchange

Phys. Rev. D **104** (2021) 032009

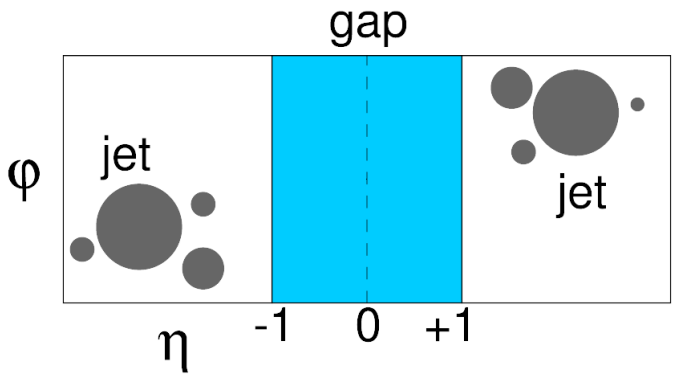

jet-gap-jet event signature in the
φ-η plane

measured by CMS

measured by CMS+TOTEM

$\sqrt{s}$ = 13 TeV, L_{int}^{CMS} = 0.66 pb^{-1}
$L_{int}^{CMS-TOTEM}$ = 0.4 pb^{-1}, β^* = 90m

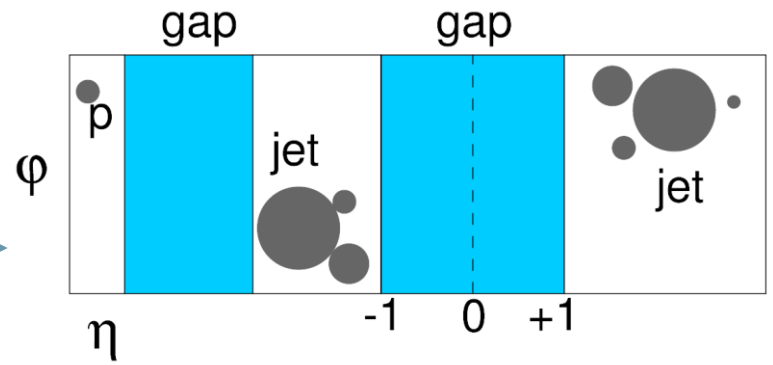

jet-gap-jet + intact proton event
signature in the φ-η plane

CMS color-singlet exchange (CSE) dijet event fractions

CMS color-singlet exchange (CSE) dijet event fractions

the fraction of color-singlet exchange dijet events, f_{CSE}, is measured in bins of $\Delta\eta_{jj} = |\eta^{jet1} - \eta^{jet2}|$, p_T^{jet2} (subleading jet p_T) and $\Delta\phi_{jj} = |\phi^{jet1} - \phi^{jet2}|$

CMS color-singlet exchange (CSE) dijet event fractions

the fraction of color-singlet exchange dijet events, f_{CSE}, is measured in bins of $\Delta\eta_{jj} = |\eta^{jet1} - \eta^{jet2}|$, p_T^{jet2} (subleading jet p_T) and $\Delta\phi_{jj} = |\phi^{jet1} - \phi^{jet2}|$

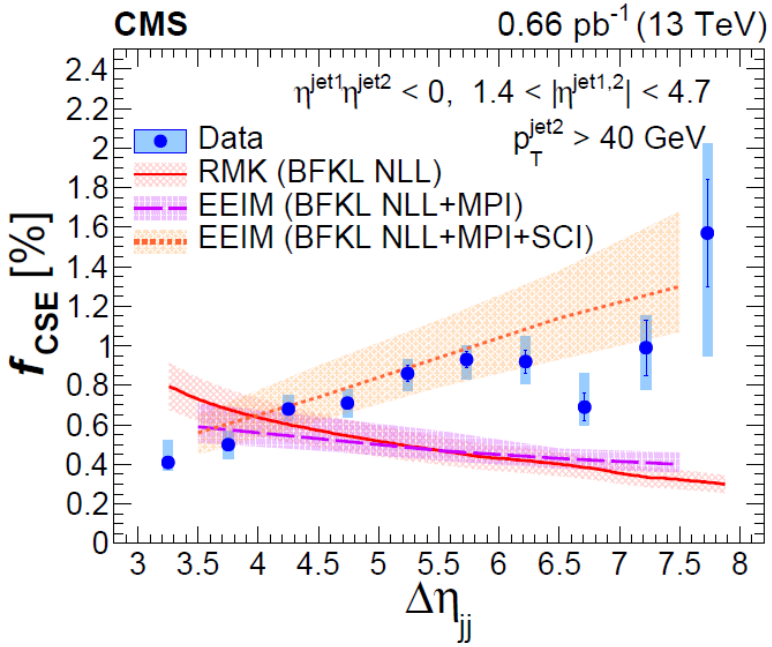

CMS color-singlet exchange (CSE) dijet event fractions

the fraction of color-singlet exchange dijet events, f_{CSE}, is measured in bins of $\Delta\eta_{jj} = |\eta^{jet1} - \eta^{jet2}|$, p_T^{jet2} (subleading jet p_T) and $\Delta\phi_{jj} = |\phi^{jet1} - \phi^{jet2}|$

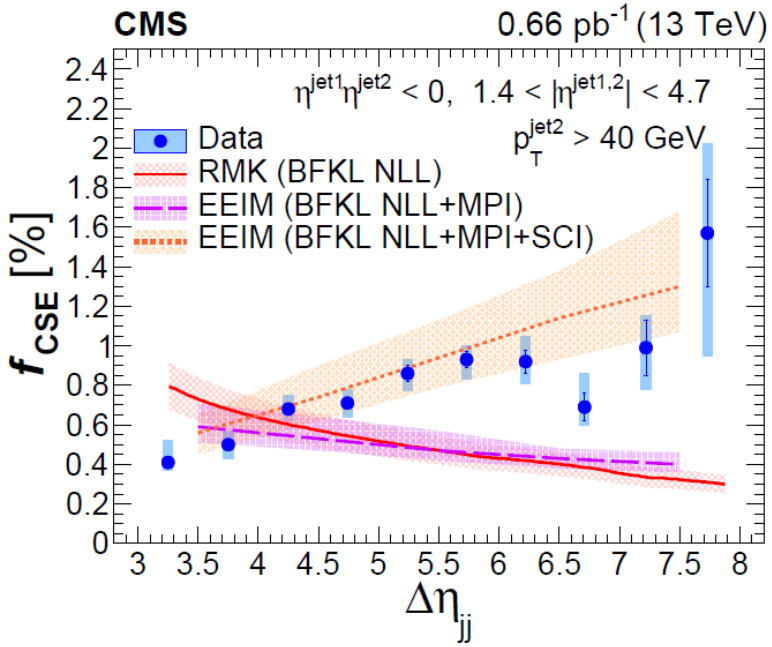

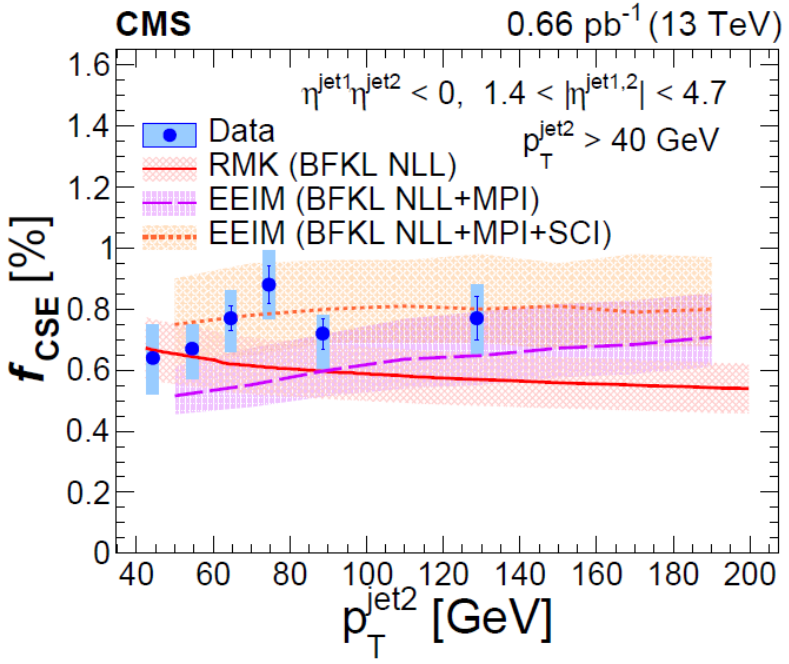

CMS color-singlet exchange (CSE) dijet event fractions

the fraction of color-singlet exchange dijet events, f_{CSE}, is measured in bins of $\Delta\eta_{jj} = |\eta^{jet1} - \eta^{jet2}|$, p_T^{jet2} (subleading jet p_T) and $\Delta\phi_{jj} = |\phi^{jet1} - \phi^{jet2}|$

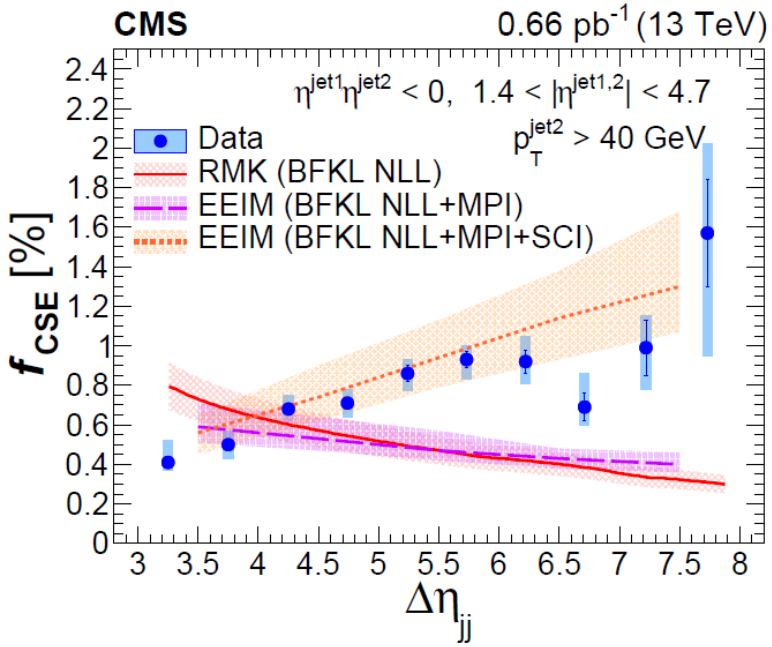

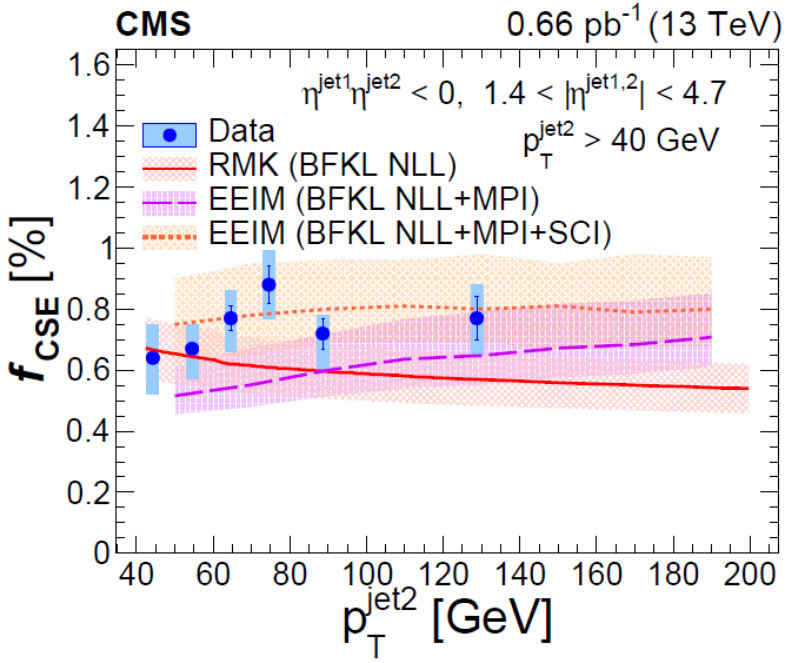

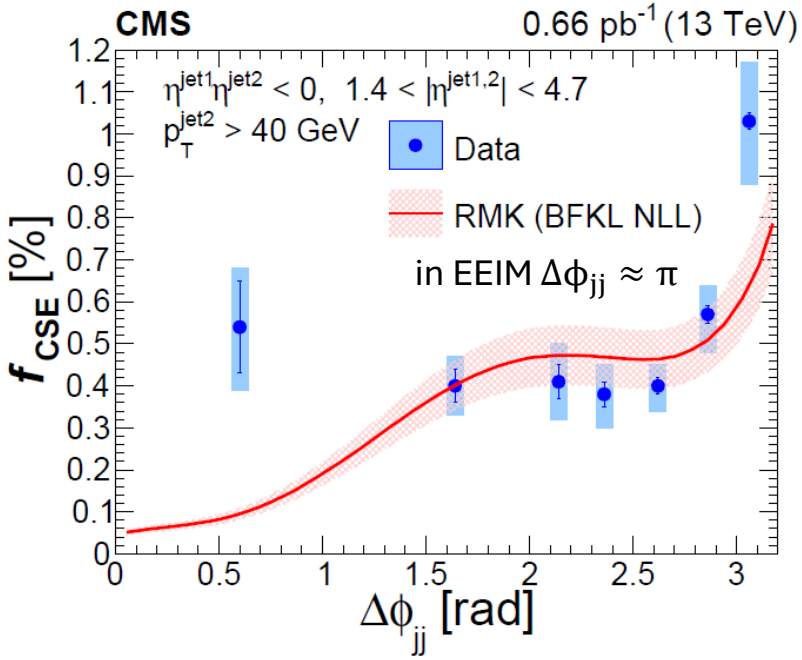

CMS color-singlet exchange (CSE) dijet event fractions

the fraction of color-singlet exchange dijet events, f_{CSE}, is measured in bins of $\Delta\eta_{jj} = |\eta^{jet1} - \eta^{jet2}|$, p_T^{jet2} (subleading jet p_T) and $\Delta\phi_{jj} = |\phi^{jet1} - \phi^{jet2}|$

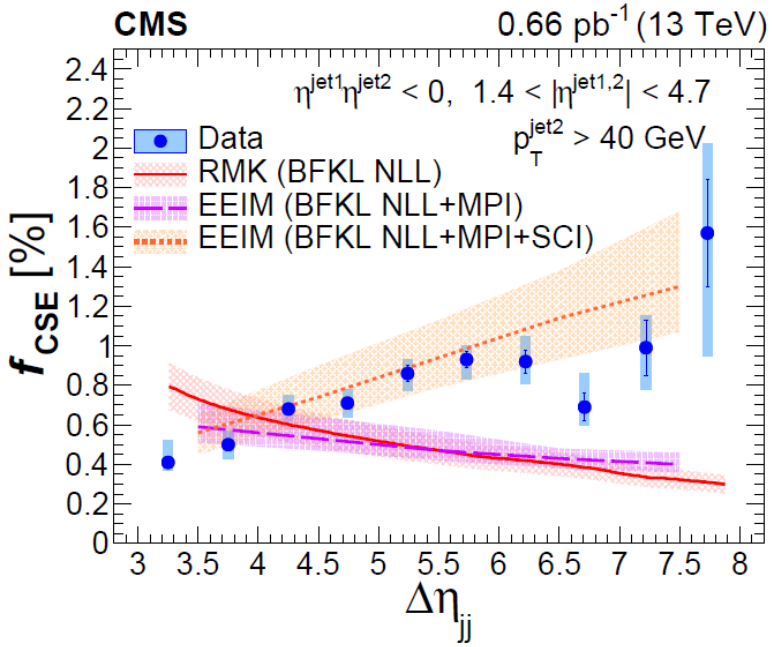

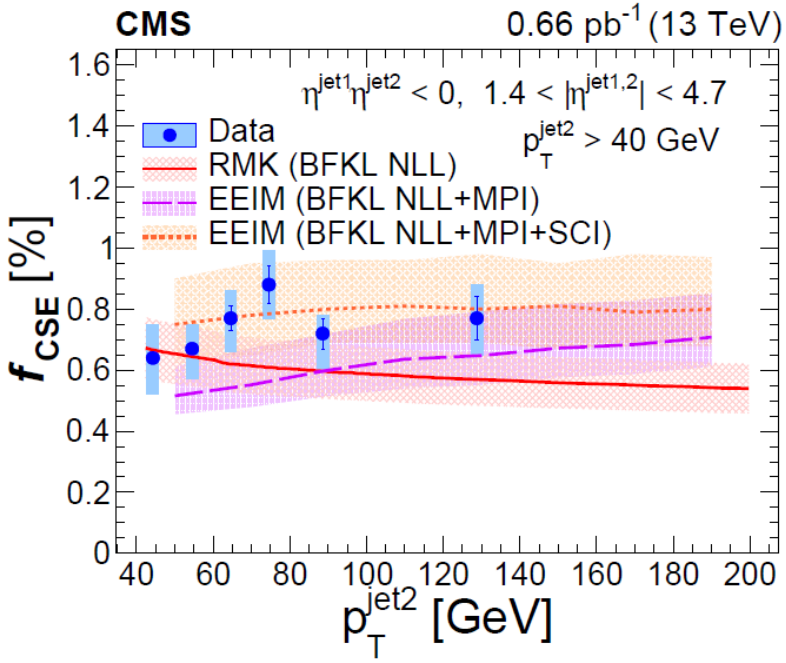

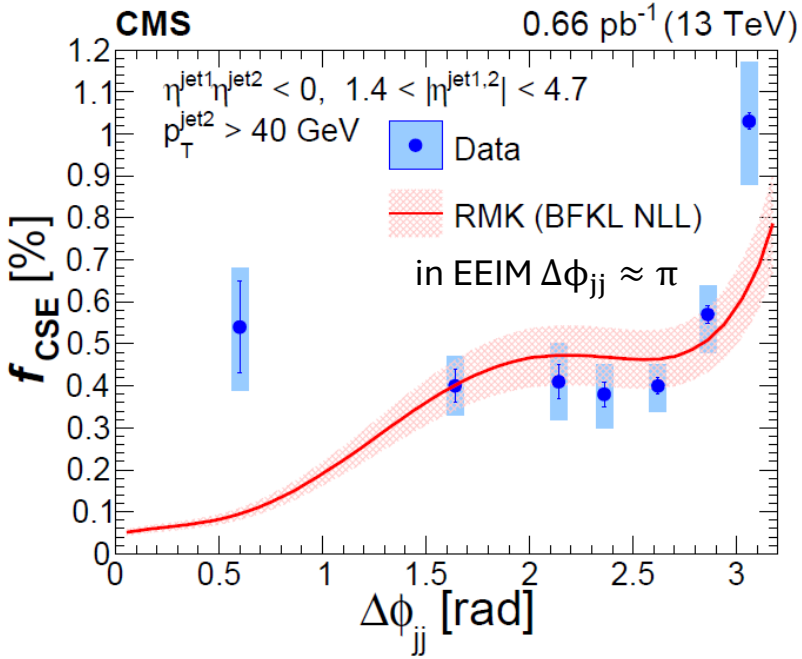

results are compared with BFKL-based calculations by Royon, Marquet, Kepka (RMK) and Ekstedt, Enberg, Ingelman, Motyka (EEIM) in NLL accuracy implemented in PYTHIA (the latter includes soft color interaction (SCI) and/or multi-parton interaction (MPI) contributions)

BFKL tests with jet-gap-jet events

BFKL tests with jet-gap-jet events

Baldenegro, González Durán, Klasen, Royon, Salomon, JHEP 2022, 250

BFKL tests with jet-gap-jet events

Baldenegro, González Durán, Klasen, Royon, Salomon, JHEP 2022, 250

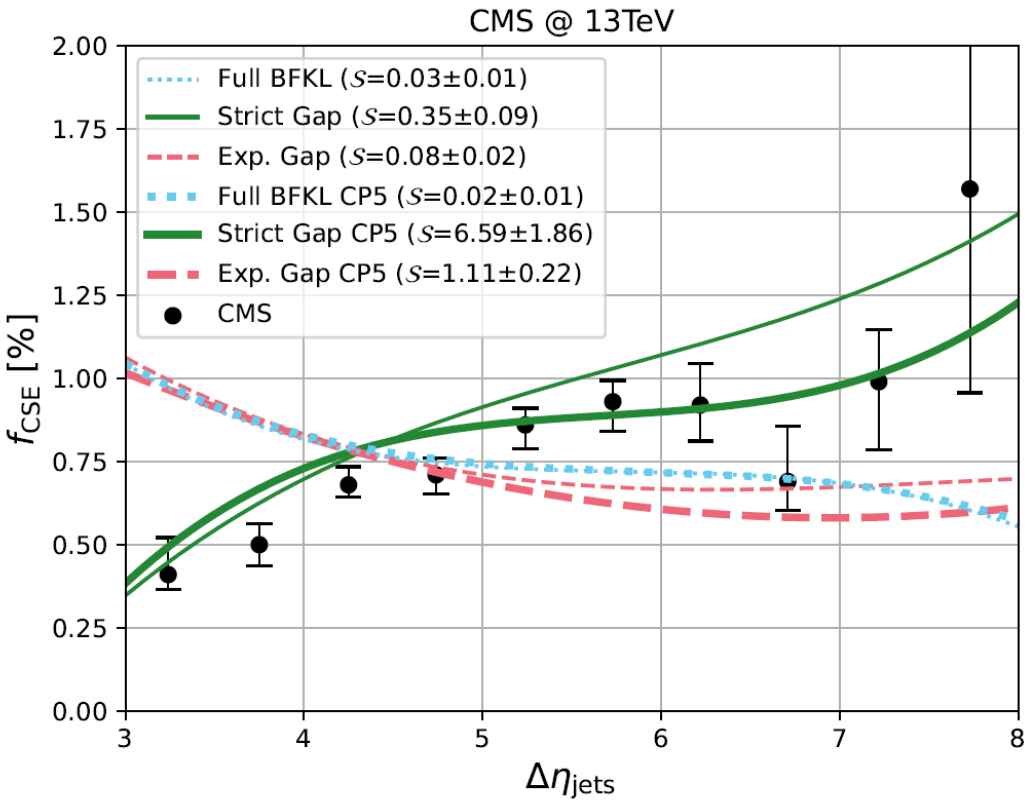

BFKL tests with jet-gap-jet events

Baldenegro, González Durán, Klasen, Royon, Salomon, JHEP 2022, 250

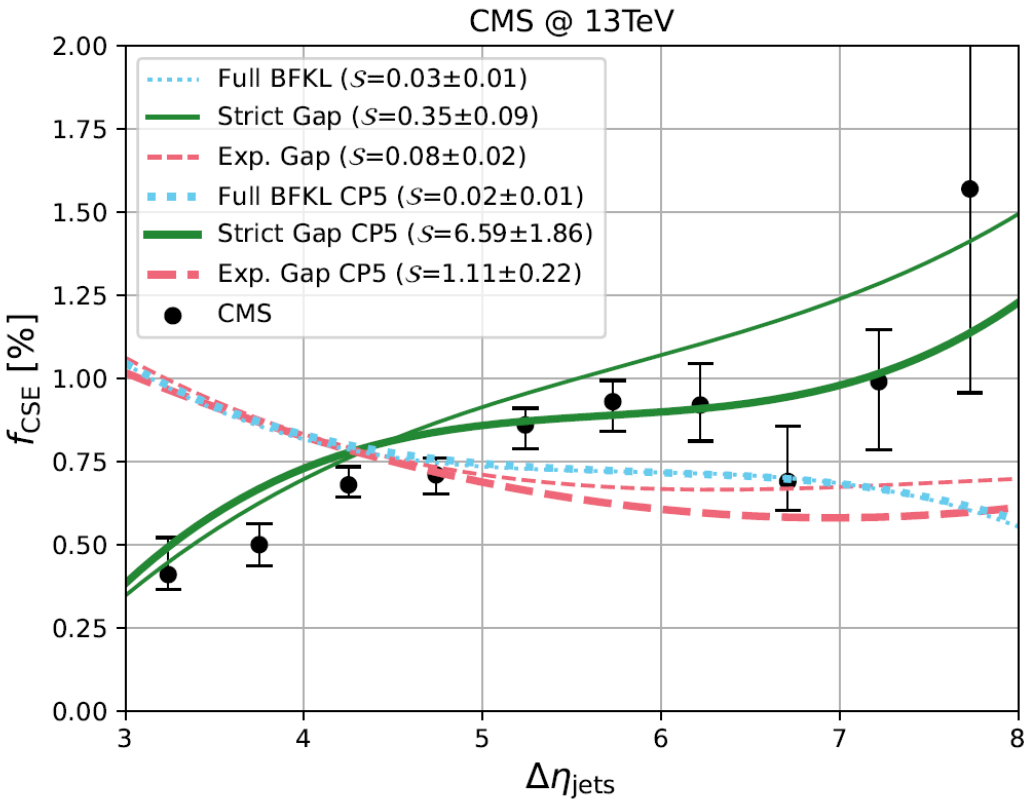

good agreement between BFKL and data but the gap definition is different in theory and data
(theory: no particles at all; experiment: no particles with p_T>200 MeV; explanation: too much ISR generated by PYTHIA)

BFKL tests with jet-gap-jet events

Baldenegro, González Durán, Klasen, Royon, Salomon, JHEP 2022, 250

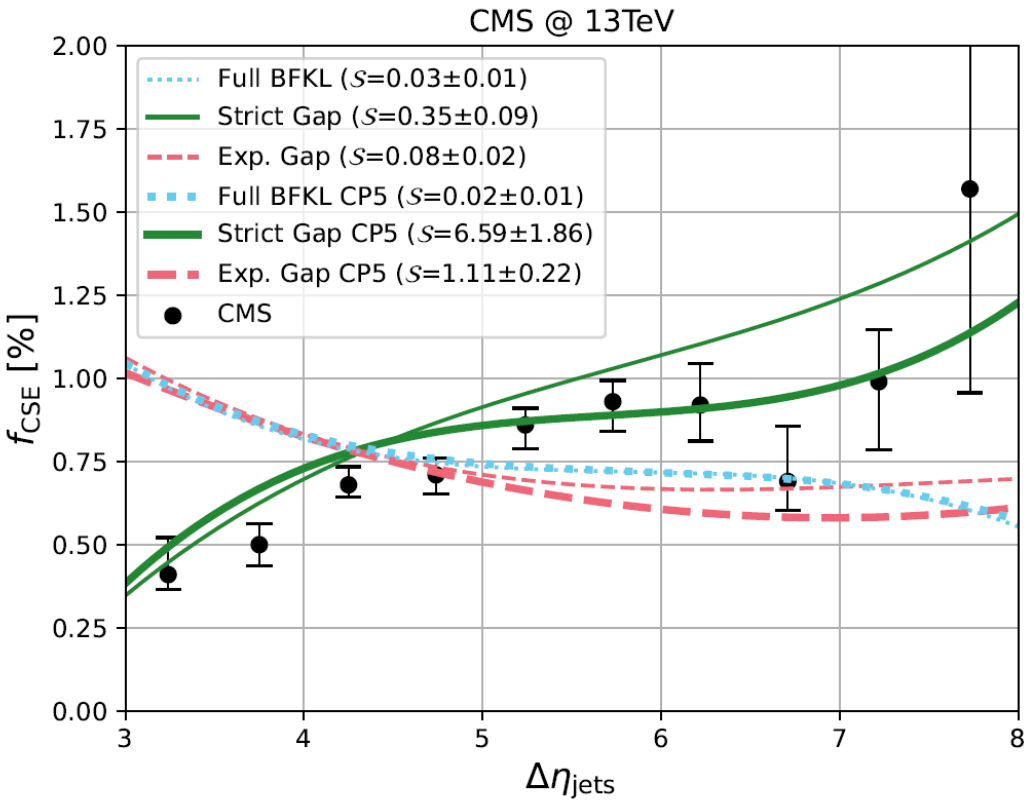

Colferai, Deganutti, Raben, Royon, JHEP 2023, 91

good agreement between BFKL and data but the gap definition is different in theory and data
(theory: no particles at all; experiment: no particles with p_T>200 MeV; explanation: too much ISR generated by PYTHIA)

BFKL tests with jet-gap-jet events

Baldenegro, González Durán, Klasen, Royon, Salomon, JHEP 2022, 250

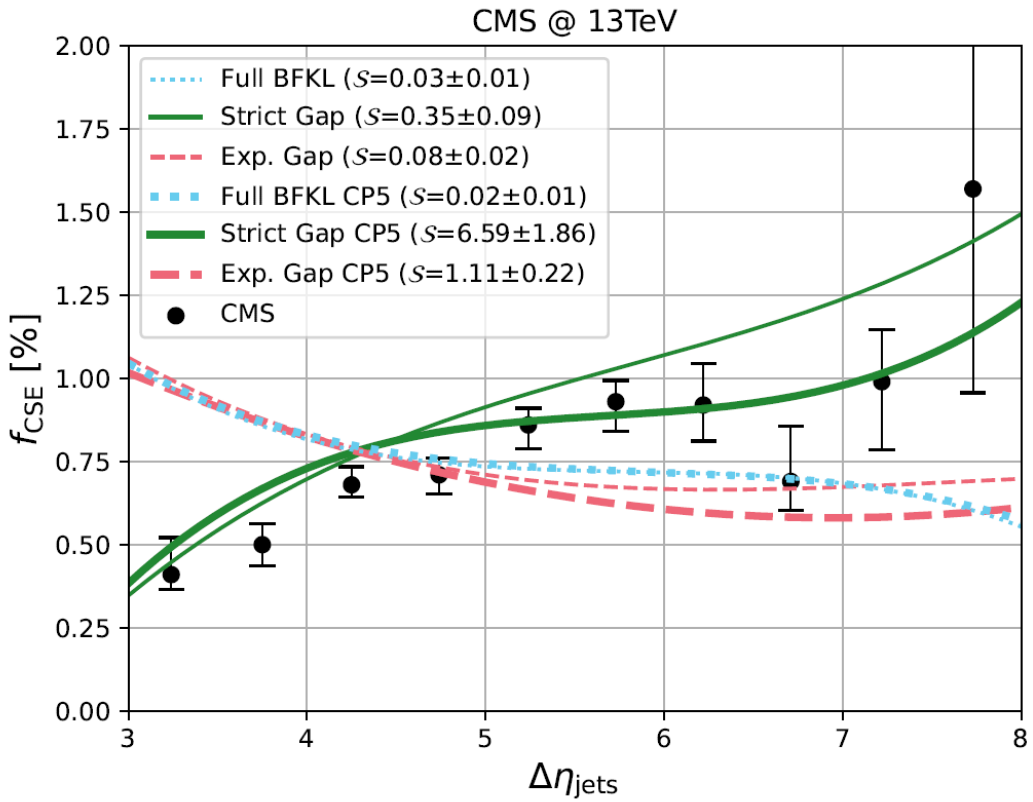

Colferai, Deganutti, Raben, Royon, JHEP 2023, 91

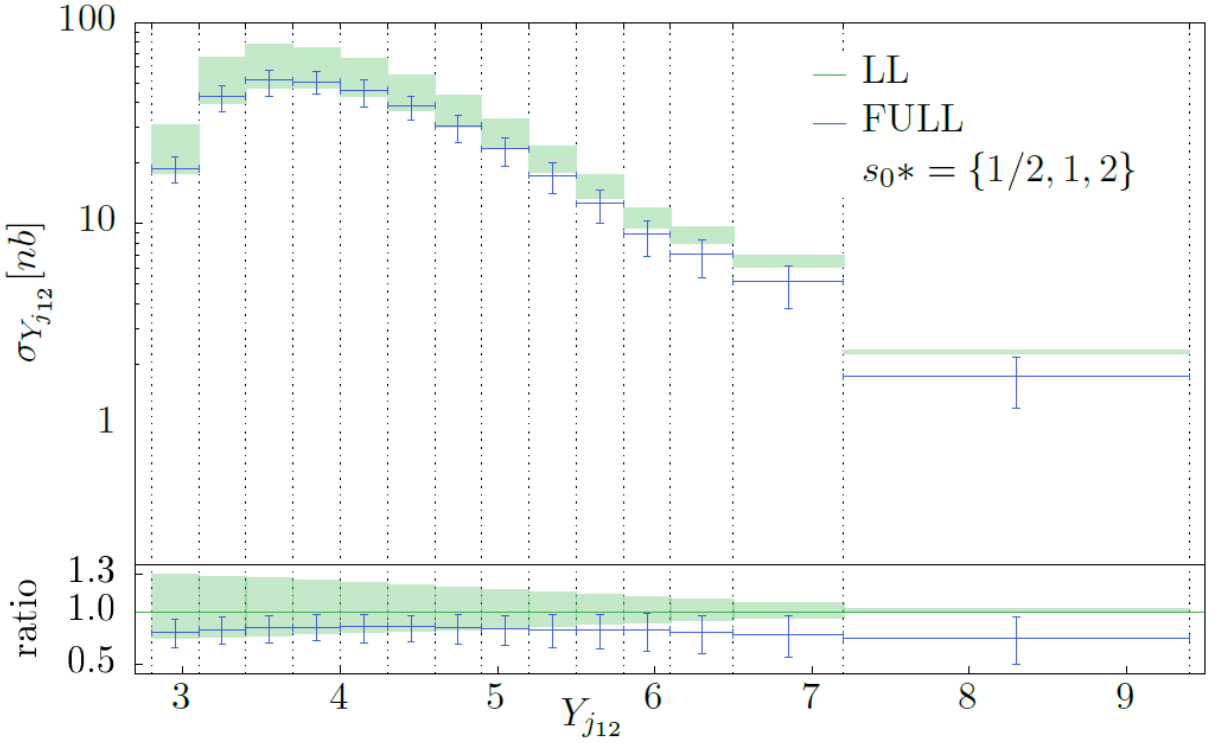

good agreement between BFKL and data but the gap definition is different in theory and data
(theory: no particles at all; experiment: no particles with p_T>200 MeV; explanation: too much ISR generated by PYTHIA)

BFKL tests with jet-gap-jet events

Baldenegro, González Durán, Klasen, Royon, Salomon, JHEP 2022, 250

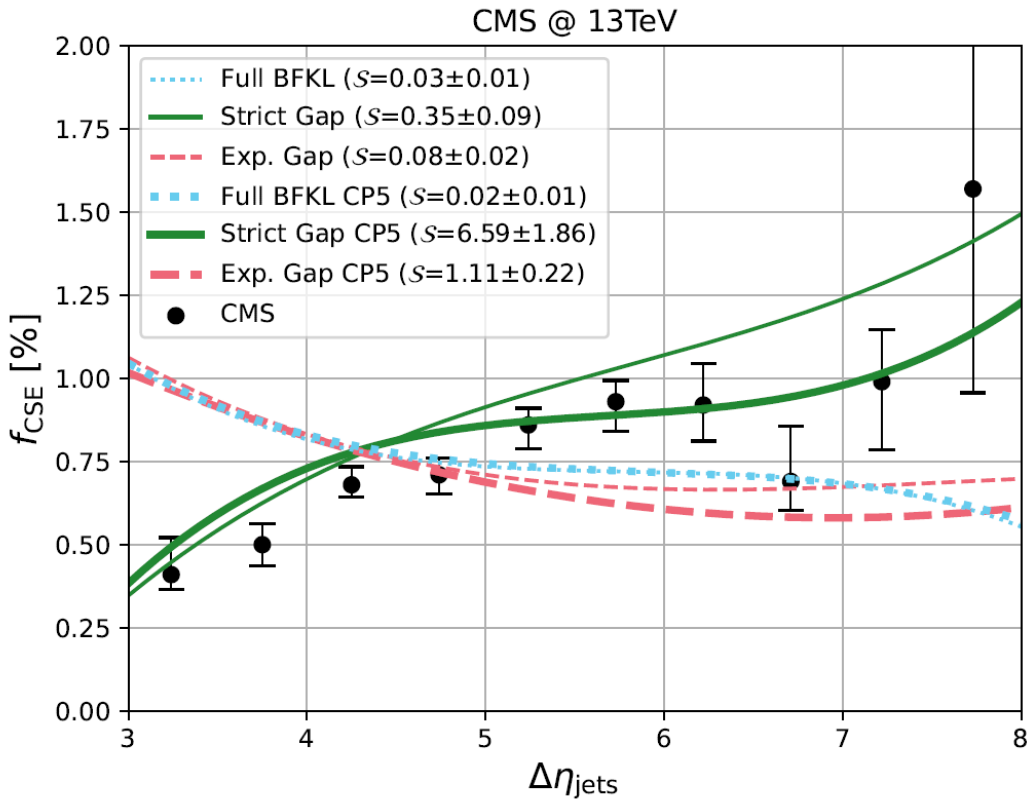

good agreement between BFKL and data but the gap definition is different in theory and data
(theory: no particles at all; experiment: no particles with p_T>200 MeV; explanation: too much ISR generated by PYTHIA)

Colferai, Deganutti, Raben, Royon, JHEP 2023, 91

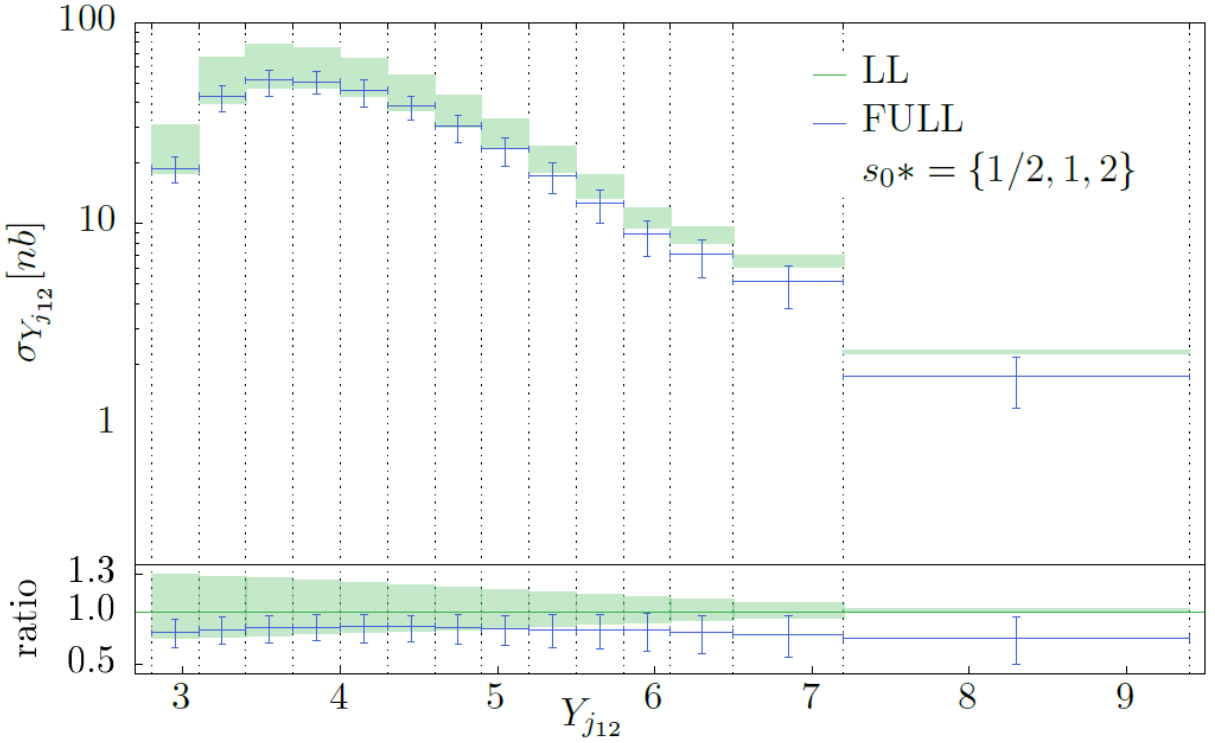

the full BFKL NLL prediction for the jet-gap-jet cross section is below the BFKL LL estimate in the whole rapidity separation range (15-20% decrease)

CMS-TOTEM CSE dijet event fractions

CMS-TOTEM CSE dijet event fractions

dominant background: uncorrelated forward protons from pile up or beam halo activity

CMS-TOTEM CSE dijet event fractions

dominant background: uncorrelated forward protons from pile up or beam halo activity

background removal based on matching between the fractional momentum losses ξ_p^{TOTEM} and ξ_p^{CMS}

CMS-TOTEM CSE dijet event fractions

dominant background: uncorrelated forward protons from pile up or beam halo activity

background removal based on matching between the fractional momentum losses ξ_p^{TOTEM} and ξ_p^{CMS}

ideally $\xi_p^{TOTEM} = \xi_p^{CMS}$, but CMS detector underestimates ξ_p,
hence $\xi_p^{CMS} - \xi_p^{TOTEM} < 0$ is required

CMS-TOTEM CSE dijet event fractions

dominant background: uncorrelated forward protons from pile up or beam halo activity

background removal based on matching between the fractional momentum losses ξ_p^{TOTEM} and ξ_p^{CMS}

ideally $\xi_p^{TOTEM} = \xi_p^{CMS}$, but CMS detector underestimates ξ_p,
hence $\xi_p^{CMS} - \xi_p^{TOTEM} < 0$ is required

limited sample size, a measurement as a function of kinematic variables is not possible: the f_{CSE} is extracted using the entire sample of events

CMS-TOTEM CSE dijet event fractions

dominant background: uncorrelated forward protons from pile up or beam halo activity

background removal based on matching between the fractional momentum losses ξ_p^{TOTEM} and ξ_p^{CMS}

ideally $\xi_p^{TOTEM} = \xi_p^{CMS}$, but CMS detector underestimates ξ_p,
hence $\xi_p^{CMS} - \xi_p^{TOTEM} < 0$ is required

limited sample size, a measurement as a function of kinematic variables is not possible: the f_{CSE} is extracted using the entire sample of events

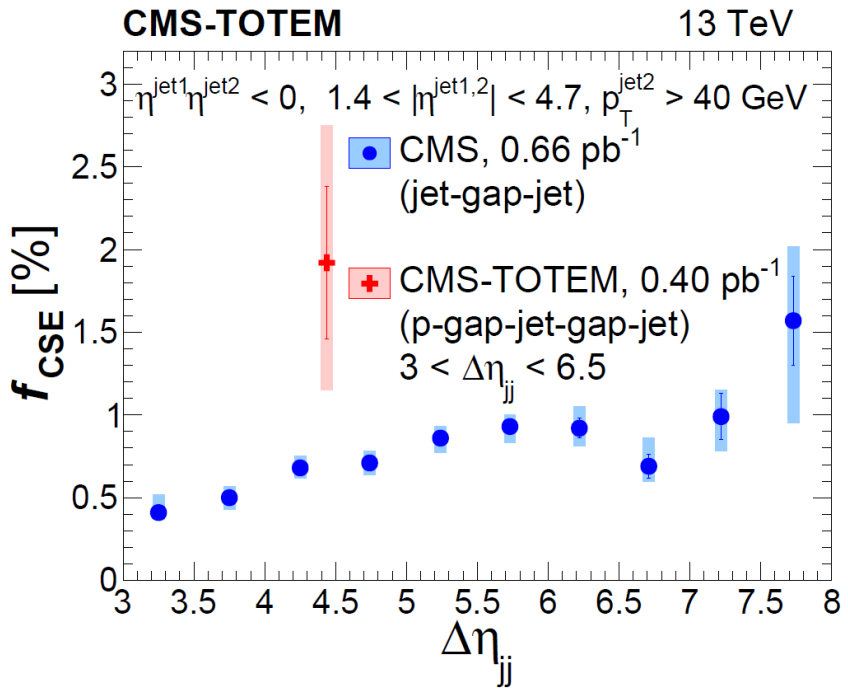

CMS-TOTEM CSE dijet event fractions

dominant background: uncorrelated forward protons from pile up or beam halo activity

background removal based on matching between the fractional momentum losses ξ_p^{TOTEM} and ξ_p^{CMS}

ideally $\xi_p^{TOTEM} = \xi_p^{CMS}$, but CMS detector underestimates ξ_p,
hence $\xi_p^{CMS} - \xi_p^{TOTEM} < 0$ is required

limited sample size, a measurement as a function of kinematic variables is not possible: the f_{CSE} is extracted using the entire sample of events

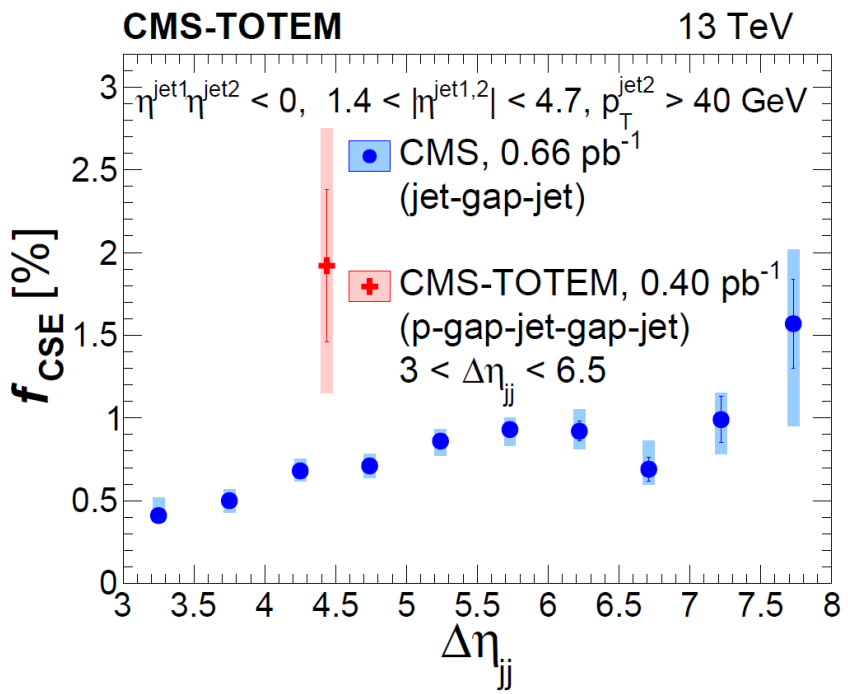

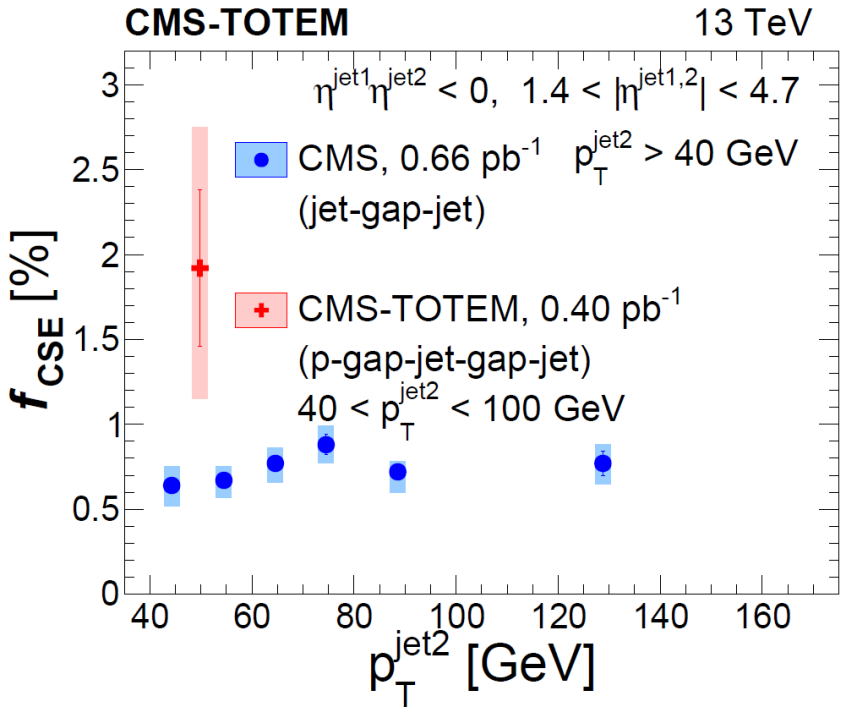

Single-diffractive (SD) dijet production

Single-diffractive (SD) dijet production

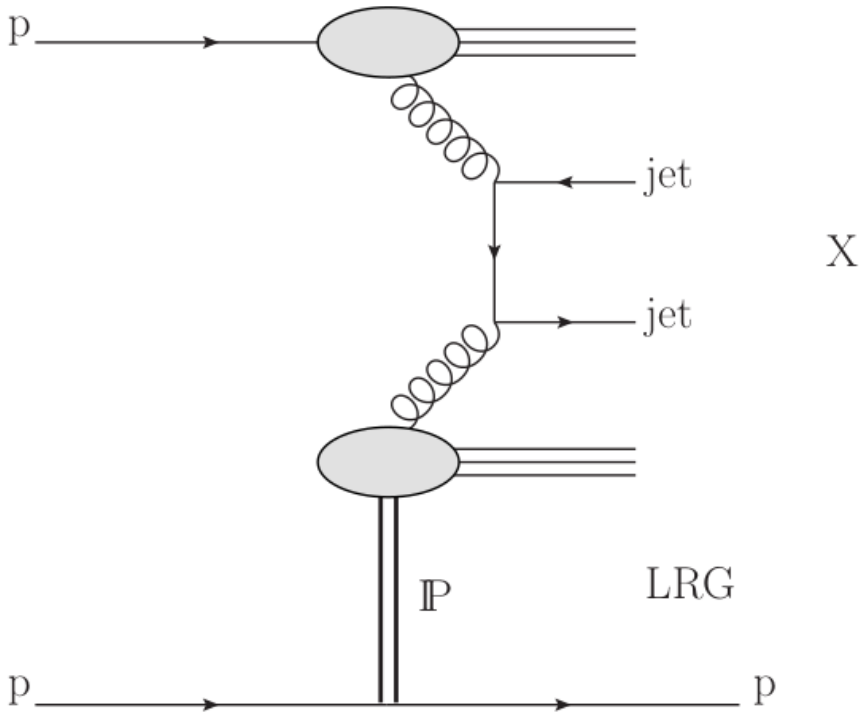

Schematic diagram of single-diffractive dijet production with hard gg → dijet scatteing process; the qq and gq initial states also contribute

Single-diffractive (SD) dijet production

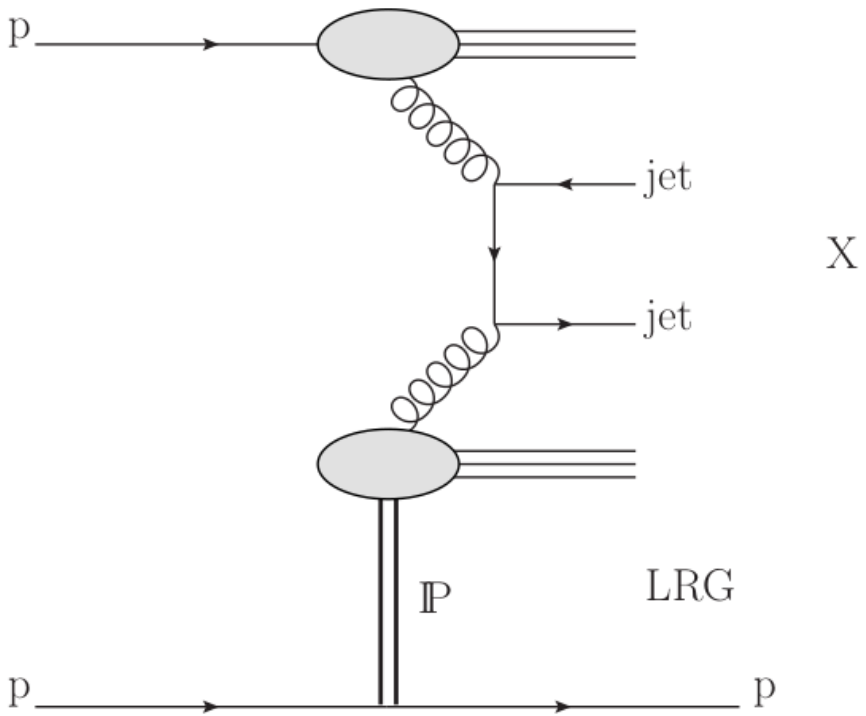

Schematic diagram of single-diffractive dijet production with hard gg → dijet scatteing process; the qq and gq initial states also contribute

high-p_T jets are measured in CMS, the scattered proton is measured in the TOTEM detectors

Single-diffractive (SD) dijet production

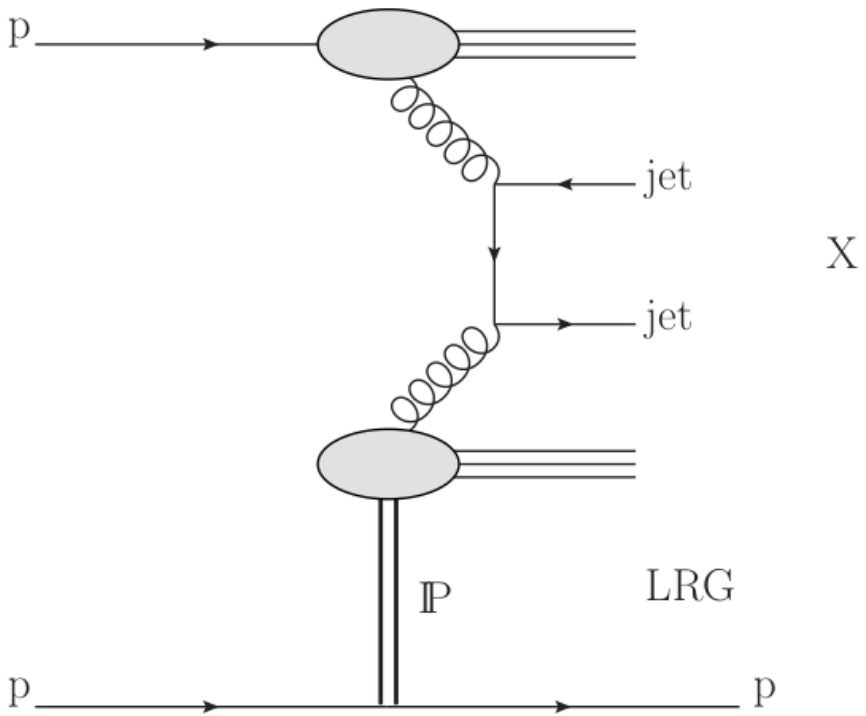

Schematic diagram of single-diffractive dijet production with hard gg → dijet scatteing process; the qq and gq initial states also contribute

high-p_T jets are measured in CMS, the scattered proton is measured in the TOTEM detectors

data collected at $\sqrt{s}$ = 8 TeV in a dedicated run (β^* = 90m, L_{int} = 37.5 nb^{-1})

Single-diffractive (SD) dijet production

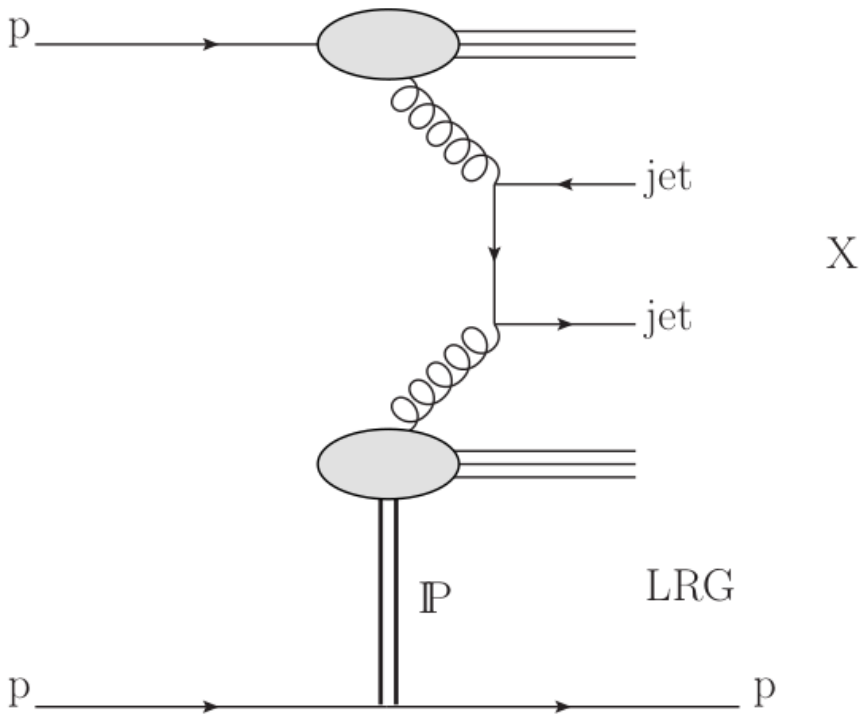

Schematic diagram of single-diffractive dijet production with hard gg → dijet scatteing process; the qq and gq initial states also contribute

high-p_T jets are measured in CMS, the scattered proton is measured in the TOTEM detectors

data collected at $\sqrt{s}$ = 8 TeV in a dedicated run (β^* = 90m, L_{int} = 37.5 nb^{-1})

matching between ξ_p^{TOTEM} and ξ_p^{CMS} to suppress pileup and beam halo events: $\xi_p^{CMS} - \xi_p^{TOTEM} \leq 0$

Single-diffractive (SD) dijet production

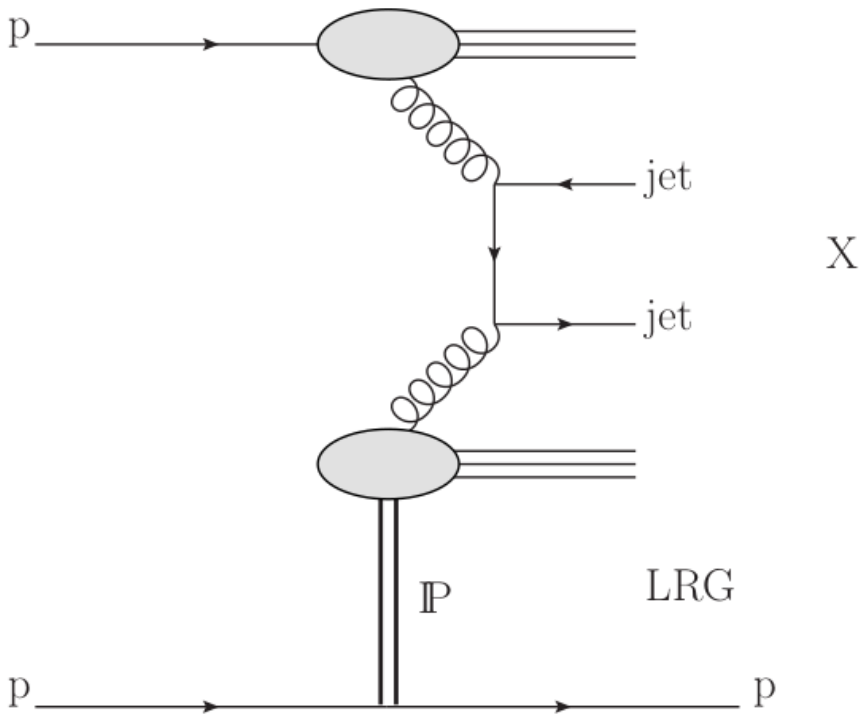

Schematic diagram of single-diffractive dijet production with hard gg → dijet scatteing process; the qq and gq initial states also contribute

high-p_T jets are measured in CMS, the scattered proton is measured in the TOTEM detectors

data collected at $\sqrt{s}$ = 8 TeV in a dedicated run (β^* = 90m, L_{int} = 37.5 nb^{-1})

matching between ξ_p^{TOTEM} and ξ_p^{CMS} to suppress pileup and beam halo events: $\xi_p^{CMS} - \xi_p^{TOTEM} \leq 0$

this is the first measurement of hard diffraction with a measured intact proton at LHC

Single-diffractive (SD) dijet production

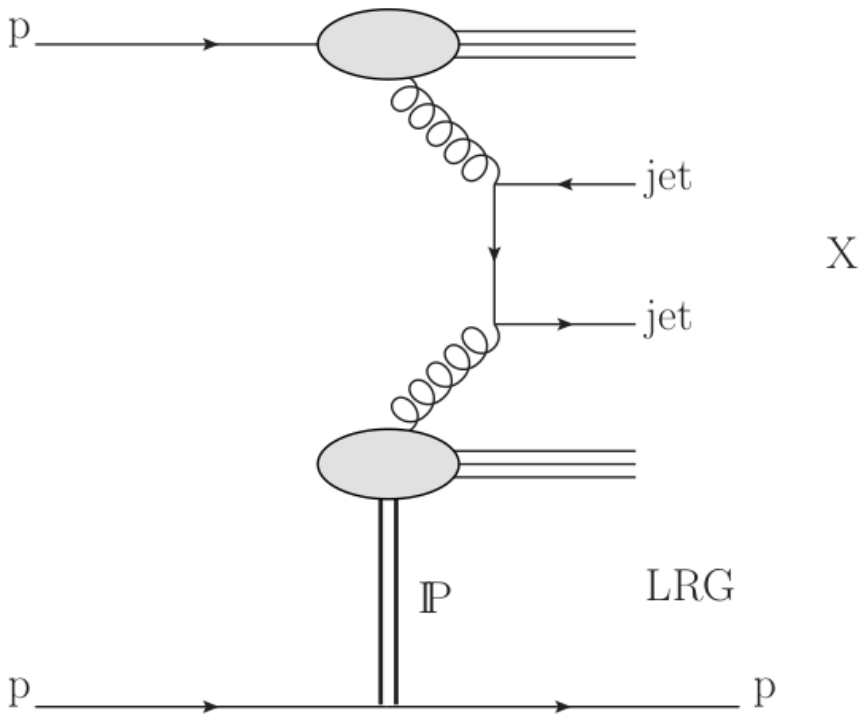

Schematic diagram of single-diffractive dijet production with hard gg → dijet scatteing process; the qq and gq initial states also contribute

high-p_T jets are measured in CMS, the scattered proton is measured in the TOTEM detectors

data collected at $\sqrt{s}$ = 8 TeV in a dedicated run (β^* = 90m, L_{int} = 37.5 nb^{-1})

matching between ξ_p^{TOTEM} and ξ_p^{CMS} to suppress pileup and beam halo events: $\xi_p^{CMS} - \xi_p^{TOTEM} \leq 0$

this is the first measurement of hard diffraction with a measured intact proton at LHC

Eur. Phys. J. C 80 (2020) 1164

Single-diffractive (SD) dijet production

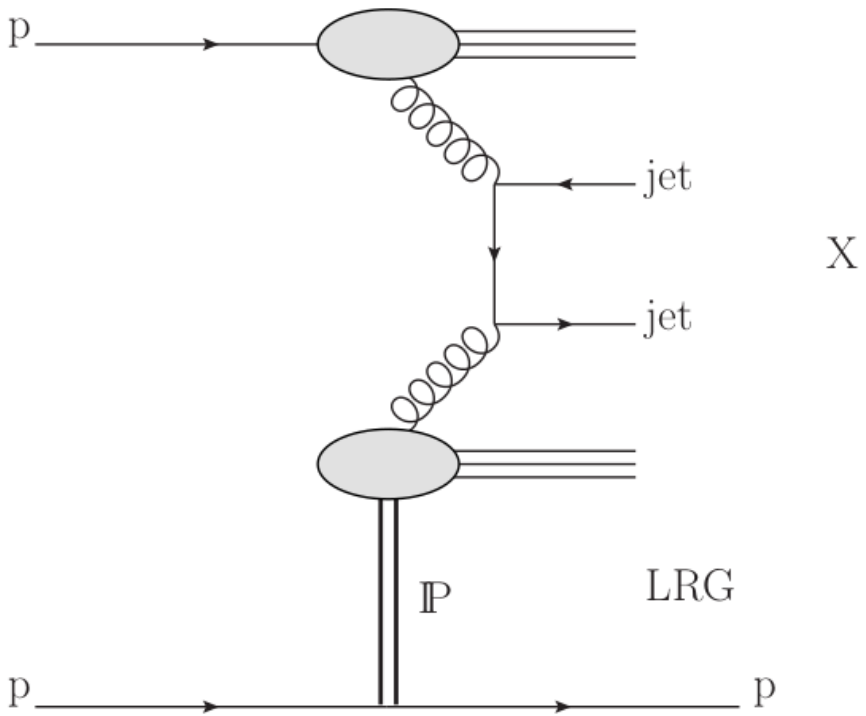

Schematic diagram of single-diffractive dijet production with hard gg → dijet scatteing process; the qq and gq initial states also contribute

Eur. Phys. J. C 80 (2020) 1164

high-p_T jets are measured in CMS, the scattered proton is measured in the TOTEM detectors

data collected at $\sqrt{s}$ = 8 TeV in a dedicated run (β^* = 90m, L_{int} = 37.5 nb^{-1})

matching between ξ_p^{TOTEM} and ξ_p^{CMS} to suppress pileup and beam halo events: $\xi_p^{CMS} - \xi_p^{TOTEM} \leq 0$

this is the first measurement of hard diffraction with a measured intact proton at LHC

hard diffractive processes are described in terms of a convolution of diffractive parton distribution functions (dPDFs, measured at HERA) and hard scattering cross sections (calculated in pQCD)

SD dijet results

SD dijet results

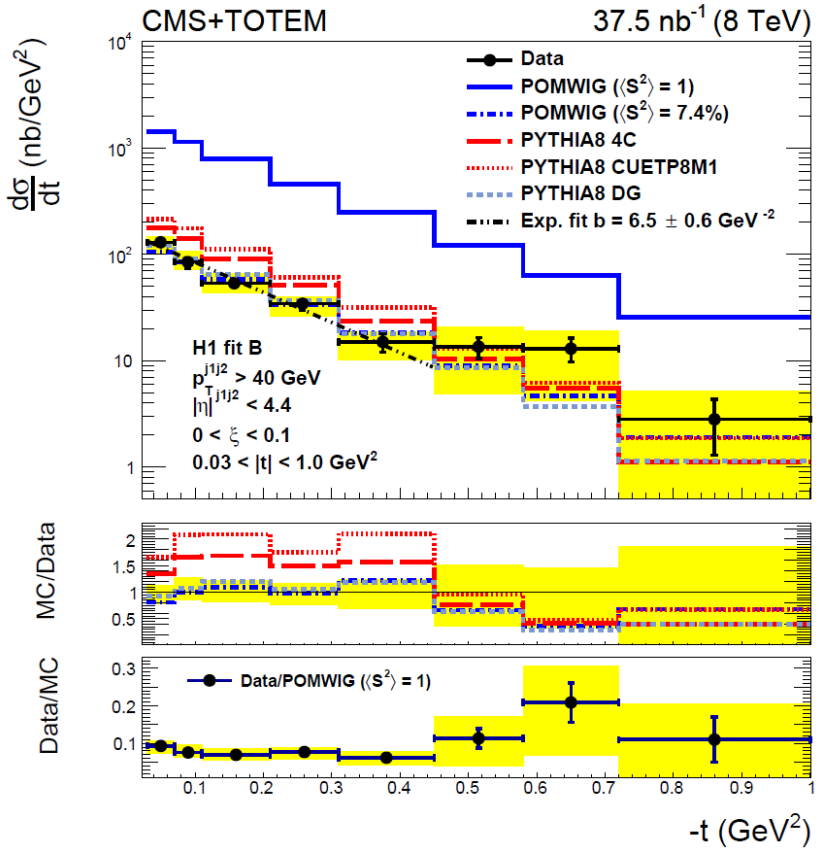

SD dijet results

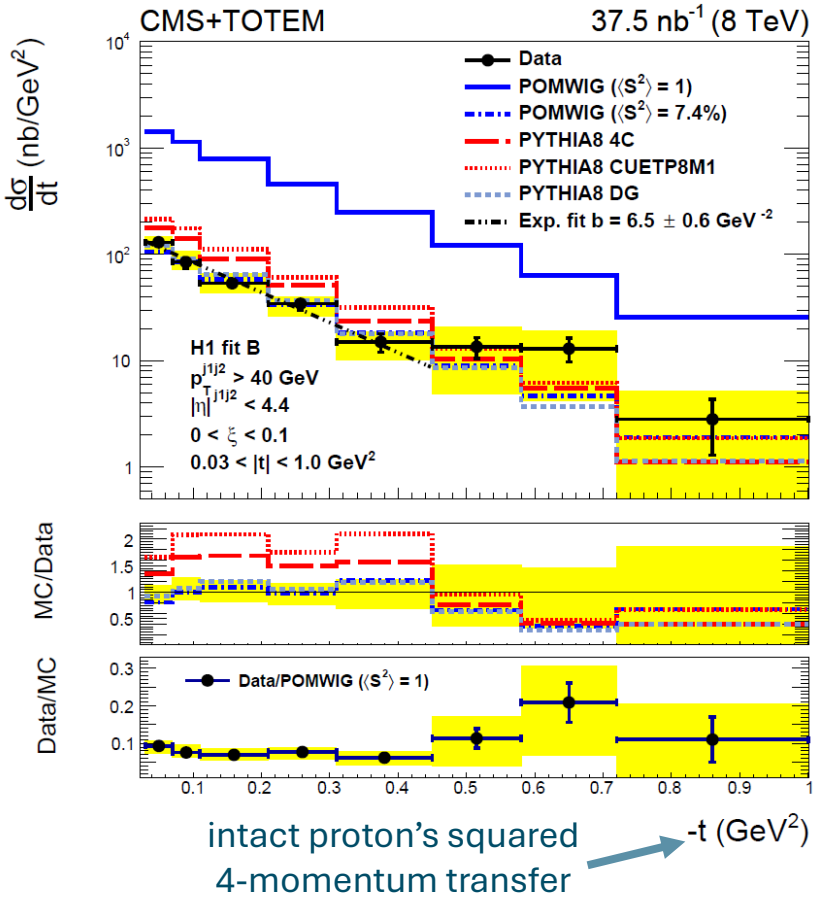

intact proton's squared 4-momentum transfer

SD dijet results

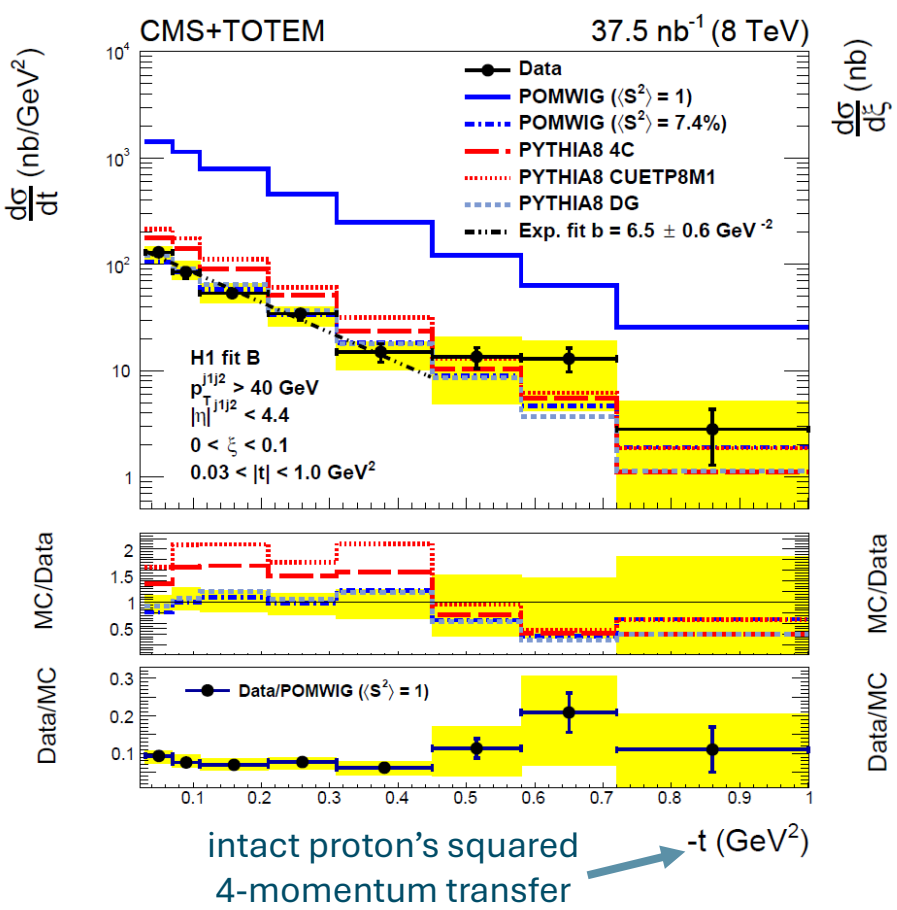

intact proton's squared 4-momentum transfer

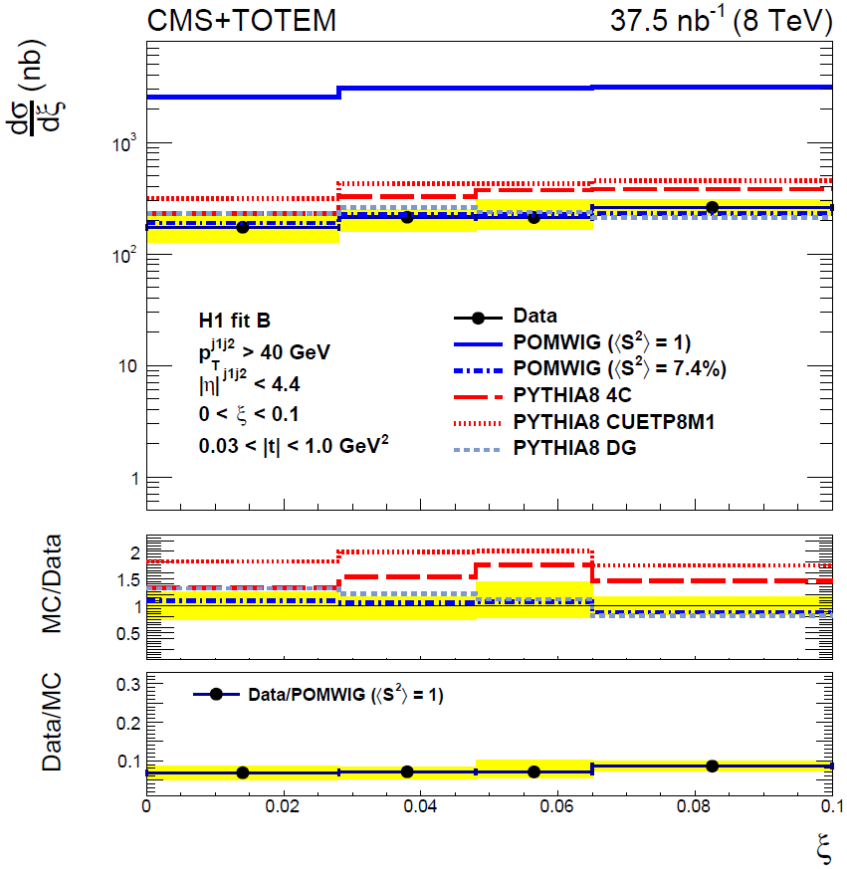

SD dijet results

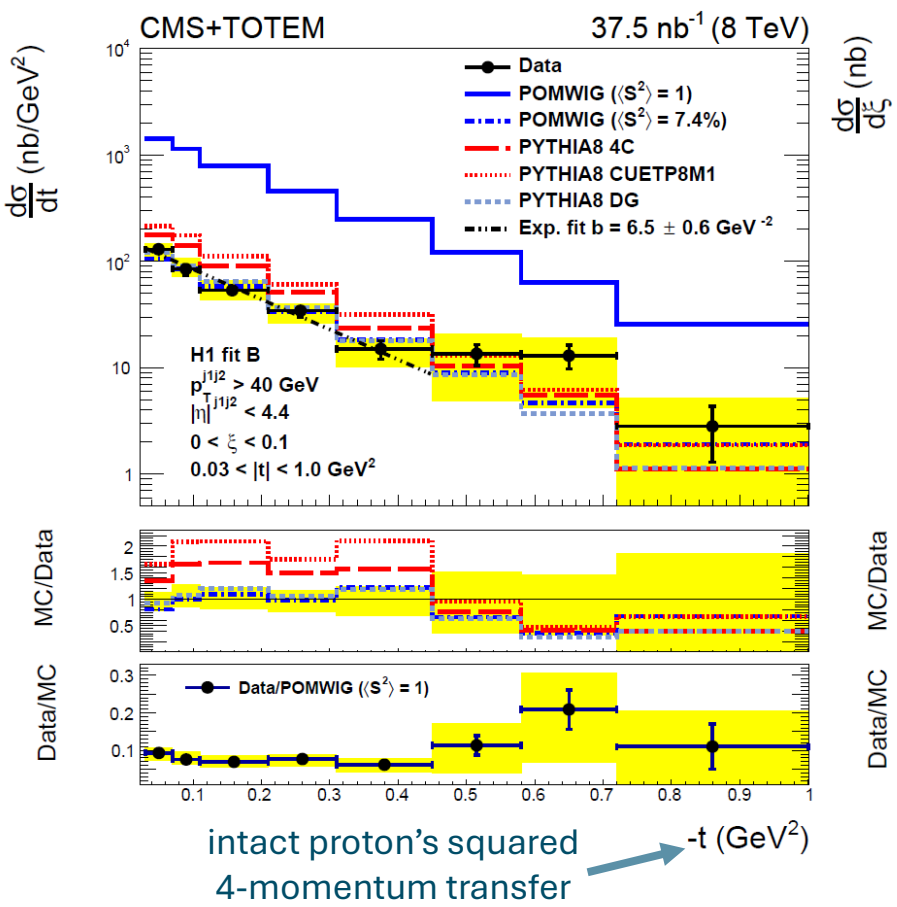

intact proton's squared 4-momentum transfer

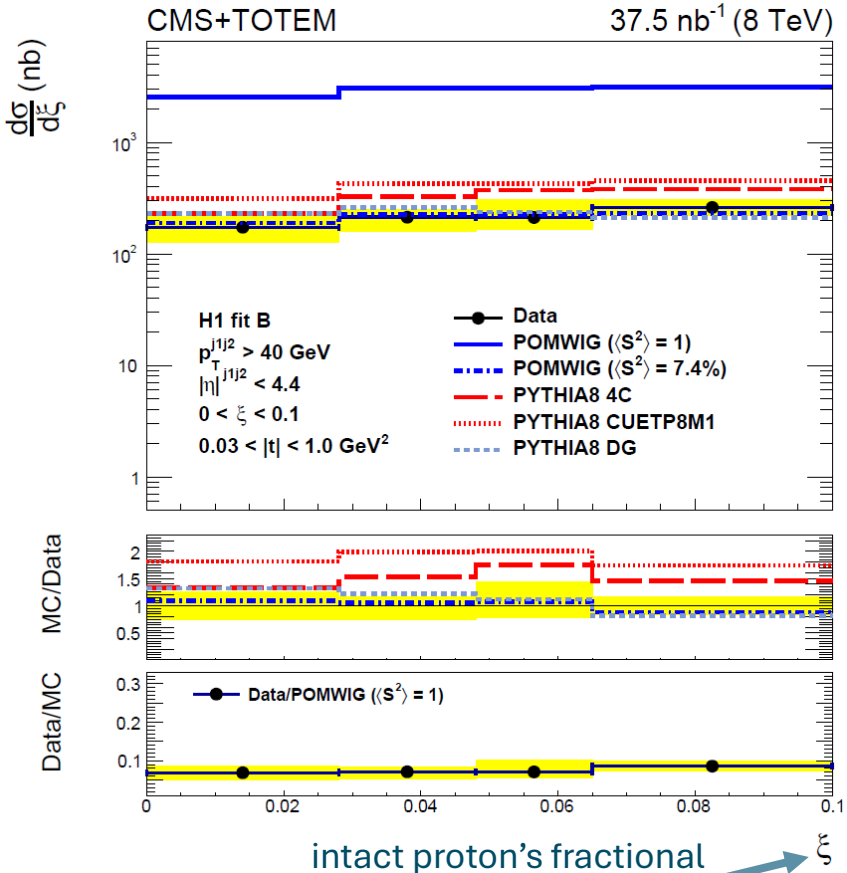

intact proton's fractional momentum loss

SD dijet results

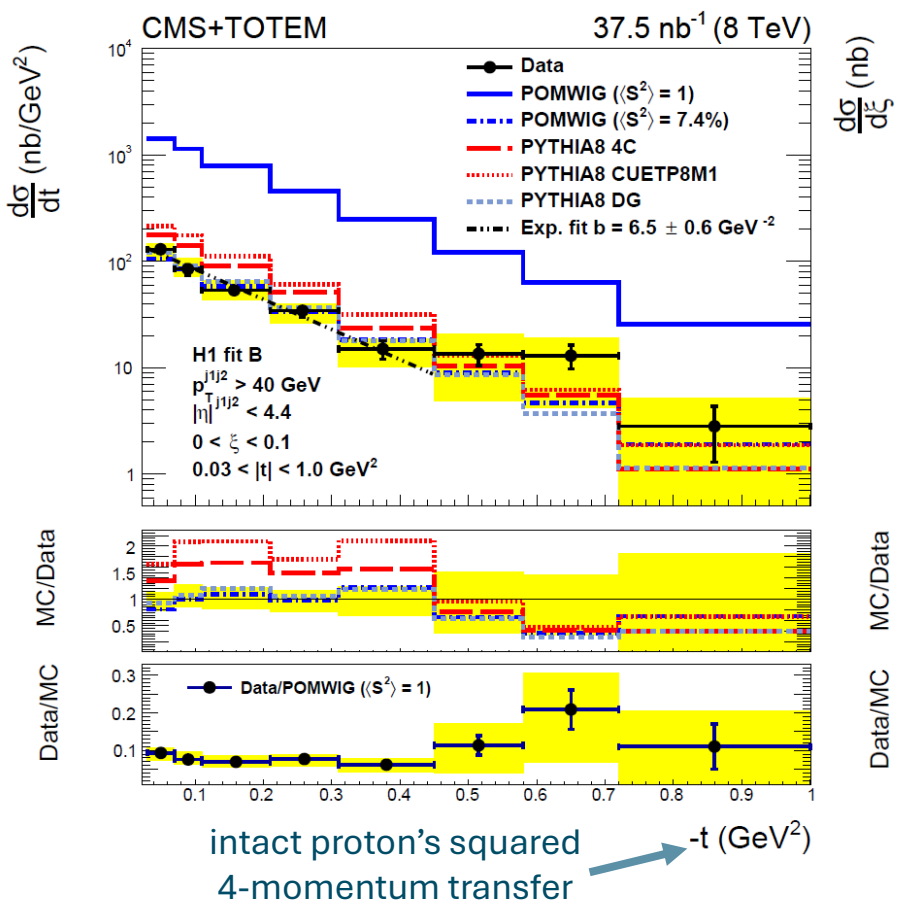

intact proton's squared 4-momentum transfer

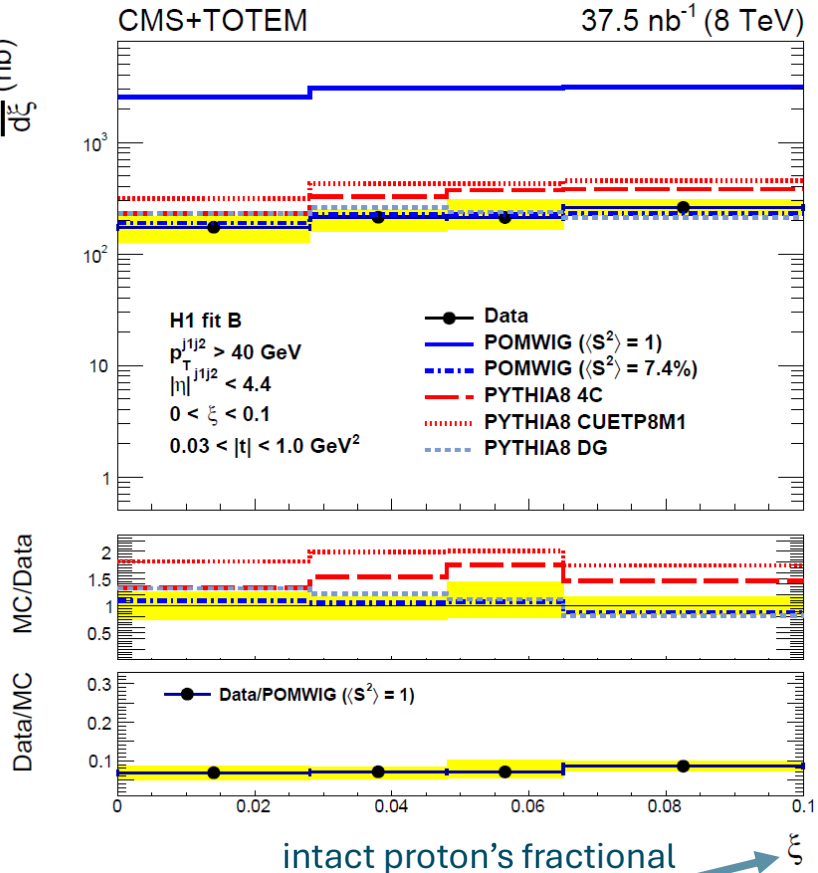

intact proton's fractional momentum loss

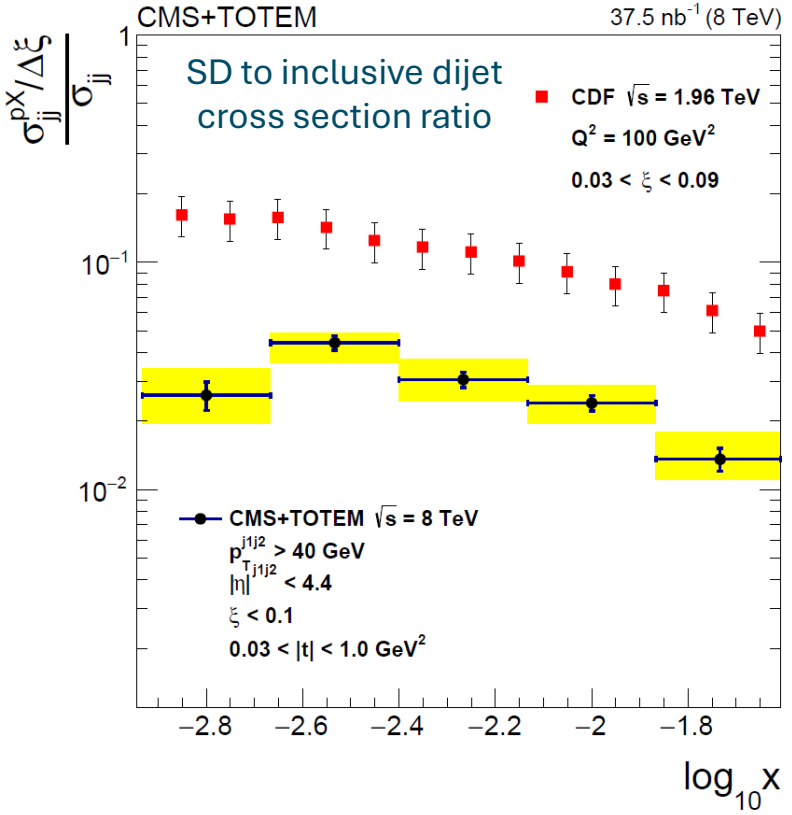

SD dijet results

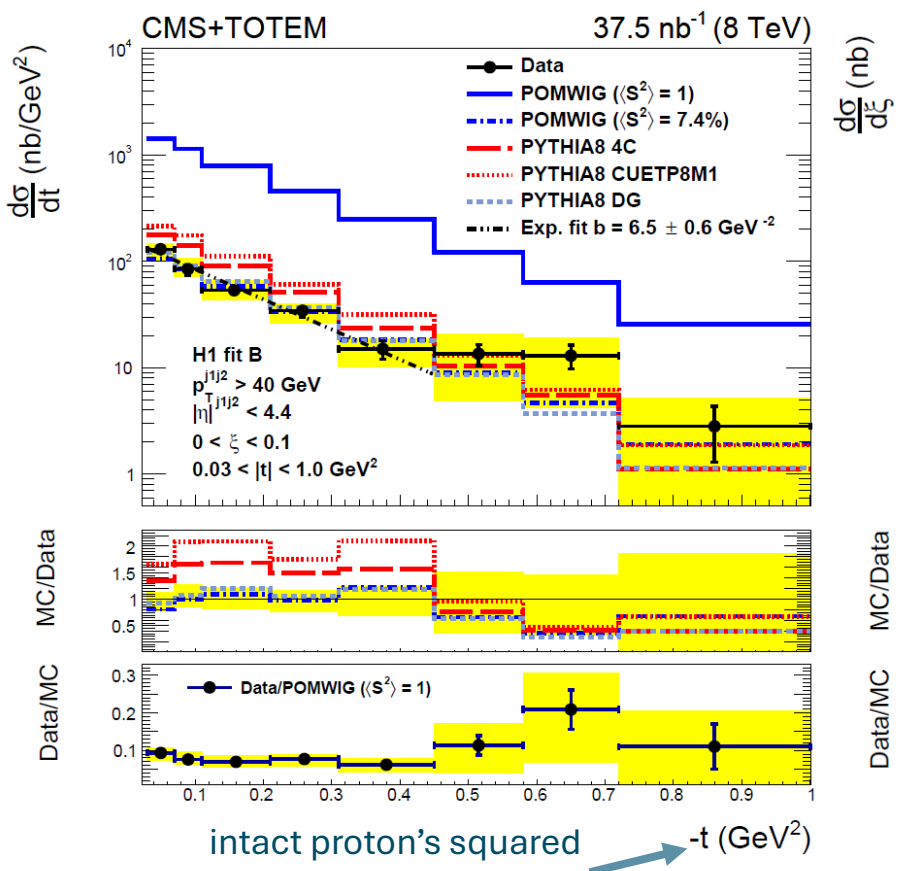

intact proton's squared 4-momentum transfer

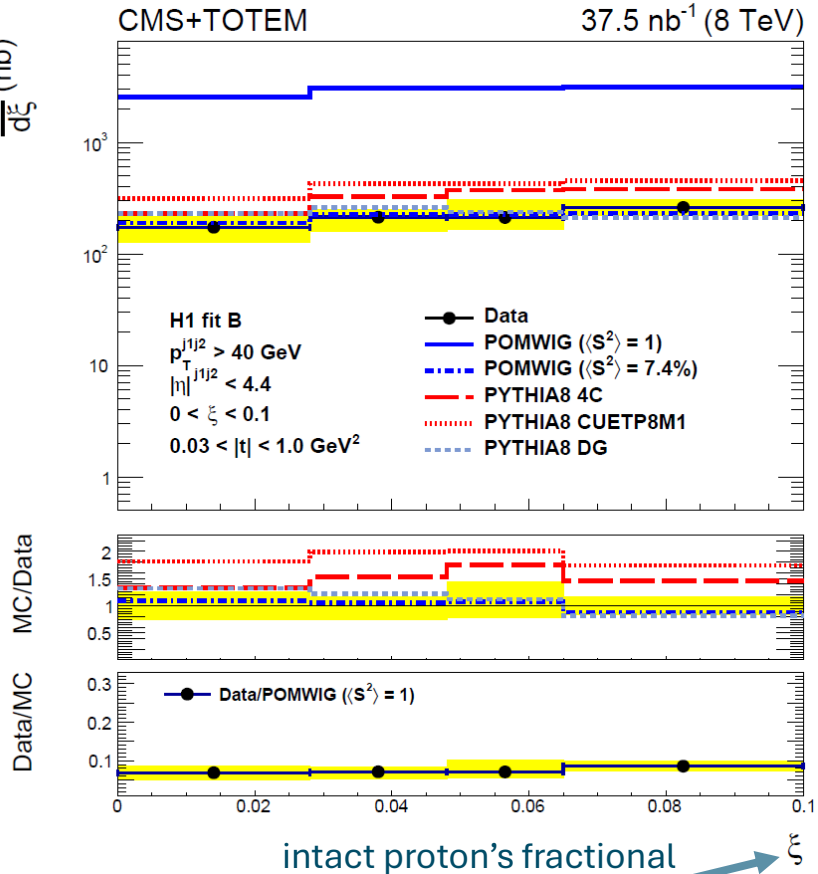

intact proton's fractional momentum loss

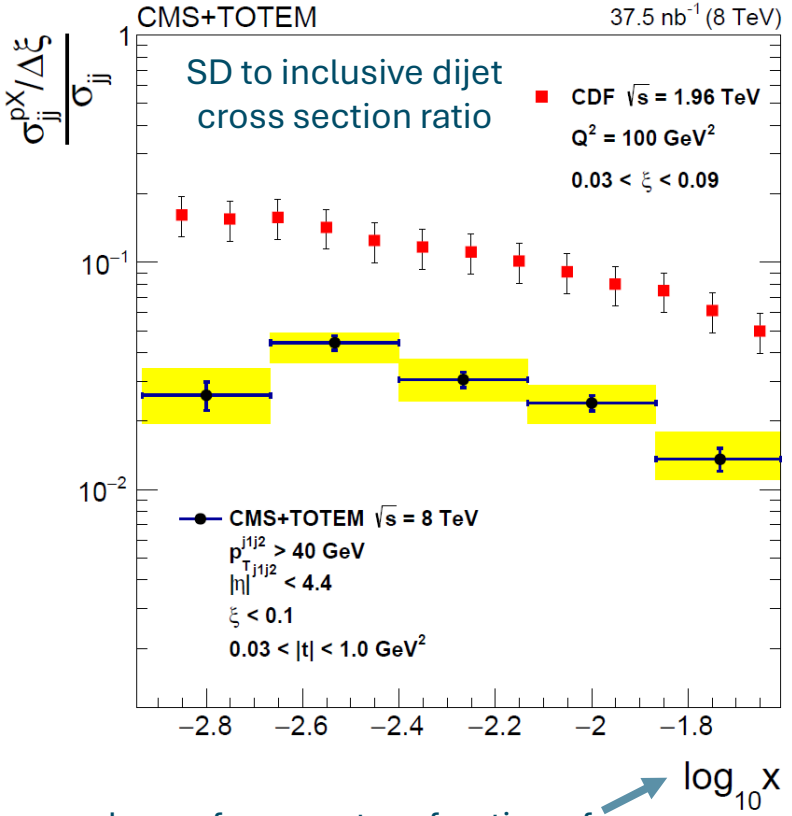

$\log_{10}$ of momentum fraction of partons initiating the hard scattering

SD dijet results

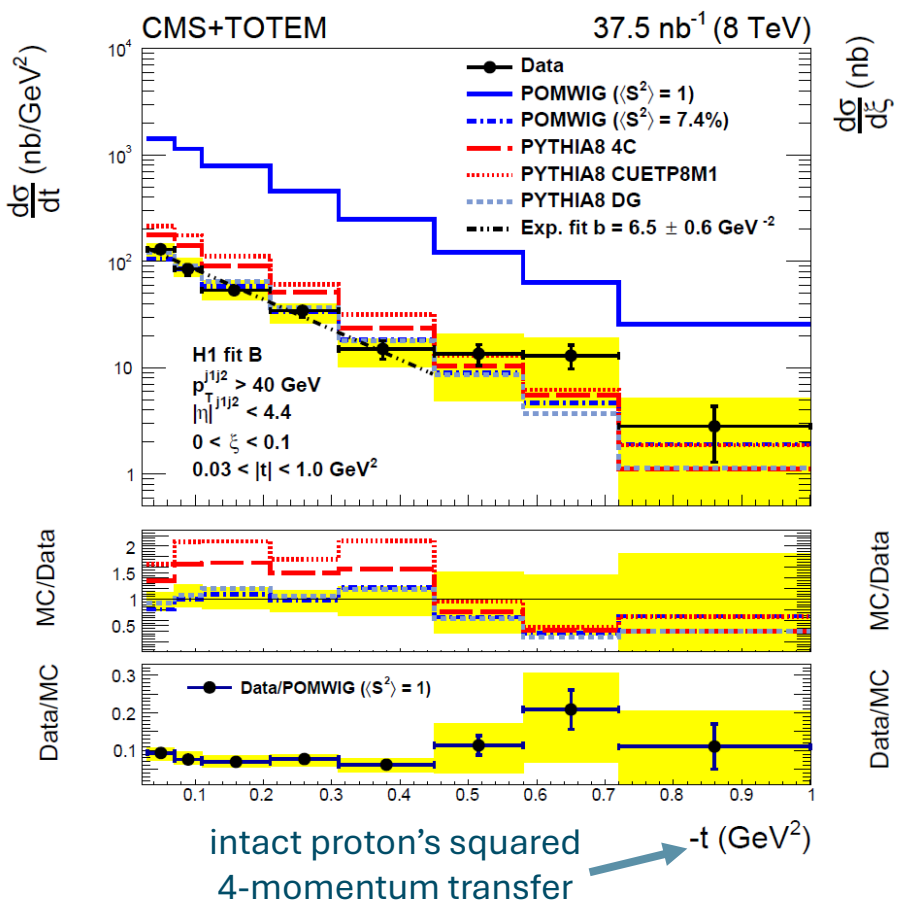

intact proton's squared 4-momentum transfer

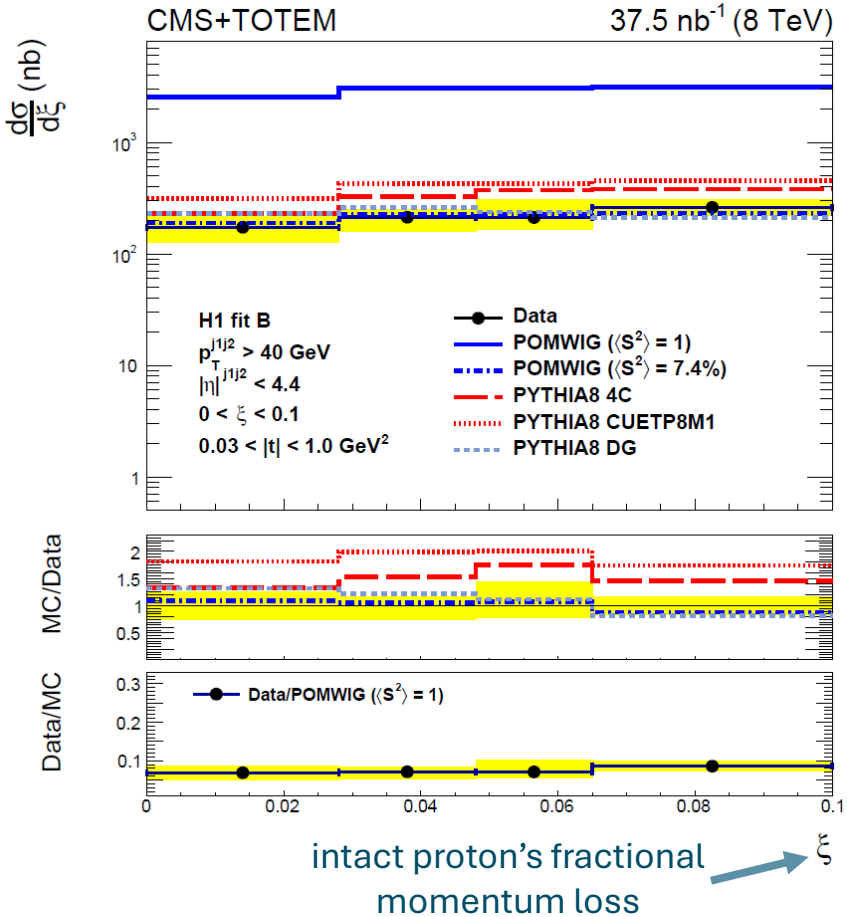

intact proton's fractional momentum loss

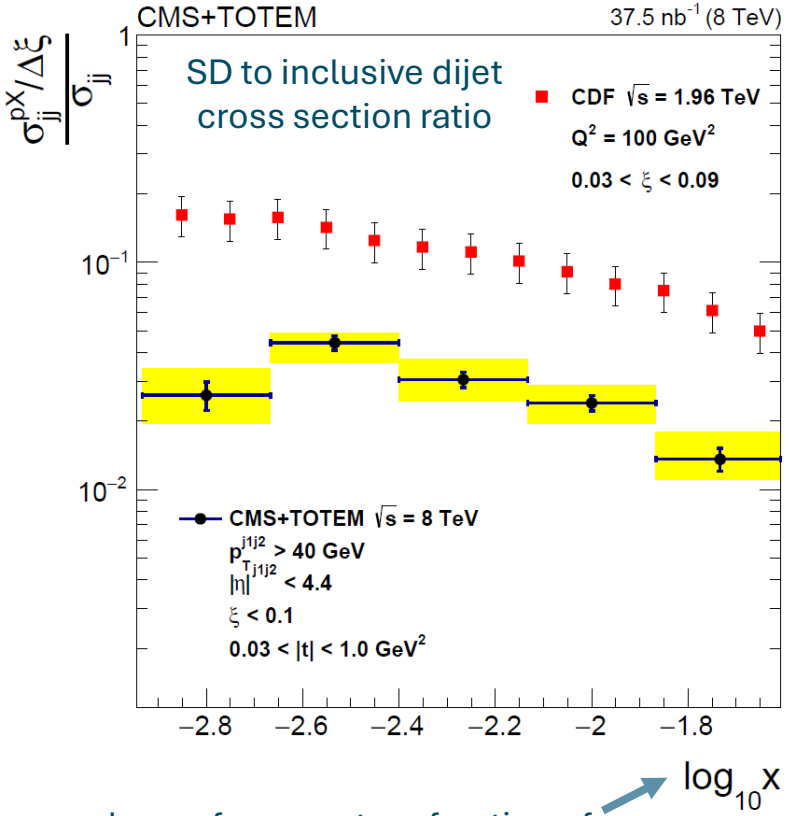

$\log_{10}$ of momentum fraction of partons initiating the hard scattering

POMWIG (with $\langle S^2 \rangle = 7.4\%$) and PYTHIA8 DG MC predictions show good agreement with the data

SD dijet results

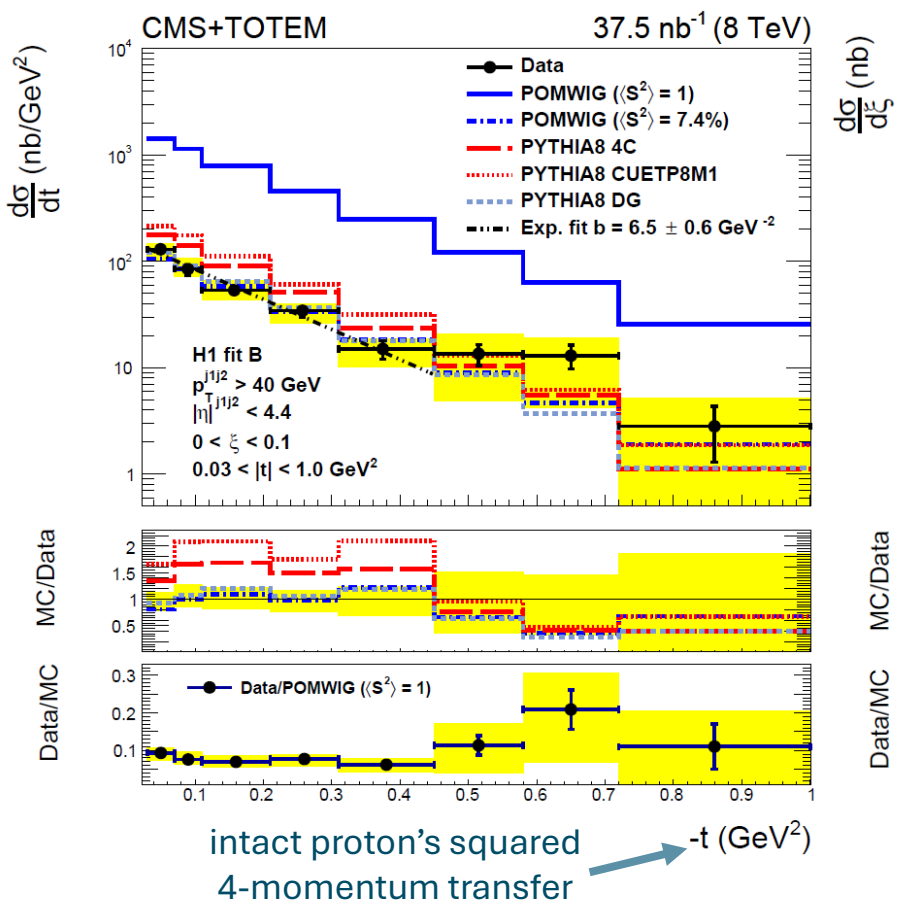

intact proton's squared 4-momentum transfer

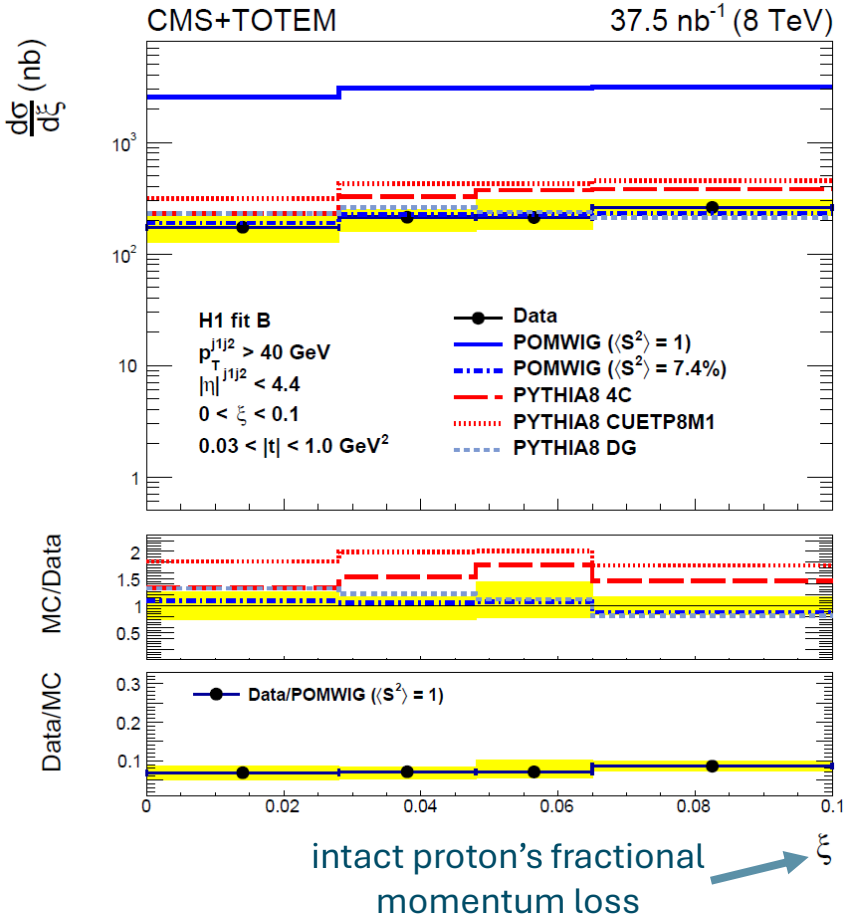

intact proton's fractional momentum loss

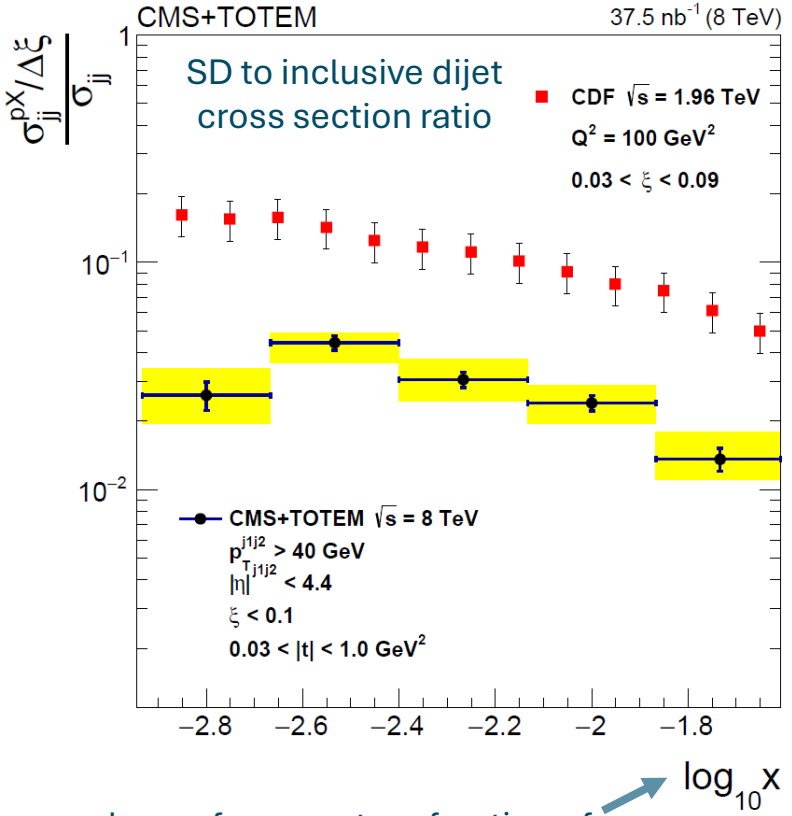

$\log_{10}$ of momentum fraction of partons initiating the hard scattering

POMWIG (with $\langle S^2 \rangle = 7.4\%$) and PYTHIA8 DG MC predictions show good agreement with the data

the t distribution up to about 0.4 GeV^2 is well described by an exponential function

SD dijet results

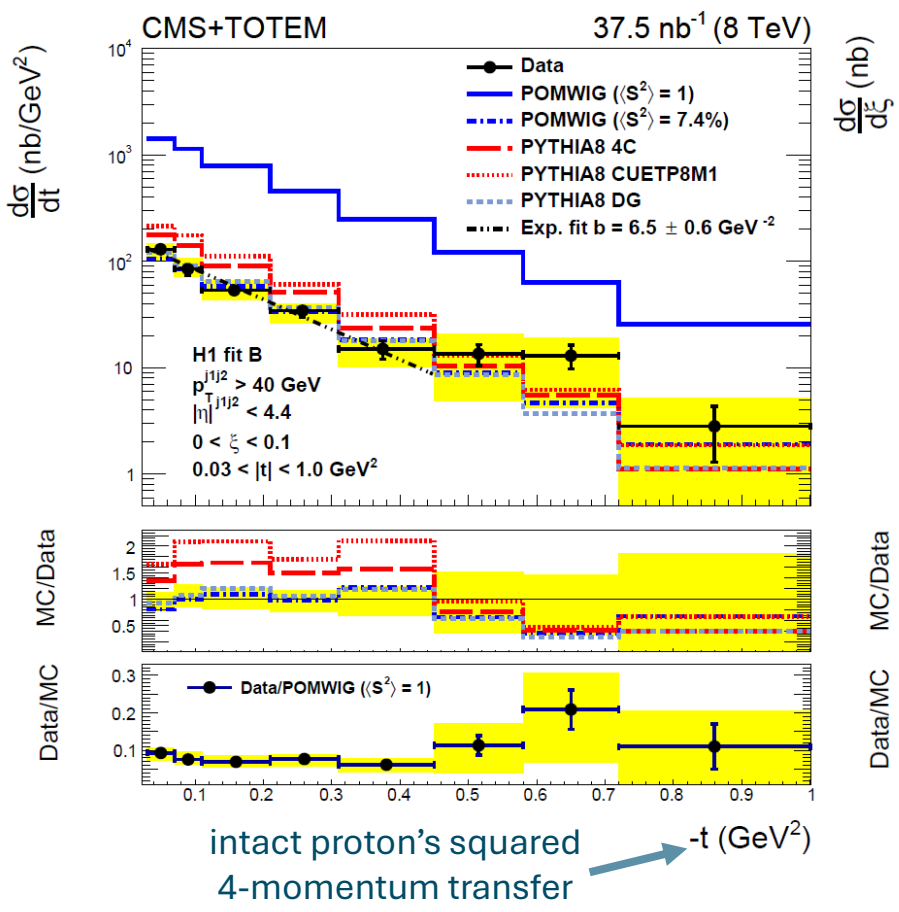

intact proton's squared 4-momentum transfer

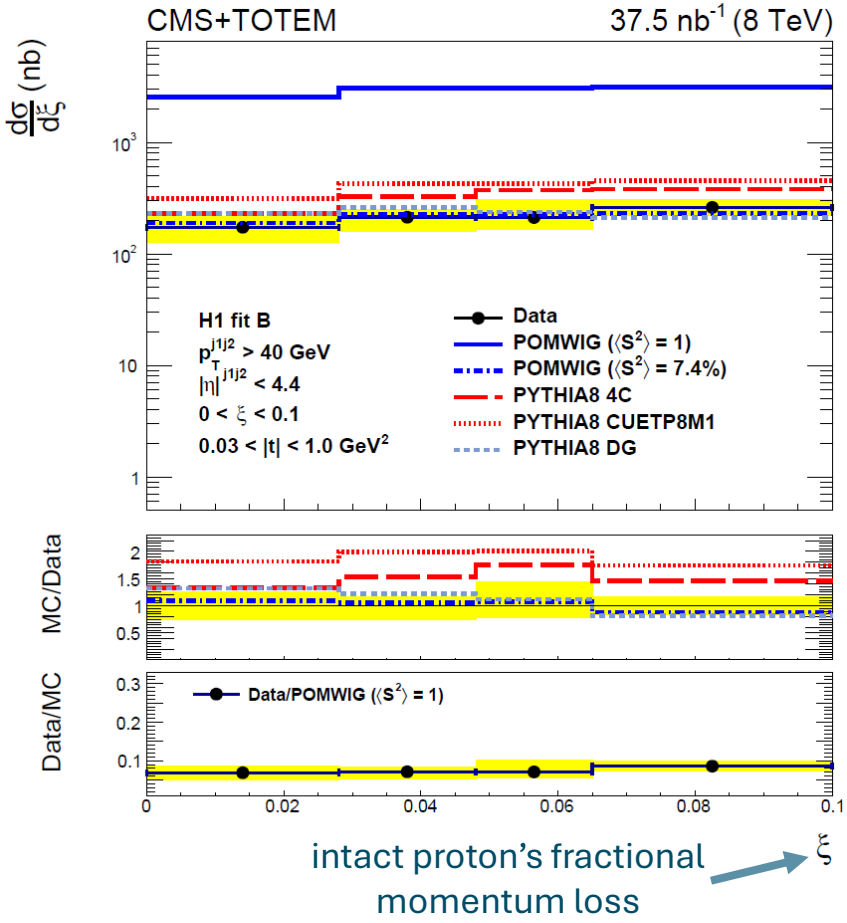

intact proton's fractional momentum loss

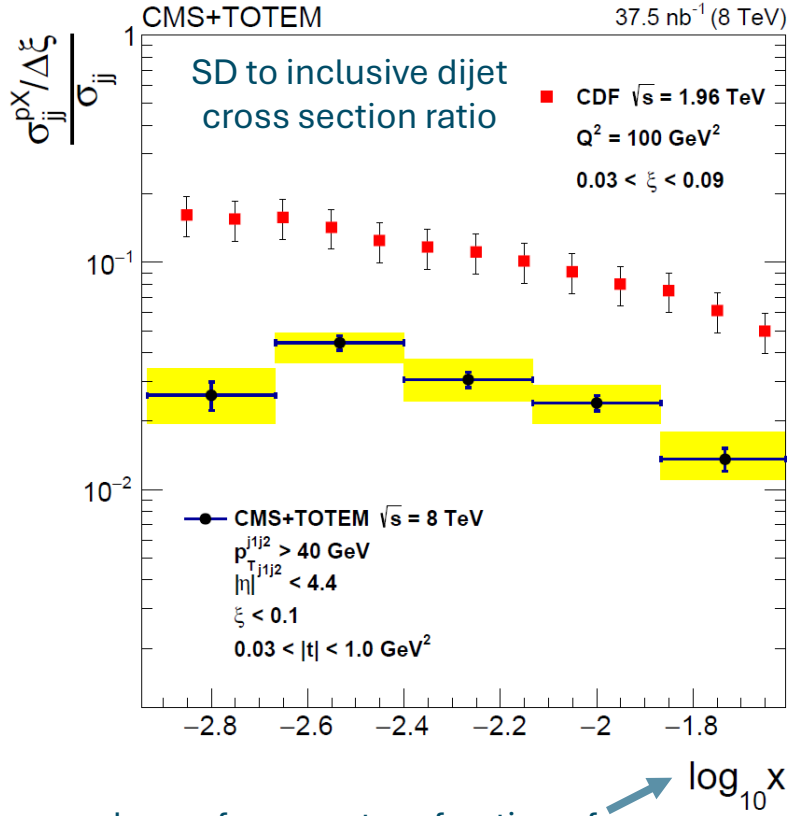

$\log_{10}$ of momentum fraction of partons initiating the hard scattering

POMWIG (with $\langle S^2 \rangle = 7.4\%$) and PYTHIA8 DG MC predictions show good agreement with the data

the t distribution up to about 0.4 GeV^2 is well described by an exponential function

as compared to the Tevatron CDF results, SD dijet production is further suppressed at the LHC

Summary

- various diffractive processes measured jointly by CMS and TOTEM in pp collisions
- first time observation of a parabolic minimum in the distribution of the azimuthal angle difference of the final state protons in central exclusive production;
- various physical parameters related to pomeron physics extracted/tuned
- good agreement between BFKL and jet-gap-jet measurements
- first measurement of hard diffraction with a measured intact proton at LHC

Thank you for your attention!

Supported by the
NKFIH grants K147557 and **2020-2.2.1-ED-2021-00181**; and
by the **Research Excellence Programme and the Flagship Research Groups Programme of the Hungarian University of Agriculture and Life Sciences**.